

AMERICAN UNIVERSITY OF BEIRUT

TIME DOMAIN ESTIMATION OF INFANT RESPIRATORY
MECHANICAL PROPERTIES AND LUNG VOLUME DURING
HIGH FREQUENCY OSCILLATORY VENTILATION

by
SAMER ABDEL MASSIH BU JAWDEH

A thesis
submitted in partial fulfillment of the requirements
for the degree of Master of Engineering
to the Department of Mechanical Engineering
of the Faculty of Engineering and Architecture
at the American University of Beirut

Beirut, Lebanon
August 2014

AMERICAN UNIVERSITY OF BEIRUT

TIME DOMAIN ESTIMATION OF INFANT RESPIRATORY
MECHANICAL PROPERTIES AND LUNG VOLUME DURING
HIGH FREQUENCY OSCILLATORY VENTILATION

by
SAMER ABDEL MASSIH BU JAWDEH

Approved by:



Dr. Robert Habib, Associate Professor
Internal Medicine

Advisor

Dr. Alan Shihadeh, Professor
Mechanical Engineering

Member of Committee

Dr. Issam Lakkis, Associate Professor
Mechanical Engineering

Member of Committee

Date of thesis defense: August 11, 2014

AMERICAN UNIVERSITY OF BEIRUT

THESIS, DISSERTATION, PROJECT RELEASE FORM

Student Name: Bu Jawdeh Samer Abdel Massih
Last First Middle

Master's Thesis Master's Project Doctoral Dissertation

I authorize the American University of Beirut to: (a) reproduce hard or electronic copies of my thesis, dissertation, or project; (b) include such copies in the archives and digital repositories of the University; and (c) make freely available such copies to third parties for research or educational purposes.

I authorize the American University of Beirut, three years after the date of submitting my thesis, dissertation, or project, to: (a) reproduce hard or electronic copies of it; (b) include such copies in the archives and digital repositories of the University; and (c) make freely available such copies to third parties for research or educational purposes.

Samer A. 21 Aug. 2014
Signature Date

ACKNOWLEDGMENTS

I would like to thank Dr. Robert Habib who really showed so much patience while dealing with a stubborn person such as I. From him, I learned the importance of patience and listening. I wouldn't have found a better mentor who gave me so much of his valuable time. I will never forget the many hours I spent in his office.

I would like to thank Dr. Alan Shihadeh and Dr. Issam Lakkis for all their lessons inside and outside the classroom.

My family for all their support, love, motivation, and encouragement to dream.

AN ABSTRACT OF THE THESIS OF

Samer Abdel Massih Bu Jawdeh for Master of Engineering
Major: Mechanical Engineering

Title: Time Domain Estimation of Infant Respiratory Mechanical Properties and Lung Volume During High Frequency Oscillatory Ventilation

Assessments of lung mechanics parameters and volume, and how these physiologic parameters change with treatment and during mechanical ventilation, may be of great value to clinicians caring for patients in respiratory failure and requiring mechanical respiratory support. Obtaining reliable and accurate mechanics and volume data is, however, challenging particularly in severely preterm infants whose condition requires using HFOV (High Frequency Oscillatory Ventilation) as a means of respiratory support. Additionally, these assessments generally suffer from being impractical, entail interrupting the HFOV support, and require different methods for lung mechanics and lung volume assessments. This thesis research tested the hypothesis that a model-based approach for the analysis of HFOV time-domain pressure, flow, volume ventilation data measured at multiple mean airway pressure (P_{aw}) and pressure amplitude (ΔP) settings will provide a practical and minimally intrusive means of obtaining reliable and physiologically sensible lung mechanical/volume parameters, and can potentially guide clinical management of this vulnerable infant population. The developed method does not interrupt the mechanical support of the infant and for the first time attempts to simultaneously obtain respiratory resistance and compliance estimates, separate airway and tissue mechanical properties and estimate alveolar lung volume. This thesis research developed and compared three mathematical models that were applied in inverse-fashion (model fitting of experimental data) to available previously collected infant data in the context of physiologically driven and evidence-based simplifying assumptions. The physiologic applicability of the results (parameter estimates) was assessed through direct comparisons to available infant data in the relevant medical research literature.

CONTENTS

ACKNOWLEDGEMENTS.....	v
ABSTRACT.....	vi
LIST OF ABBREVIATIONS.....	ix
Chapter	
I. INTRODUCTION.....	1
II. LUMPED ELEMENT MODELS.....	3
A. Single Airway, Uni-alveolar Model.....	3
B. Lumped Element Model.....	4
C. Previous Studies.....	5
III. METHODS.....	7
A. Multiple Settings Inverse Modeling.....	7
B. Current Data.....	9
C. Multiple Settings Strategy for Cg and Ct.....	9
D. Fitting Across Paw Only (Single ΔP).....	12
E. Fitting Across Multiple Paws and Multiple ΔP Settings.....	13

IV. RESULTS AND DISCUSSION	17
A. Individual Baby Results	17
B. Baby Results Summarized.....	20
C. Averaged Baby Results	28
D. Literature	32
E. Conclusion	38
F. Future Scope	39
BIBLIOGRAPHY	40

Appendix

A. Other Research Results	45
B. Data Selection and Preparation for Fitting	47
C. Baby and Model Guide.....	50
D. Averaged Baby Results	56
E. Inertance Effect.....	59
F. Individual Baby Results.....	68

ABBREVIATIONS

C	Compliance
HFOV	High frequency oscillatory ventilation
I	Inertance
P	Pressure
ΔP	Peak to peak oscillatory pressure
p	Ratio of tissue to airway tidal volume
R	Resistance
t	Time
V	Volume
V _o	Mean lung volume

SUBSCRIPTS

alv	alveolar
aw	airway
g	gas
rs	respiratory system
t	tissue
tr	trachea

CHAPTER I

INTRODUCTION

Preterm infants are susceptible to significant respiratory distress and failure, and may be associated with substantial morbidity and mortality. Several respiratory mechanical support modalities have been developed to assist infants achieve adequate ventilation and oxygenation. These methods of support include both invasive mechanical ventilation and noninvasive (e.g., Nasal Continuous Positive Airway Pressure or NCPAP) modalities. Mechanical ventilation (MV) approaches have traditionally been based on conventional, low (or breathing) frequency with high tidal volumes with varying success. Alternatively, a newer modality that is more frequently used in the most preterm (i.e., sickest) infants is High Frequency Oscillatory Ventilation (HFOV).

HFOV is a high frequency (well above breathing rates), low volume (oscillatory) strategy that may lead to less risk of volutrauma and hence may be presumed to be superior to conventional MV methods [1]. The management of HFOV treated infants is, however, more complex particularly in choosing the optimal settings for the ventilator support. The primary HFOV settings are the mean airway pressure (P_{aw}), the pressure oscillation amplitude (ΔP), fundamental ventilation frequency (f ; 5 - 15 Hz), and inspiratory to expiratory time ratio (I:E; 1:2 - 1:3). The set P_{aw} is designed to inflate the lungs to a certain operating lung volume that will facilitate optimal oxygenation [2]. The choice of ΔP , and to some degree the frequency, will determine the oscillatory tidal volume amplitudes that will be effectively ventilating the lungs.

To date, management of HFOV treated infants has relied heavily on physician experience and intuition, on indirect indicators, and on some degree on trial and error. These facts about HFOV management render it more an art rather than a science based on objective criteria given the lack of information on the respiratory system's response while varying HFOV settings. This limitation has led many groups to investigate how best can clinicians optimize HFOV settings [2-9]. Many of the suggested approaches to optimize settings have focused on means of measuring respiratory mechanics, lung volumes and gas exchange parameters such as oxygenation and ventilation (removal of CO₂) [10-25]. These approaches have been mostly hampered by being tedious, require additional equipment, disrupt the clinical setting and may also require interrupting the delivery of the HFOV support.

Currently, there is no clinically applicable technique capable of providing insight on respiratory compliance, resistance, and lung volume simultaneously. Yet, if such comprehensive information about the underlying lung mechanics and volumes during HFOV treatment (including how these may change with adjustment of ventilator settings) were attainable in a practical, reliable and accurate manner, doctors will be better situated to help these sick infants and with minimal risk and disruption.

The objective of the current research is to develop and test a practical and non-disruptive modeling based approach to obtain comprehensive information about airway and respiratory (lung) tissue mechanical properties and lung volumes during HFOV, and how these change with HFOV settings. Here, we hypothesized that simultaneous consideration (inverse modeling) of pressure, flow and volume data during HFOV support collected at multiple and systematic adjustments of support levels (Paw and ΔP) will provide such detailed information.

CHAPTER II

LUMPED ELEMENT MODELS

A. Single Airway, Uni-alveolar Model

Ideally, we would like to know as much as possible about the respiratory system behavior. Several studies have developed various models and studied them in numerous techniques [26,27]. One major physical respiratory model that captures several physically important elements is a single tube representing the main airway and its extending branches (Figure 2.1). The tube is connected to one large sphere that combines all the alveoli into one massive bundle. Based on this model, we identify six lung elements. First, the tube contributes an airway resistance (R_{aw}) and an airway inertance (I_{aw}). These two airway elements cause the pressure to drop to alveolar pressure (P_{alv}) at the end of the airway. The degree to which lung volume changes with response to pressure is known as tissue compliance (C_t). The higher the change in volume for the same pressure the more the lung is compliant. The lung tissue will also contribute with a tissue resistance (R_t) and tissue inertance (I_t). In addition, part of the airway tidal volume (V_{aw}) reaching the alveoli causes change in lung volume (V_t), whereas the remaining part will be compressed inside the alveoli (V_g). The latter adds a gas compression (C_g) factor to our model that captures the amount of V_{aw} that has been compressed inside the lung. Finally, concerning the airway, it is a compliant airway in the sense that its radius varies depending on the HFOV settings. More specifically, these six elements could vary as HFOV settings are changed. Mean lung volume (V_o) will vary as well.

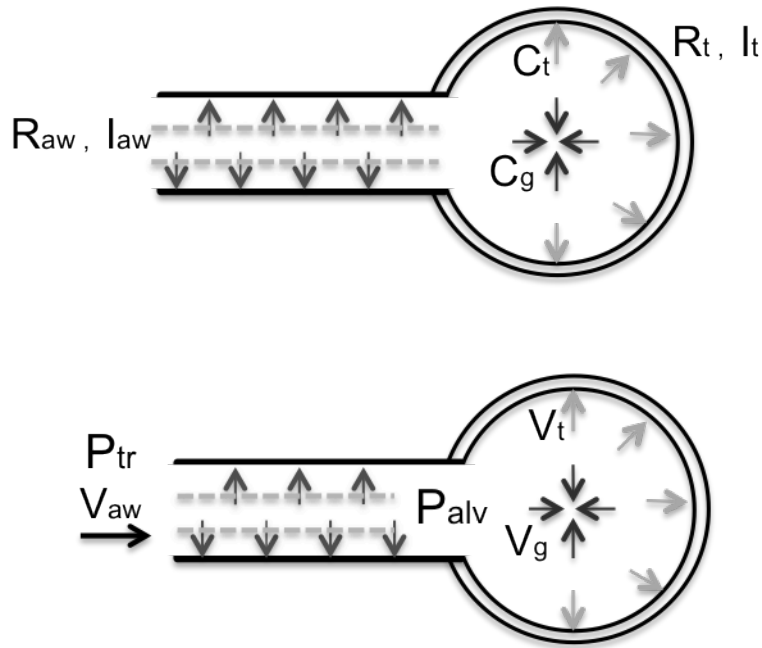


Figure 2.1: Lung Model. Model includes six distinct parameters R_{aw} , I_{aw} , C_g , R_t , I_t , and C_t . HFOV sets P_{tr} , and as a result, a certain V_{aw} will enter the airway. V_{aw} will depend on the values of the lung parameters

B. Lumped Element Model

Based on the 6-element model, we can represent the six various elements through a lumped element electrical circuit. Inertances can be modeled with inductors, compliances with capacitors, and resistances with resistors (Figure 2.2)

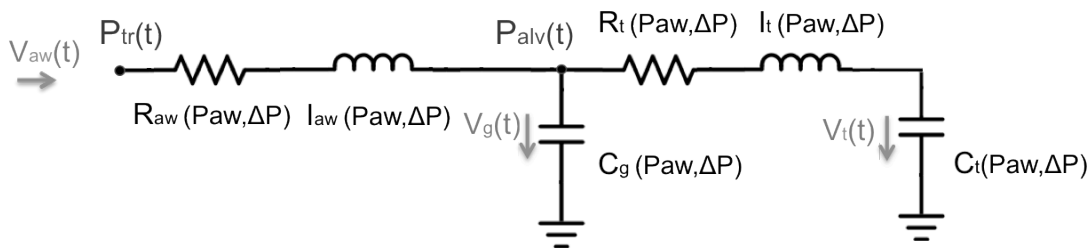


Figure 2.2: Six-element equivalent electrical lumped model. P_{tr} , P_{alv} , V_{aw} , V_t , and V_g vary with time, whereas R_{aw} , R_t , C_g , C_t , I_t , and I_{aw} are P_{aw} and ΔP dependent.

The essence of this model is that it separates airway and tissue properties via an alveolar gas compression shunt compartment. Use of this model, if possible and

justifiable, in both the forward and inverse direction can provide a basis for a better understanding of respiratory mechanics during HFOV. This, however, has not been attempted in any prior studies.

C. Previous Studies

Singh et al. recently measured tracheal pressure (P_{tr}) and Flow (\dot{V}_{aw}) in 11 HFOV-supported preterm infants collected at multiple combinations of P_{aw} and ΔP [3]. The data, at any given $P_{aw}/\Delta P$ setting combination, attempted to fit a 3-element model composed of a resistor, capacitor, and inductor which capture the overall dynamics of the respiratory system without separation of airway and tissue compartments (Figure 2.3). Through this model, identification of an overall respiratory compliance (C_{rs}) and an overall respiratory resistance (R_{rs}) with a high degree of confidence was achieved. In addition, the data showed that a respiratory inductance (I_{rs}) was not identified suggesting that at the used HFOV frequencies (10-15 Hz) an inductance is not needed to explain P_{tr} and \dot{V} measurements. Therefore, measurements from a single set of HFOV settings may be well explained using only a 2-element (RC) lumped model of infant respiratory mechanics.

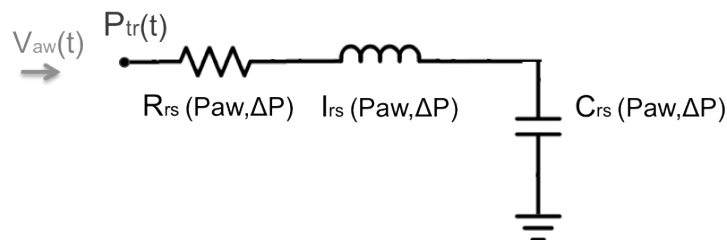


Figure 2.3: Three-element RIC model. The model captures the overall behavior of the respiratory system but fails to capture the behavior of the airway and tissue

The findings by Singh et al. of a lack of an inertance effect would then suggest that the 6-element topology needed to separate airway from tissue properties through an alveolar gas compartment might be reduced to a 4-element topology consisting of R_{aw} , R_t , C_g , and C_t (Figure 2.4)

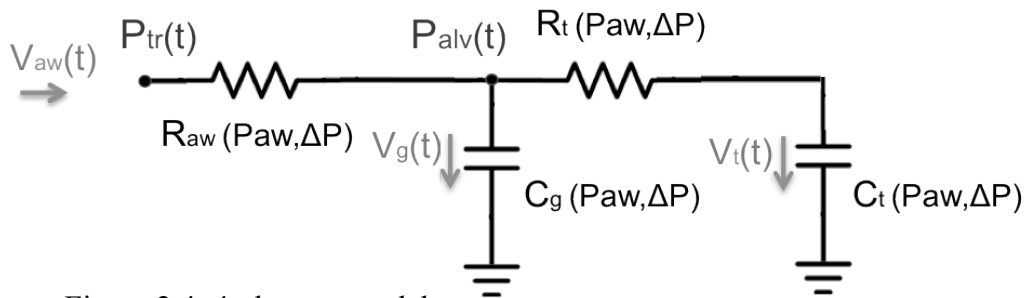


Figure 2.4: 4-element model.

Several groups have attempted to compare (separate) tissue and airway resistance using a variety of techniques [e.g., 28,29]. Kaczka et al. measured tissue and airway resistance over a wide frequency range and showed that tissue resistance (R_t) values decrease substantially with increasing frequencies to very low values approaching zero at about 4 to 5 Hz. For frequencies above 4 Hz, the dissipative (resistance) properties may be attributed to airway resistance (R_{aw}) only [28]. Incorporating this finding into our reduced 4-element topology will further simplify the lumped element representation of respiratory mechanics during HFOV to a 3-element RCC (R_{aw} , C_g , C_t) topology as depicted in figure 2.5. Where the two compliance elements are in parallel such that their effects on pressure flow dynamics are essentially inseparable and acting as a single compliance ($C_{rs}=C_g+C_t$). This, indeed, is both consistent and explanatory of the aforementioned findings by Singh et al.

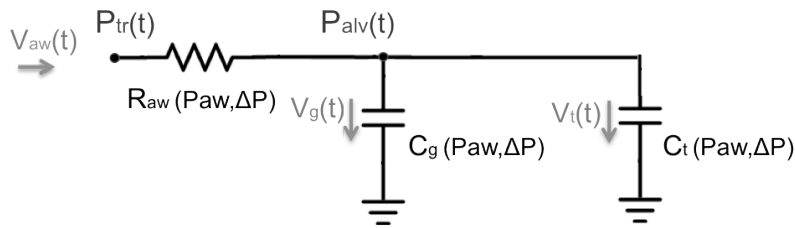


Figure 2.5: 3-element RCC model.

To summarize, the fact that R_t is not identifiable presents a major restriction. In this particular case, it becomes topologically impossible, if we employ the same strategy of Singh et al. and try to fit single settings, to separate C_g from C_t because in the electrical analog two capacitors in parallel are reduced to one, and we can only uniquely identify their resultant ($C_g + C_t$). Thus, we would have failed in our main objective to separate the compartments, and we would be fitting a 2-element model similar to what Singh et al. presented. The current thesis, as described in chapter III, proposes a novel approach based on the simultaneous inverse model analysis of multiple HFOV measurements where P_{aw} and ΔP are systematically adjusted.

CHAPTER III

METHODS

A. Multiple Settings Inverse Modeling

Singh et al. in studying their data only analyzed and reported one single setting (one ΔP for one P_{aw}). We believe that single setting measurements cannot be used to partition airway and tissue properties in the 3-element model, nor can they be used to estimate lung volume or how it may change with varying settings. We are proposing that inverse modeling of pressure and flow HFOV data at multiple settings will provide an objective manner for partitioning airway from tissue properties and estimating alveolar gas volume.

Considering this technique, we shall apply two fitting possibilities. Fitting measurements across P_{aw} and one ΔP setting, or we can fit across P_{aw} and multiple ΔP settings. In either case, certain physiological assumptions will be used. These assumptions mainly capture how elements vary across settings. Again, we claim that fitting multiple settings simultaneously under appropriate assumptions will probably facilitate in estimating elements, which were non-identifiable in single measurements. To further explain, for a 3-element, in the case of single measurements, there is $M*N*3$ parameters where M is the number of P_{aw} settings and N the number of ΔP settings. Since the three elements vary with P_{aw} and ΔP , we have 3 elements at each single setting. However, by taking assumptions that these elements behave or vary in a certain manner across different settings, we directly reduce the number of unknown parameters. This particular reduction aids in parameter estimation.

B. Current Data

The data we shall fit is taken from Singh et al. In their study, measurements were first taken by increasing P_{aw} to a maximum and then returning to baseline. In total, we have 7 mean airway pressures; however, for the time being, we shall restrict our study to the inflation phase of the lung, which includes 4 mean airway pressures. In addition, at each P_{aw} , 3 different ΔP settings were also altered (100%, 150%, and 50%). Figure 3.1 shows flow and tracheal pressure at one P_{aw} setting and for three ΔP settings.

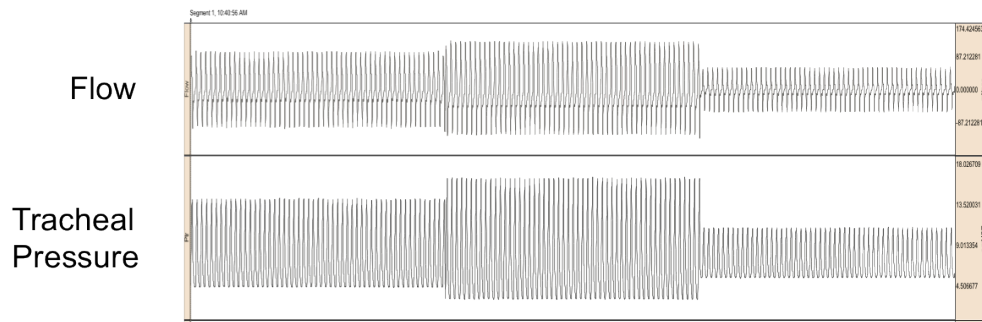


Figure 3.1: Example measured tracheal pressure and flow data from an infant shown at a single P_{aw} setting with multiple ΔP s.

In our study, we shall also use the method of Singh et al. and fit each setting alone (single P_{aw} ΔP setting) to find an overall respiratory compliance and resistance (2 Element Fit). These shall be compared to the results we shall obtain while fitting across settings using our methods developed in the following sections.

C. Multiple Settings Strategy for C_g and C_t

To further aid in separating C_g from C_t in fitting combined data, we shall invoke a physical derivation based on our respiratory system model. Recall that in case R_t is almost zero, the actual infant respiratory mechanics is close to a 3-element RCC model;

therefore, identifying unique values for C_g and C_t is not possible. The main idea behind our strategy is that a fraction (p) of V_{aw} entering the airway will cause the lung volume to change, whereas the remaining fraction will be compressed (Figure 3.2 top). Thus, we are interested in finding that fraction. C_g is based on total lung volume (V_{alv}). V_{alv} is a function of V_o and $p \times V_{aw}$ (Figure 3.2 bottom).

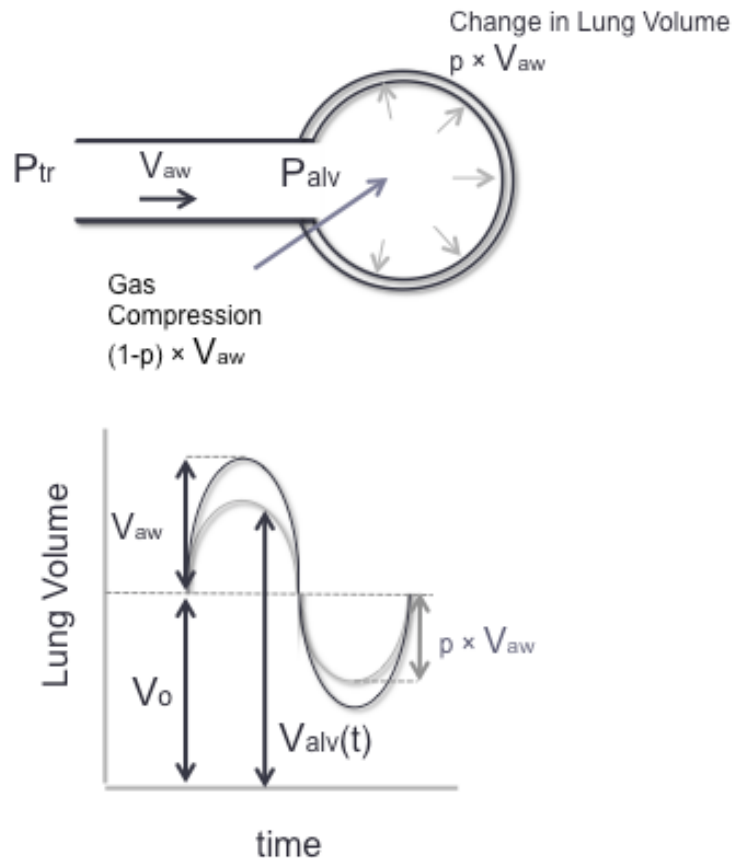


Figure 3.2: Multiple Settings Strategy. The model considers that a fraction (p) of V_{aw} causes a change in lung volume. The remaining fraction ($1-p$) is compressed. Thus the total lung volume at any time (t) is $V_{alv}(t)$.

Through this powerful yet simple strategy, we can go further and actually equate time dependent compliances ($C_g(t)$ and $C_t(t)$). Physically this is more accurate since lung volume oscillates. Furthermore, in the 3-element RCC, the ratio p depends on the values of C_g and C_t . In fact, p is equal to C_t divided by the addition of both

compliances. In light of this, we can present the values of Cg and Ct in time. We can take averages to eliminate this dependence.

$$V_{av}(t) = V_o + p \times V_{aw}(t)$$

$$C_g(t) = \frac{V_{av}(t)}{1033 - 64} = \frac{V_o + p \times V_{aw}(t)}{1033 - 64}$$

$$\therefore p = \frac{C_t}{C_t + C_g}$$

$$C_t(t) = \frac{p}{1-p} C_g = \frac{p}{1-p} \times \frac{V_o + p \times V_{aw}(t)}{1033 - 64}$$

In case we want to eliminate time dependence of parameters by considering averages, then the equations approximate to:

$$V_{av} \cong V_o + p \times \frac{\Delta V_{aw}}{2}$$

$$C_g \cong \frac{V_o}{1033 - 64} + p \times \frac{\Delta V_{aw}}{2(1033 - 64)}$$

$$C_t \cong \frac{p}{1-p} \times \left(\frac{V_o}{1033 - 64} + p \times \frac{\Delta V_{aw}}{2(1033 - 64)} \right)$$

Using the equations derived, we apply them in equation relating pressure to flow and volume in the 3-element RCC model, which is given by:

$$P_{tr} = R_{aw} \dot{V}_{aw} + \frac{V_{aw}}{C_g + C_t}$$

By replacing Cg and Ct by the equations derived and combing data over settings, we hypothesize to find values for Raw, Vo, and p. From the latter two, we then find Cg and Ct.

D. Fitting Across Paw Only (Single ΔP)

In case we are fitting across Paw and single ΔP setting, we have to select a certain behavior for the elements.

Mean Lung Volume (V_o):

$$V_o = v_o + v_1 \left(\frac{P_{aw} - \min(P_{aw})}{\max(P_{aw}) - \min(P_{aw})} \right)^{v_2} \quad v_o > 0 \quad v_1 > 0 \quad v_2 > 0$$

V_o is selected to behave in a power-law fashion with 3 degrees of freedom (v_o , v_1 and v_2). By using power-law and restricting the latter three parameters to positive values, we can limit the behavior to increase with Paw. We select this behavior based on the know physiology stating that V_o increases with mean airway pressure.

Airway Resistance (Raw):

$$R_{aw} = r_o + \frac{r_2}{P_{aw}} \quad r_o > 0$$

Raw behaves in a hyperbolic fashion with respect to Paw. Raw will have two parameters (r_o and r_2) and only r_o is restricted to positive values. Through these parameters Raw has the freedom to either increase or decrease across Paw. In case both parameters are positive, Raw will decrease with Paw. This is our primary expectation since airways are compliant and can expand with increasing Paw. On the other hand, if r_2 were negative then Raw would increase with Paw. In either case, we do not limit Raw in order to see if the results mimic our expectations. Of course, negative Raw values are rejected.

Ratio of Tissue to Airway Tidal Volume (p):

$$p = \frac{P_2 V_o}{V_o} \quad 0 \leq p_2 \leq \frac{V_o}{v_o}$$

The amount of gas compression (1-p) is dependent on V_o . In other words, the larger V_o is, the higher is the ability of the lung to compress and the smaller the p value is. Hence, p should vary inversely with V_o . We use one parameter p_2 to model p and restrain p_2 to provide positive p values between 0 and 1.

The final equations governing lung mechanics across P_{aw} shall be as such:

The following parameters for the elements across P_{aw} single ΔP_{tr} setting shall be applied

$$\rightarrow V_o = v_o + v_1 \left(\frac{P_{aw} - \min(P_{aw})}{\max(P_{aw} - \min(P_{aw}))} \right)^{v_2} \quad v_o > 0 \quad v_1 > 0 \quad v_2 > 0$$

$$\rightarrow p = \frac{P_2 V_o}{V_o} \quad p_2 > 0$$

$$\rightarrow R_{aw} = r_o + \frac{r_2}{P_{aw}} \quad r_o > 0$$

$$\rightarrow V_{adv} = V_o + p \times V \quad V_o > 0$$

$$\rightarrow C_g = \frac{V_{adv}}{969}$$

$$\rightarrow C_t = \frac{C_g \times p}{1 - p}$$

Note: This process reduced the problem from solving 8 elements (C_g , C_t , and R_{aw} at each setting) to solving 18 (6x3) parameters (r_1 , r_2 , v_o , v_1 , v_2 , p_2) across multiple P_{aw} one ΔP_{tr} setting.

We shall refer to this model as Model 1.

E. Fitting Across Multiple Paws and Multiple ΔP Settings

The equations utilized in the first strategy will also be used; however we only add parameters to capture element change with ΔP . In particular, we shall add ΔP dependence for R_{aw} (r_1 and α_r) and C_t (α_{Ct}). By doing so we are assuming that lung volume does not vary with ΔP . We later relax this assumption by allowing lung volume

to change with ΔP (α_{valv}). If that is the case, Ct will automatically be ΔP dependent and there is no need to use α_{Ct} .

We shall refer to the model which assumes lung volume to be ΔP dependent as Model 2, whereas the latter as Model 3.

Mean Lung Volume (V_o):

Model 2:

$$V_o = v_o + v_1 \left(\frac{P_{aw} - \min(P_{aw})}{\max(P_{aw} - \min(P_{aw}))} \right)^{v_2} \quad v_o > 0 \quad v_1 > 0 \quad v_2 > 0$$

Assuming V_o is independent of ΔP , the lung will behave as in Model 1.

Model 3:

$$V_o = \left(v_o + v_1 \left(\frac{\Delta P_{aw}}{\max(\Delta P_{aw})} \right)^{v_2} \right) \times \left(\frac{\Delta P}{\max(\Delta P)} \right)^{\alpha_{v_1}} \quad v_o > 0 \quad v_1 > 0 \quad v_2 > 0$$

By adding a multiplicative factor we can allow ΔP lung variation. The magnitude of this variation will depend on α_{v_1} value. As its absolute value increases then V_o becomes more dependent on ΔP .

Airway Resistance (R_{aw}):

$$R_{aw} = r_o + \frac{r_2}{P_{aw}} + r_1 \times \frac{\Delta P}{\max(\Delta P)} \times P_{aw}^{\alpha_r}$$

The basic behavior of R_{aw} will be as in model 1 (r_o and r_2). To model R_{aw} behavior across ΔP we also used a hyperbola function based on ΔP . However, we observed that at higher P_{aw} s ΔP effects are more evident. In order to quantify this finding, we added a P_{aw} multiplicative factor raised to a parameter α_r . Thus as P_{aw} increases the ΔP effect can increase as we require. This combination allows R_{aw} , for

example, to be a decreasing hyperbola across P_{aw} at ΔP 50% while an increasing hyperbola at ΔP 100%.

Ratio of Tissue to Airway Tidal Volume (p):

$$p = \frac{P_2 V_o}{V_o} \quad 0 \leq p_2 \leq \frac{V_o}{v_o}$$

p shall behave as in model 1. Since it is based V_o . In case we use Model 2, it shall not vary with ΔP . It will when Model 3 is applied. This is also true for C_t .

Tissue Compliance (Ct) for Model 2:

$$C_t = \frac{C_g \times p}{1 - p} \times \left(\frac{\Delta P}{\max(\Delta P)} \right)^{\alpha_{Ct}}$$

In case we use Model 2 and do not allow lung volume to vary with ΔP , then we shall allow C_t to vary instead. We add a multiplicative factor dependent on ΔP to C_t .

As a summary, the parameters over P_{aw} and ΔP settings shall vary as such

Model 2:

$$\rightarrow V_o = v_o + v_1 \left(\frac{P_{aw} - \min(P_{aw})}{\max(P_{aw} - \min(P_{aw}))} \right)^{v_2}$$

$$\rightarrow p = \frac{p_2 v_o}{V_o}$$

$$\rightarrow R_{aw} = r_o + \frac{r_2}{P_{aw}} + r_1 \times \frac{\Delta P}{\max(\Delta P)} \times P_{aw}^{\alpha_r}$$

$$\rightarrow V_{av} = \frac{V_o + p \times V}{969}$$

$$\rightarrow C_g = \frac{V_{av}}{969}$$

$$\rightarrow C_t = \frac{C_g \times p}{1 - p} \times \left(\frac{\Delta P}{\max(\Delta P)} \right)^{\alpha_{Ct}}$$

Model 3:

In this model the assumption that V_o is ΔP independent shall be relaxed. C_t will no longer need a parameter to vary with ΔP . C_g , p , and R_{aw} will behave as in Model 2.

$$\rightarrow V_o = \left(v_o + v_1 \left(\frac{\Delta P_{aw}}{\max(\Delta P_{aw})} \right)^{v_2} \right) \times \left(\frac{\Delta P}{\max(\Delta P)} \right)^{\alpha_{v_1}}$$

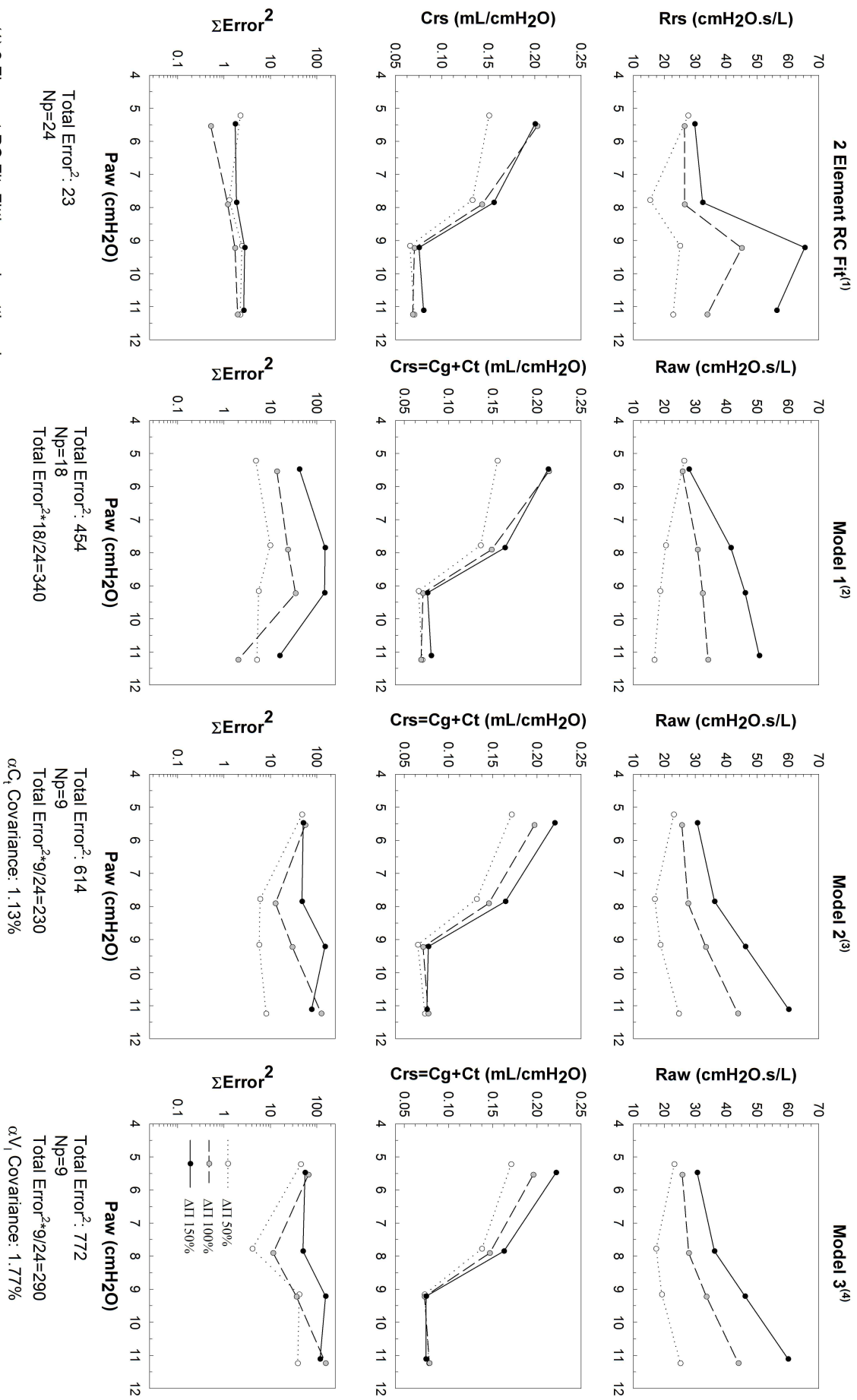
$$\rightarrow C_t = \frac{C_g \times p}{1 - p}$$

CHAPTER IV

RESULTS AND DISCUSSION

A. Individual Baby Results

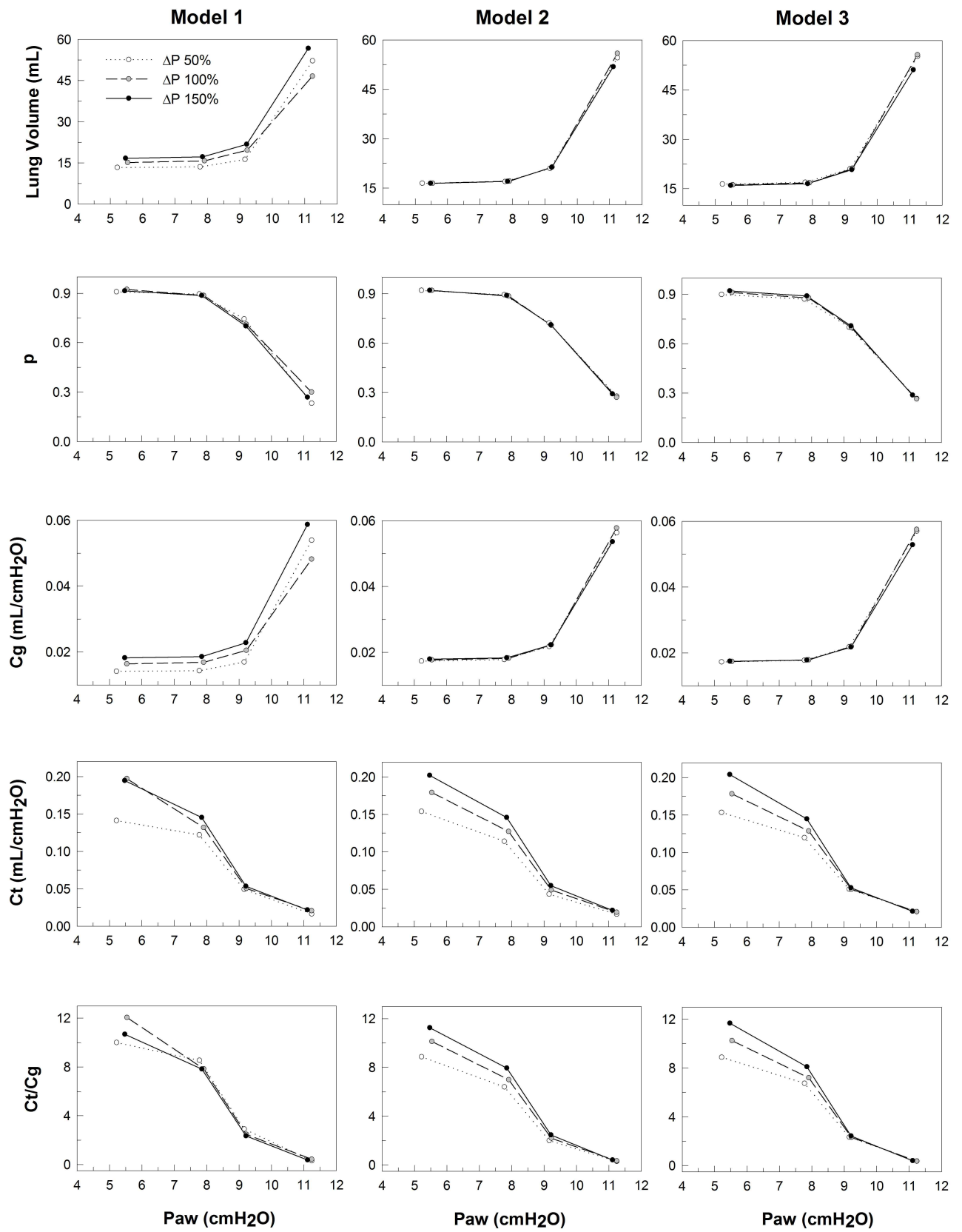
Data for 8 infants was analyzed separately using the traditional 2-element RC fit applied to a single setting measurement in addition to the three modeling approaches developed in this research. Figure 4.1 shows Baby 1 respiratory system results (Crs and Rrs) for the 2 Element Fit, Model 1, Model 2, and Model 3. Since Rt is non-existent in our models, Raw can be compared to Rrs in a 2-element fit, while Cg+Ct can be compared to Crs. Figure 4.2, provides lung volume, p, Cg, Ct, and Cg and Ct/Cg results for the 3 Models only since such measurements are not possible in a 2-element fit Results for the remaining babies are provided in Appendix F.



- (1) 2 Element RC Fit: Fitting each setting alone
- (2) Model 1: Fitting multiple Paws with a single ΔP setting.
- (3) Model 2: Fitting multiple Paws with the three different ΔP settings. Assumed lung volume independent of ΔP.
- (4) Model 3: Fitting multiple Paws with the three different ΔP settings. Allowed lung volume to vary with ΔP.

Baby 1, Male, 0.872 Kg, 10 Hz Natural Frequency, Filter BP 5-15 Hz, 20 cycles per setting

Figure 4.1: Baby 1 respiratory system results.

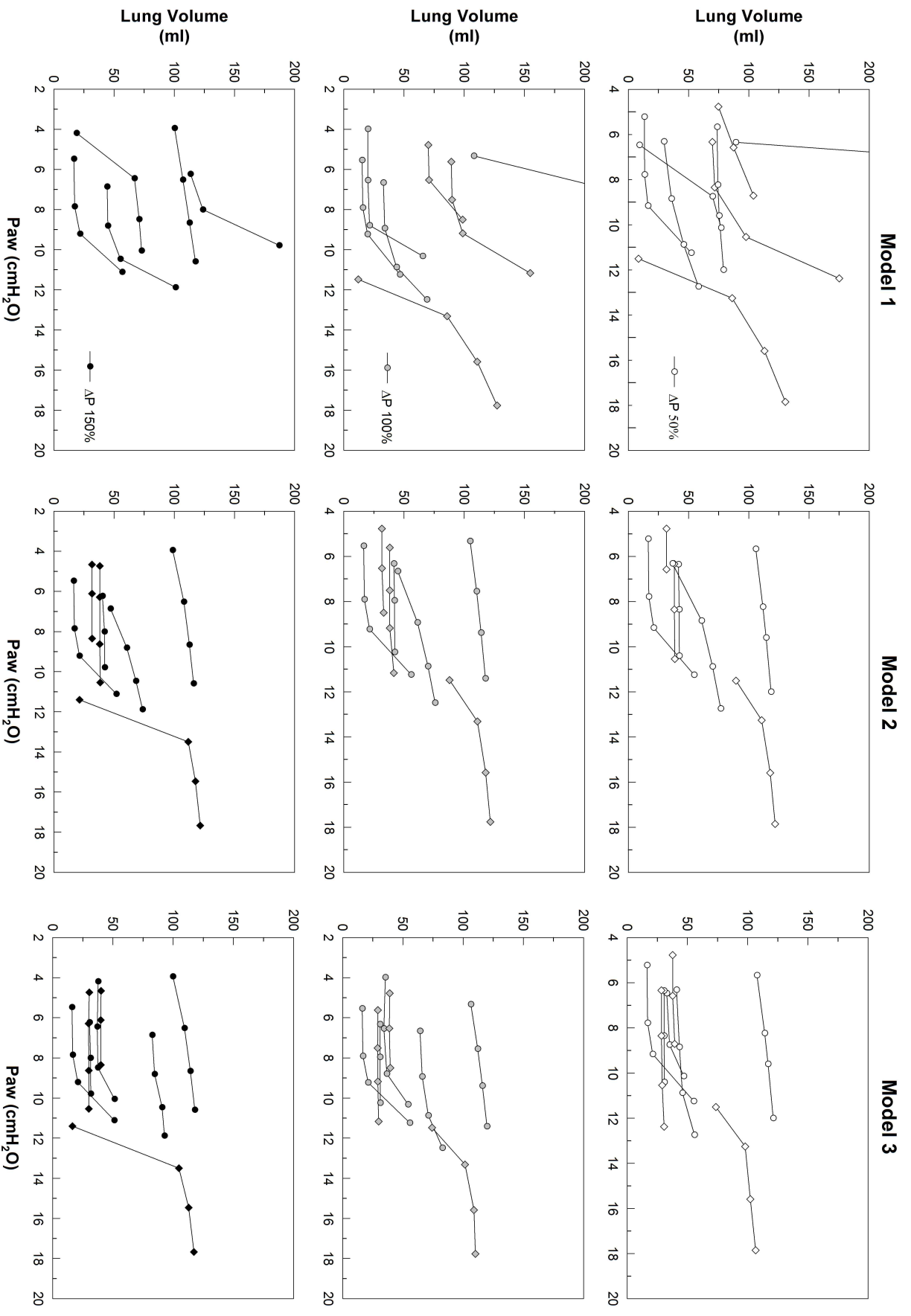


Baby 1 , Male, 0.872 Kg, 10 Hz Natural Frequency, Filter BP 5-15 Hz, 20 cycles per setting

Figure 4.2: Baby 1 lung volume, p, Cg, Ct, and Ct/Cg results.

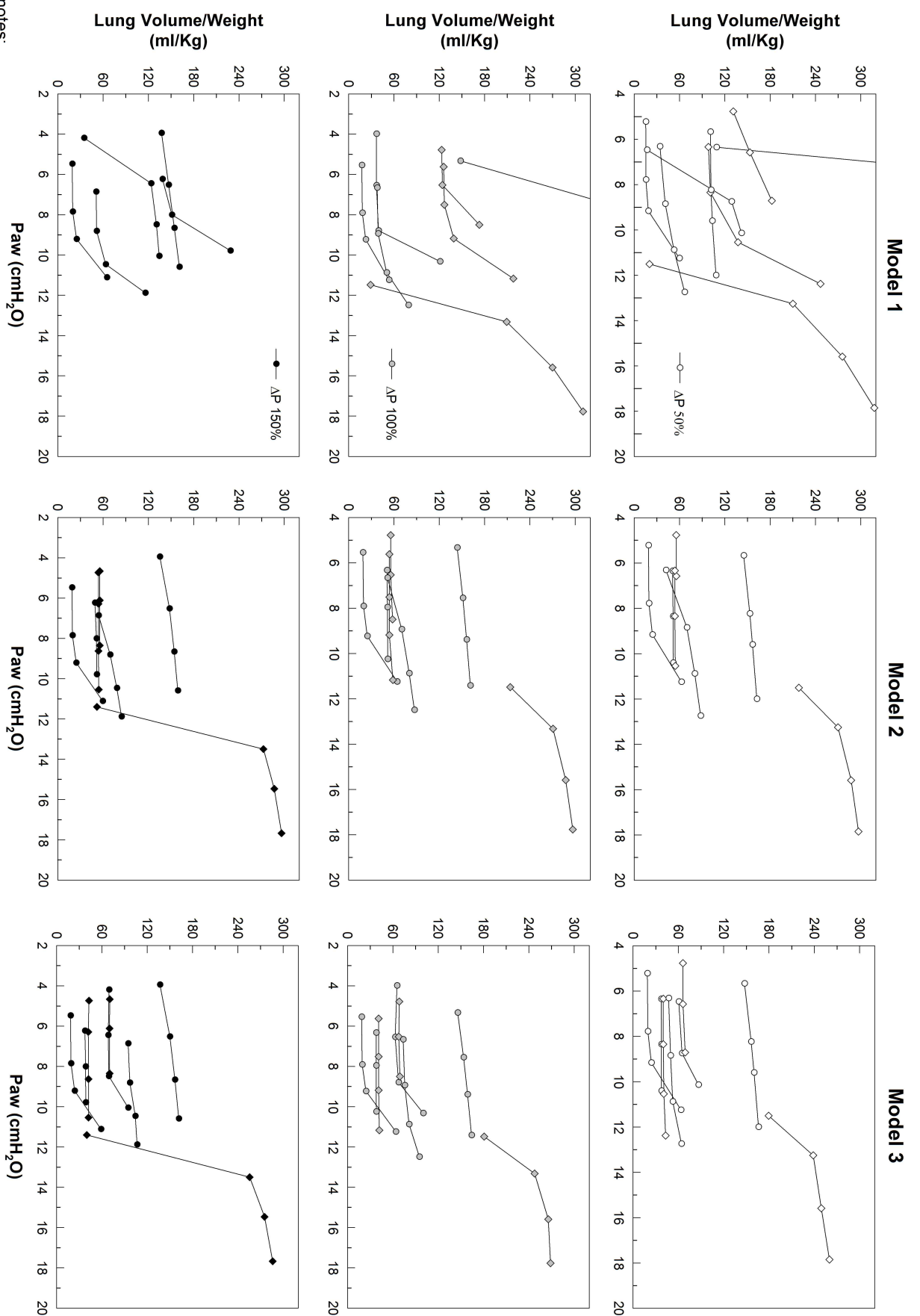
B. Baby Results Summarized

The behavior in lung mechanics among infants varies based on several factors such as HFOV settings, demographics, and respiratory disease. Figures 4.3 through 4.9 plot V_o , V_o per weight, R_{aw} , C_{rs} , C_{rs}/V_o , C_t , and C_t/V_o respectively for all studied babies at each single ΔP .



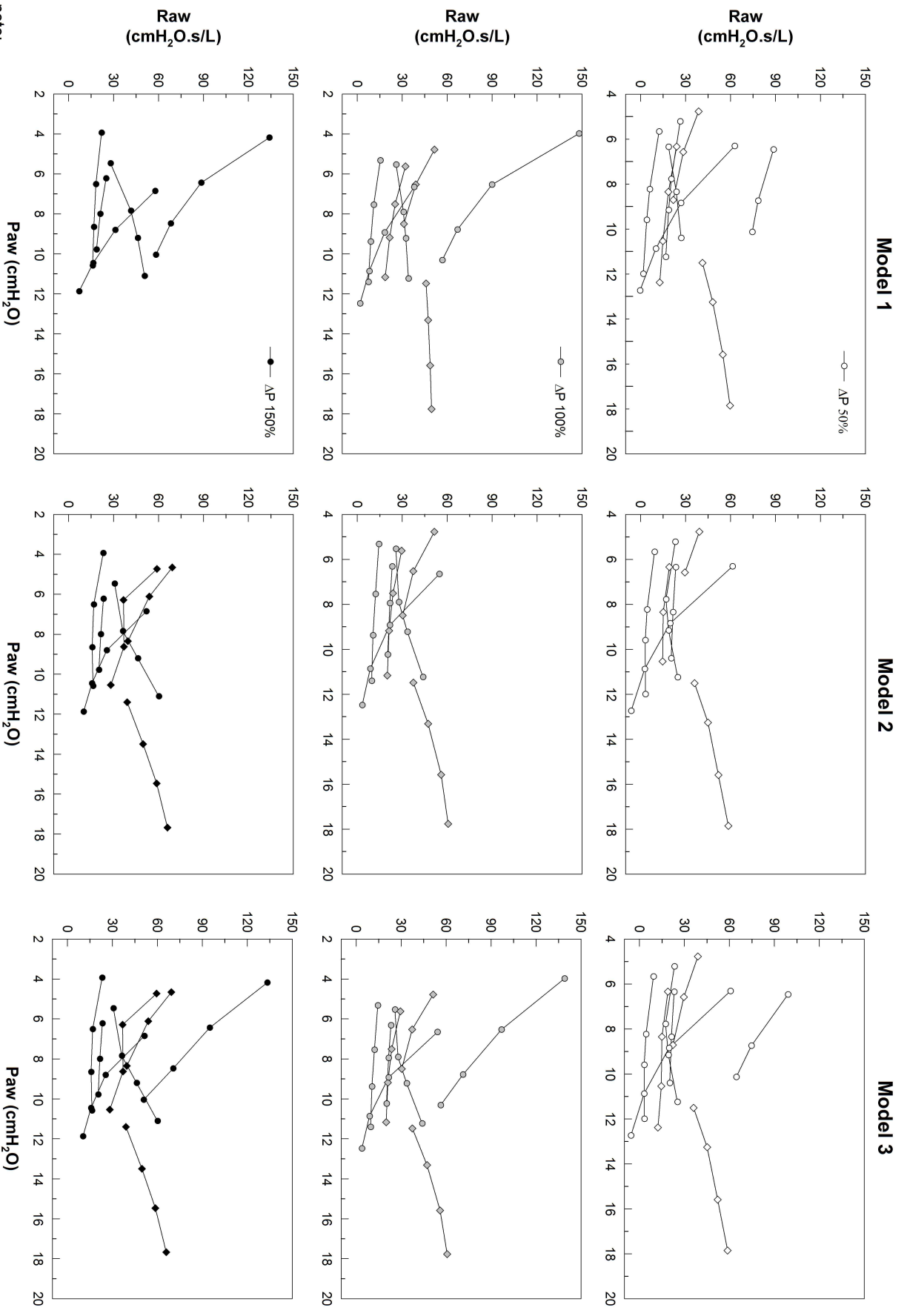
notes:
 (1) Diamond symbols are used for the babies if Model 1 fitting at ΔP 150% failed to converge.

Figure 4.3: Summary baby results. Vo.



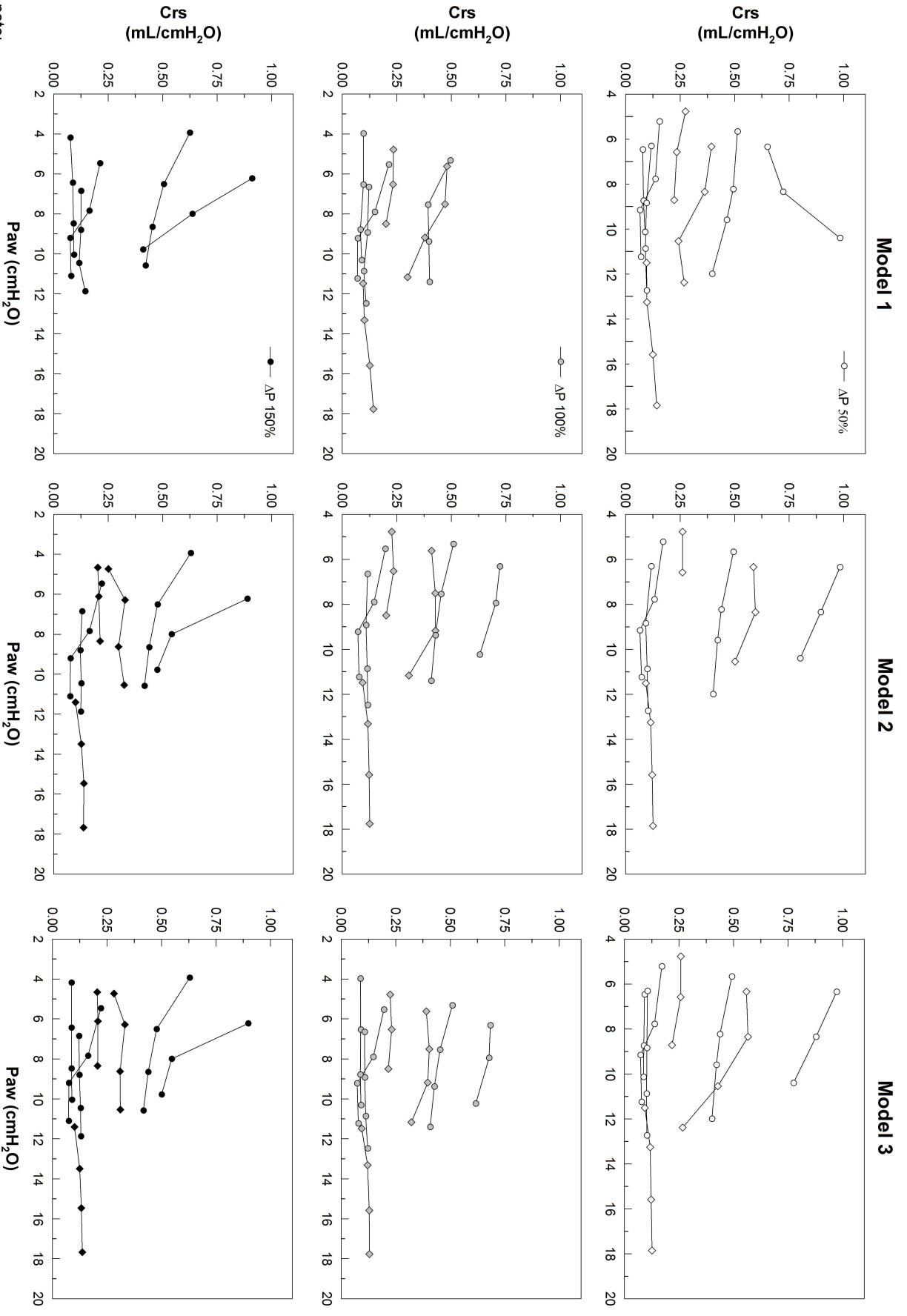
notes:
 (1) Diamond symbols are used for the babies if Model 1 fitting at ΔP 150% failed to converge.
 (2) Y-scaling was based on Model 2 or Model 3 since extreme values for babies in Model 1 were not evident in the other two models.

Figure 4.4: Summary baby results. Vo per weight.



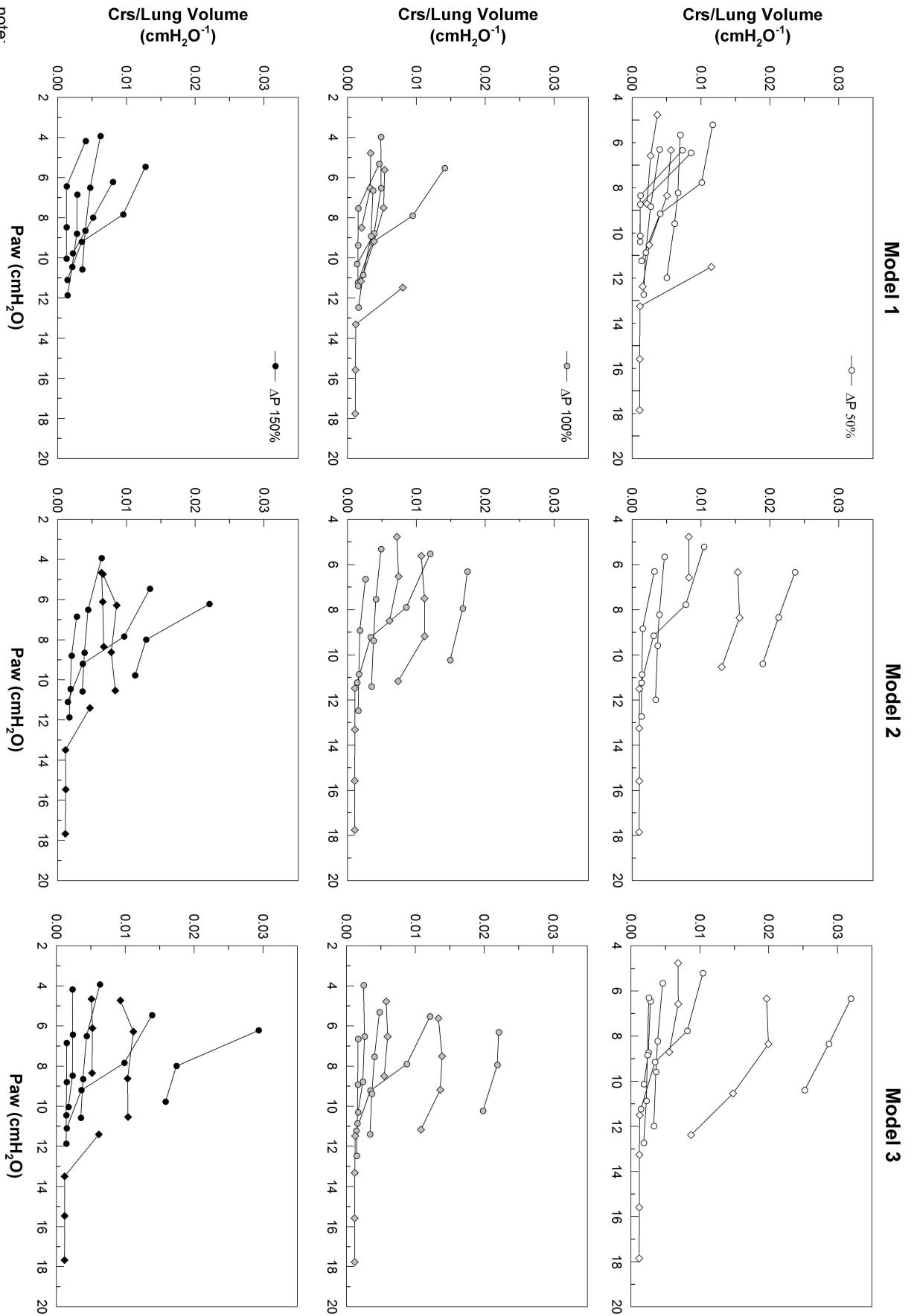
note:
 (1) Diamond symbols are used for the babies if Model 1 fitting at ΔP 150% failed to converge.

Figure 4.5: Summary baby results. Raw.



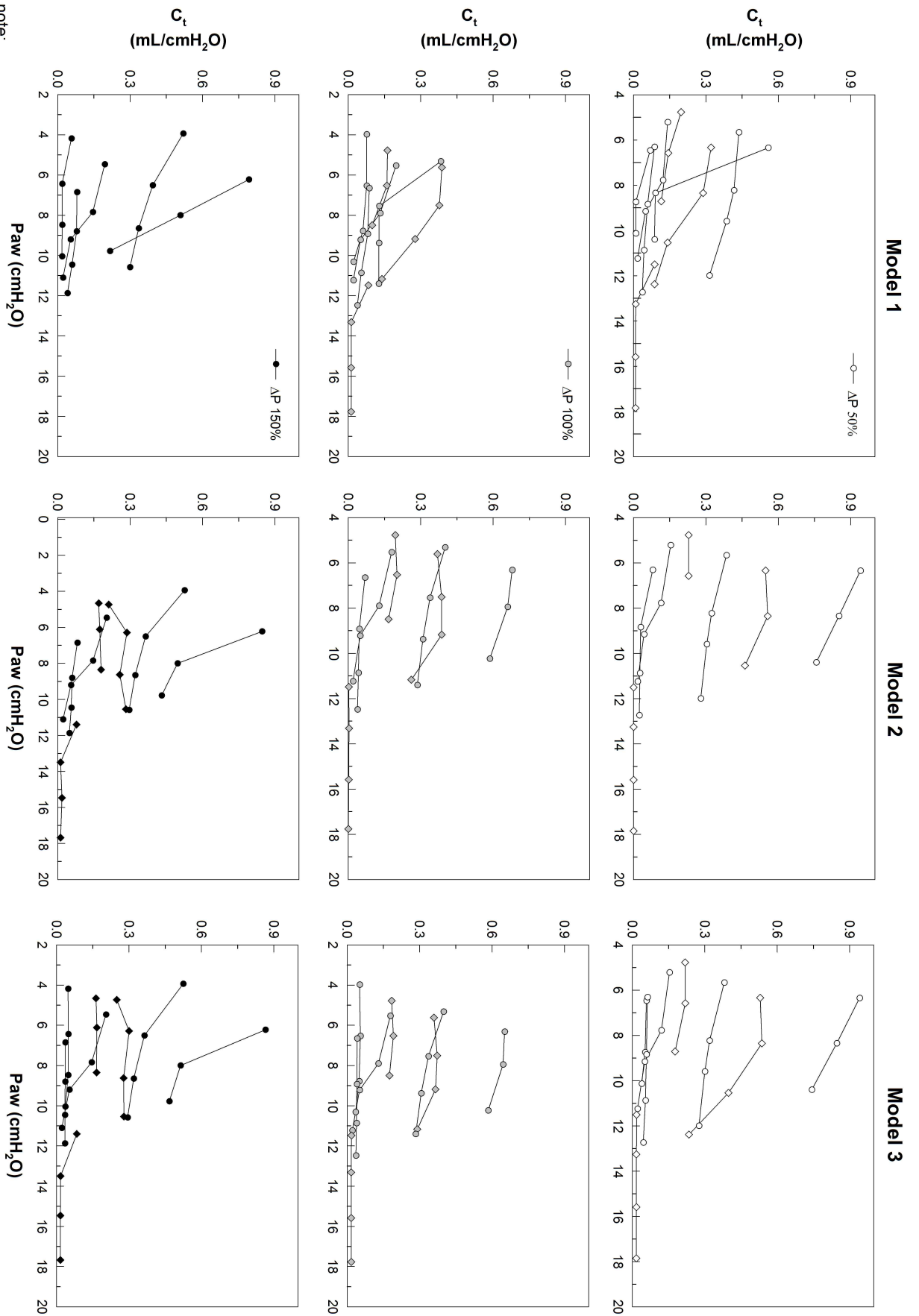
note:
 (1) Diamond symbols are used for the babies if Model 1 fitting at ΔP 150% failed to converge.

Figure 4.6: Summary baby results. Crs.



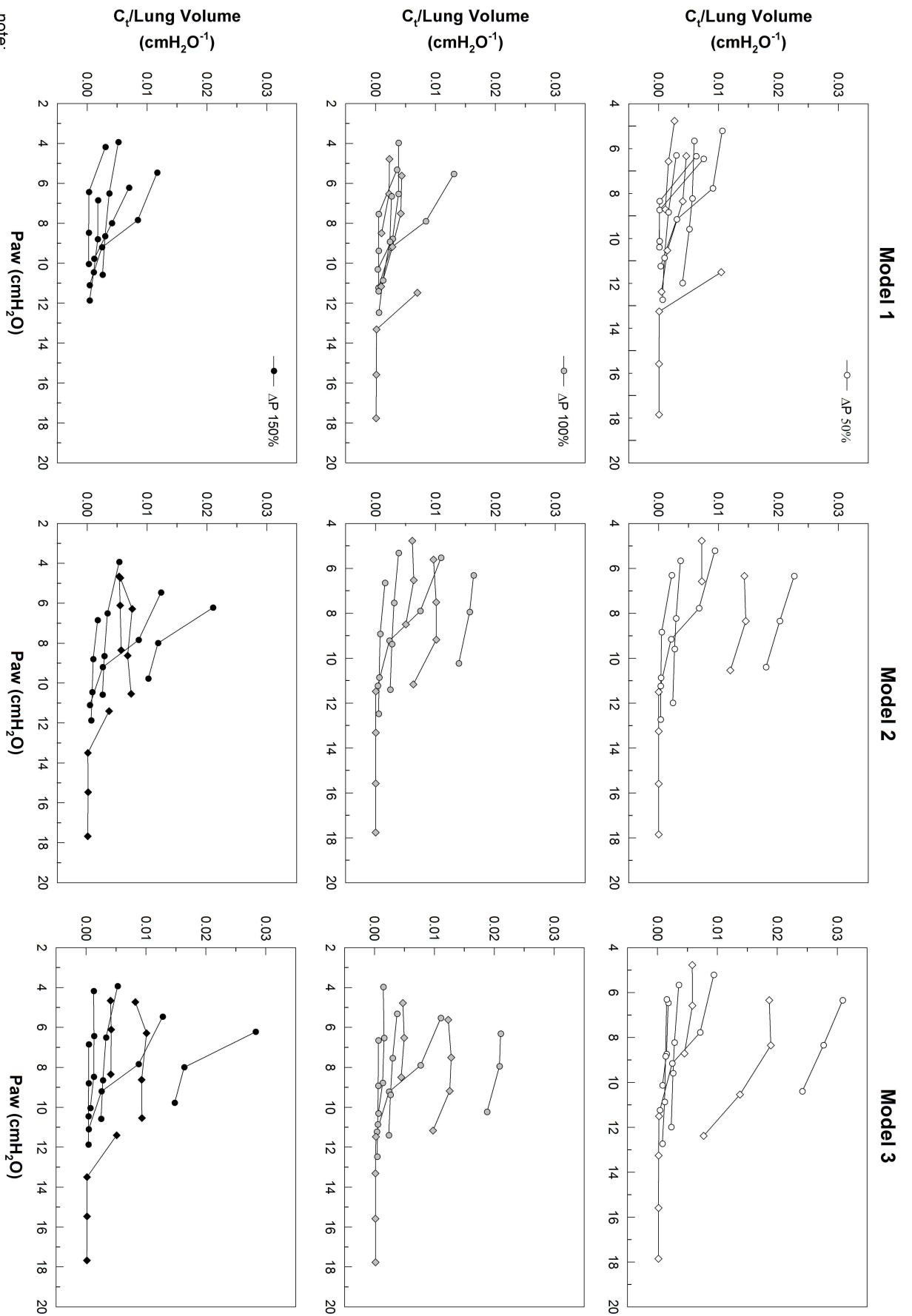
note:
 (1) Diamond symbols are used for the babies if Model 1 fitting at ΔP 150% failed to converge.

Figure 4.7: Summary baby results. Crs/Vo.



note:
 (1) Diamond symbols are used for the babies if Model 1 fitting at ΔP 150% failed to converge.

Figure 4.8: Summary baby results. Ct.



note:
 (1) Diamond symbols are used for the babies if Model 1 fitting at ΔP 150% failed to converge.

Figure 4.9: Summary baby results. Ct/Vo.

C. Averaged Baby Results

In order to point out some general trends among the infants, we can average the results obtained. Figures 4.10 and 4.11 show averaged results for Raw, Crs, Ct, Vo per weight, Crs/Vo and Ct/Vo. Averaging was done between Paw of 6.5 and 10 cmH₂O since that range included most of the infant data. In order to average, we interpolated the results of the infants from Paw 6.5 to 10 cmH₂O with an interval of 0.5 cmH₂O. Figures 17 and 18 only show the means. Means with standard error bars are shown in Appendix D.

There are differences in lung mechanics among individual babies, yet in general a certain behavior is observed for the different elements and models.

Model Selection:

The more data the model fitted, the better and more physiologically sound were the results. Thus fitting along both settings (Models 2 and 3) was better than fitting along Paw alone (Model 1). This was evident with the larger standard deviation obtained while fitting across Paw (Model 1) in comparison to fitting along both settings (Model 2 and 3). This is again, the core of our research. The more data we have and can combine on lung mechanics, the more is it possible to determine the lung elements.

Airway Resistance (Raw):

Raw decreases across Paw but increases with increasing ΔP . The primary could be explained due to the compliant nature of the airways, which expand with increasing Paw. As for the other observation, it captures the non-linear behavior of the airway.

Also, we observe that R_{aw} measured in our Models are very comparable to R_{rs} measured in the 2 Element fit. This strengthens our assumption that tissue resistance could not have contributed considerably to lung mechanics.

Lung Volume (V_o):

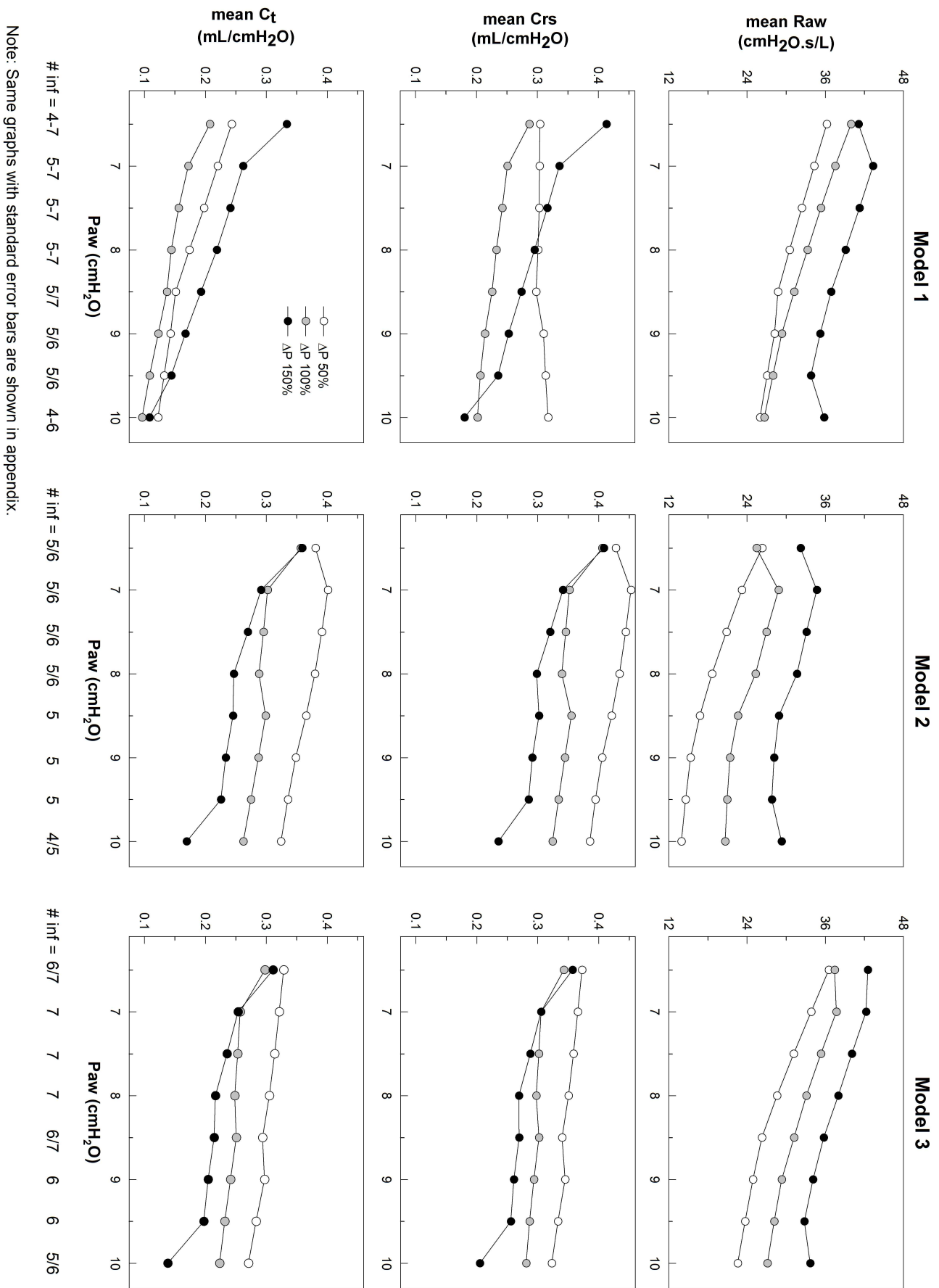
The lung (as well as C_g) behaved as we had expected. It somehow showed a behavior similar to the common sigmoidal curve observed in literature.

Tissue Compliance (C_t):

Interestingly but not surprisingly C_{rs} dropped as P_{aw} increased. As the lung volume increases to its limit the ability of the lung to comply becomes less and less. At smaller lung volumes the lung is still far from its maximum capacity so it's easier to have larger oscillations, which mean higher compliance. This could be one possible reason for this observation.

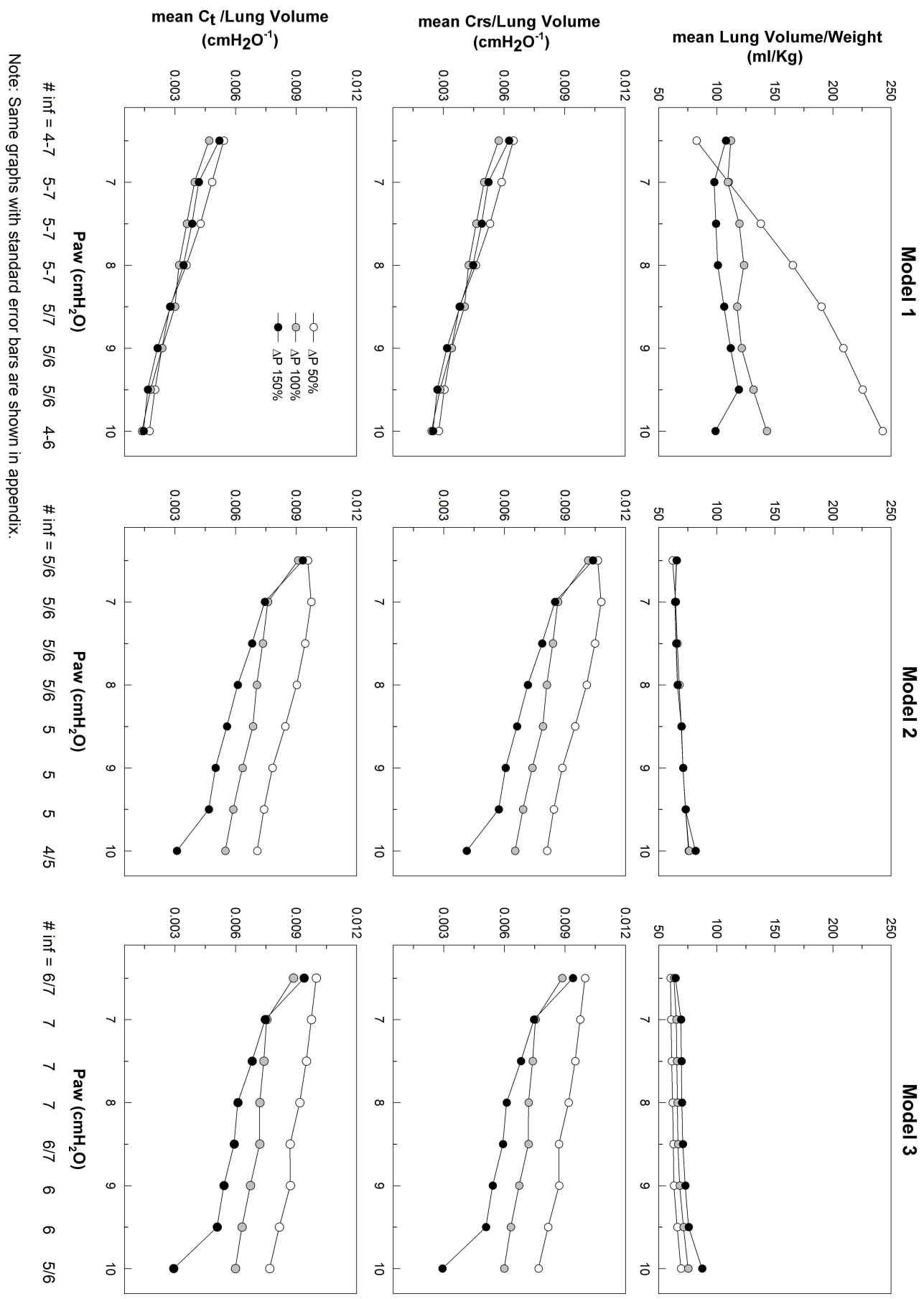
Respiratory Compliance (C_{rs}):

Since C_t was in most of the times higher than C_g , C_{rs} dropped across P_{aw} mimicking C_t . Also notice, that similar to R_{aw} , C_{rs} was close to the summation of C_g and C_t .



Note: Same graphs with standard error bars are shown in appendix.

Figure 4.10: Averaged baby results. Raw, Crs, and Ct.



Note: Same graphs with standard error bars are shown in appendix.

Figure 4.11: Averaged baby results. Vo per weight, Crs/Vo, and Ct/Vo.

D. Literature

Figures 4.12 through 4.14 plot our results (Rrs, Crs, and lung volume) compared to literature against post-conceptual age (PCA), weight and Paw.

Airway Resistance (Raw):

Compared to Baraldi, Choukron, Kalenga et al., our values were less, whereas our values are more comparable to Dorkin et al. This observation is true across age, weight, and Paw. We could have expected such a behavior because resistance drops with frequency. Despite the fact that Kalenga also used HFOV, the single occlusion technique actually measures static resistance, which could explain the discrepancy between his and our results. Also, concerning our data, we can point out, as mentioned earlier, that Raw on average drops with Paw.

Respiratory Compliance (Crs):

As in the case of resistance, Crs values obtained by Dorkin are closest to ours. Our values do share a common range with the other studies (Dimitriou, Baraldi, and Choukron); however, the shared range (0.2-0.65 ml/cmH₂O) lies mainly with values below the study means. Again, this is observed across age, weight and Paw. However, keep in mind that our babies have the least weight and age compared to the other studies.

Lung Volume:

Considering age and weight, we can divide our results into two main groups that seem equally divided. On one hand, we have many values that are much larger

compared to literature. Another portion fits well with literature studies (Kavvadia, Thome, and Vilstrup). This differs when we consider lung findings across Paw. There are some data points that are far away, but the majority of the points fit with most of the studies (Dimitriou, Vilstrup, and Thome). The possibility of this observation could lead us to conclude that Paw might be the biggest determinant of lung volume compared to weight and age.

If we are to consider the autopsy study conducted by Thurlbeck, then we find our values to be close with his measurements (Figures 4.15- 4.17). In fact, even at high Paws (6.5-10 cmH₂O), our lung values are still very much comparable to his especially if we eliminate the baby with the possible leakage (Figure 4.17 Right).

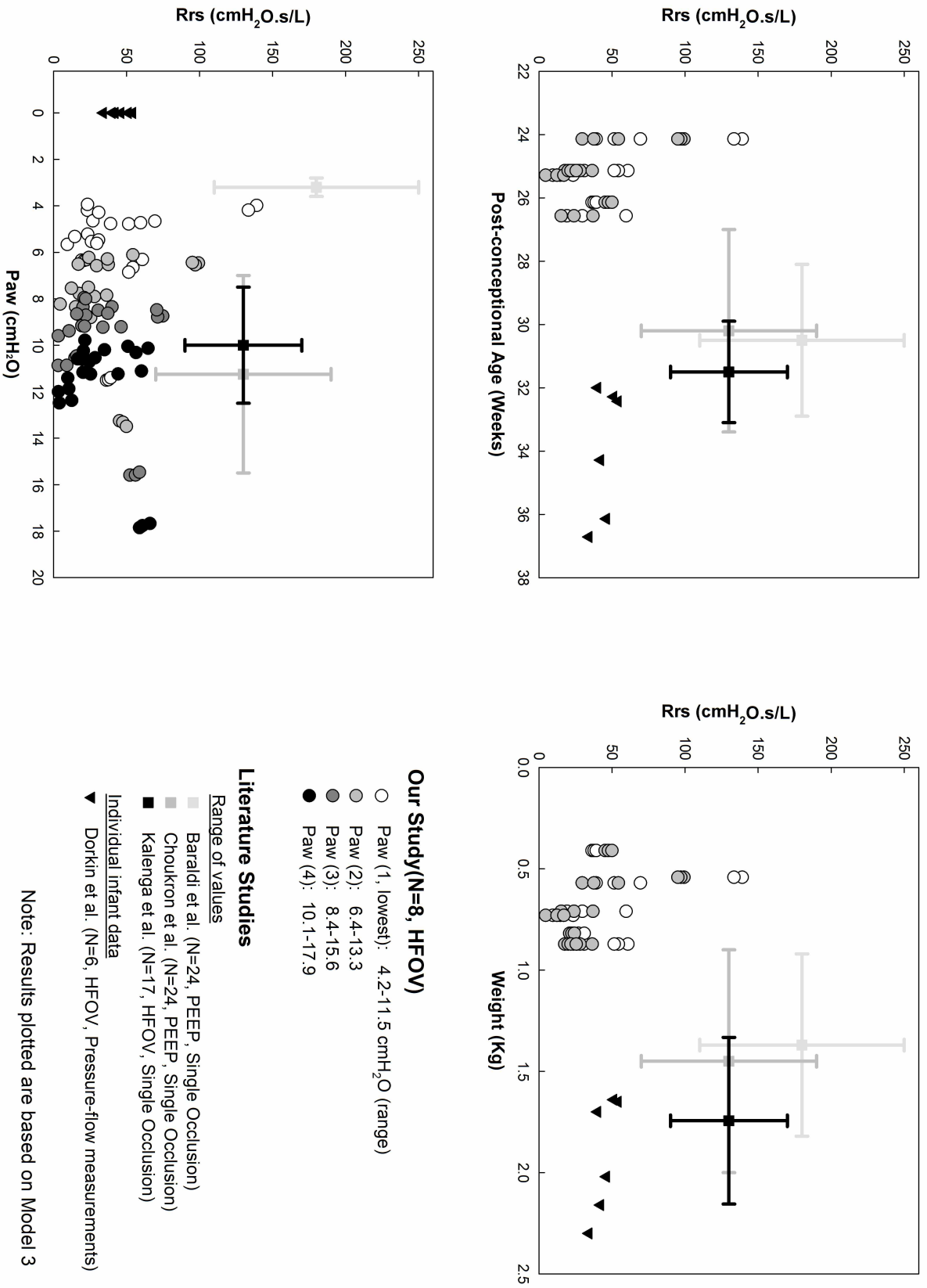


Figure 4.12: Results compared to literature. Resistance.

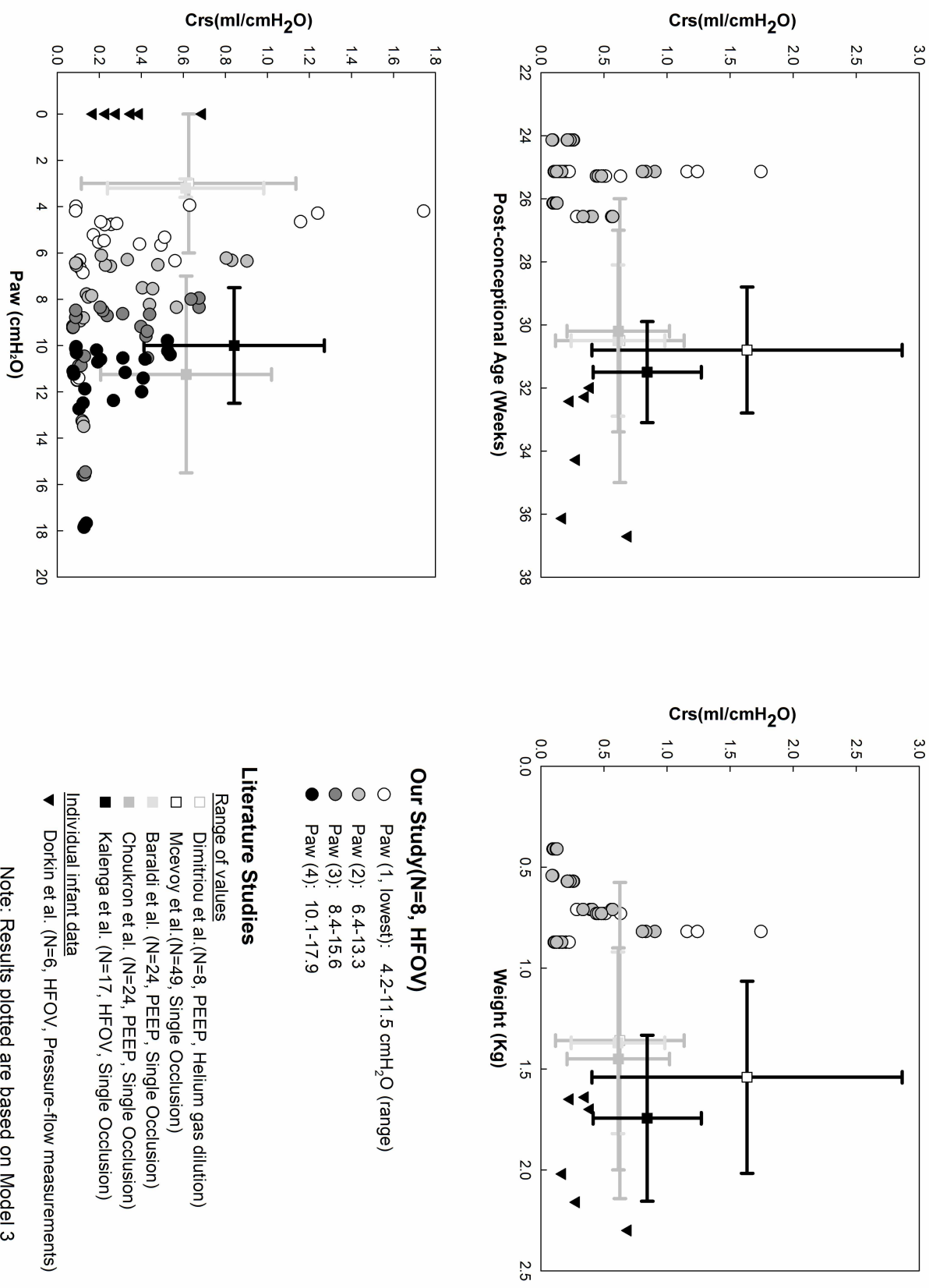


Figure 4.13: Results compared to literature. Compliance.

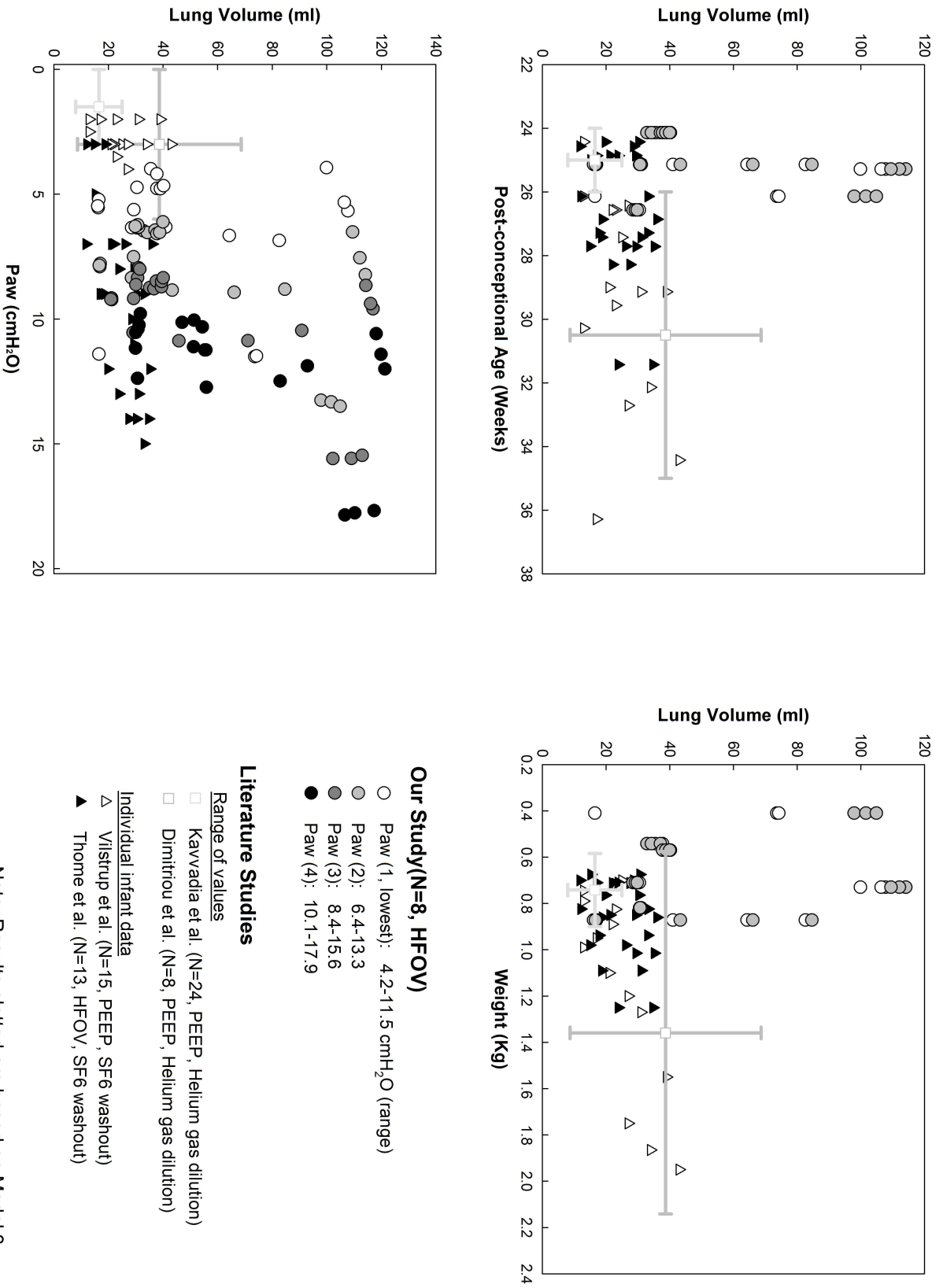


Figure 4.14: Results compared to literature. Lung volume.

Human Lung Growth in Late Gestation and in the Neonate. (Thurlbeck et al. *American Review of Respiratory Disease* 1984)

- Lung volume obtained through autopsy
- 42 infants
- Post-conceptional age (PCA): 19-42 weeks
- CRL: Crown-rump length

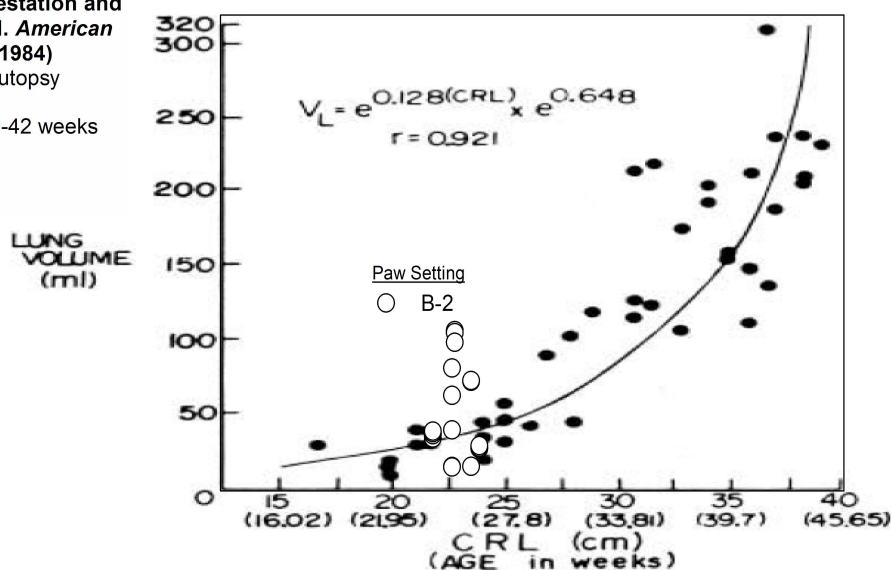


Figure 4.15: Thurlbeck et al. study (above) plots lung volume with respect to crown-lump length (CRL). Study was conducted on 42 infants and volume results were obtained through autopsy [30]. We replicate the plot (below) and plot our lowest Paw values in order to compare.

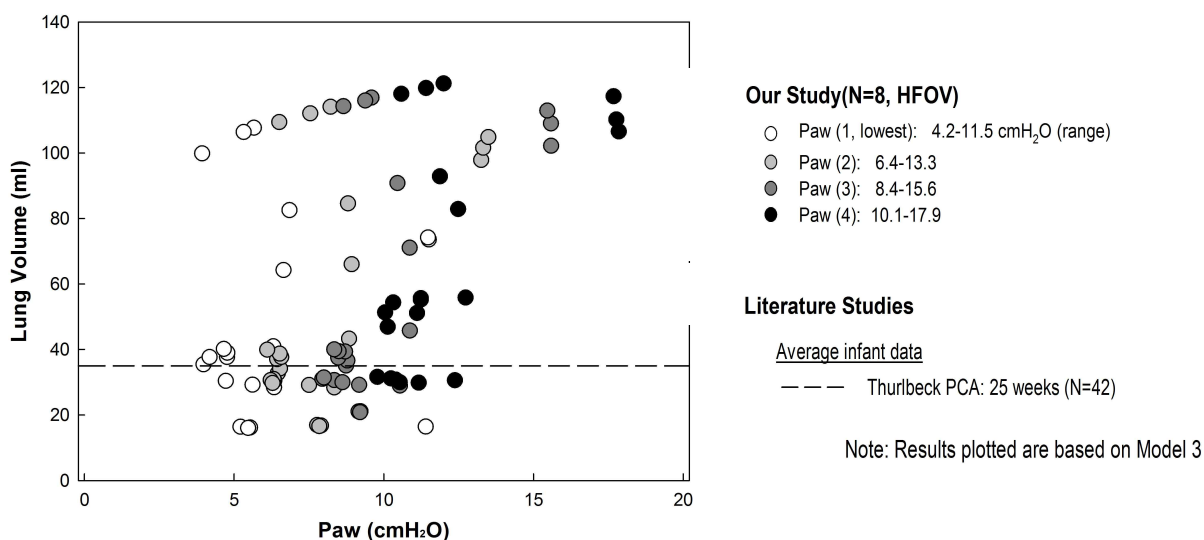


Figure 4.16: Our individual lung volume results compared to Thurlbeck's lung volume estimate equated using our infants' post-conceptional age average.

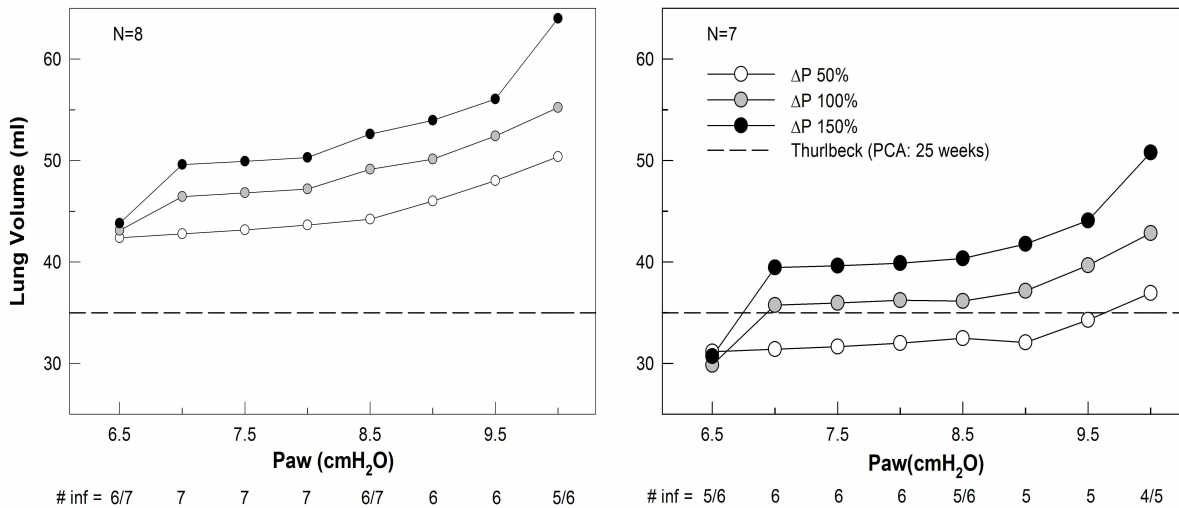


Figure 4.17: Average lung results of all babies are plotted (Left) and compared to Thurlbeck's lung volume estimate equated using our infants' post-conceptual age average. We repeat the process (Right) but eliminate one baby due to leakage possibility. Leakage is suspected because the difference between measured airway pressure and tracheal pressure is relatively high compared to normal cases. This could be an indication of leakage, which causes over-estimates in lung values.

E. Conclusion

There might be few discrepancies, which can be due to the fact that lung volume and mechanical properties are dependent on several parameters and show non-linear behavior; however, we do find a lot of resemblance with literature. In brief, we cannot claim that our method is accurate and has provided the actual respiratory elements without further validation. However, relative to literature, the results obtained so far are in general very comparable. Thus, the method could still be very promising and demands further investigation. In case further studies show the method's accuracy, then we believe that this technique, compared to others, suits best in clinical applications. The advantage is that this technique requires no intervention, occlusion, or tiresome setup. Second, with this technique we can obtain a global perspective on the respiratory

mechanics (airway resistance, compliance, and volume) only through flow and pressure measurements.

F. Future Scope

The results are promising enough in order to further investigate the flow-pressure measurement method. The most important step, in order to further test and verify this technique, is a simple experimental setup capable of mimicking lung mechanics. Lung volume in addition to compliance and resistance should be calculated through our technique and compared with the actual physical values. In addition, the effect of leakage, which is a main concern in this method, should be investigated.

Concerning the modeling, it can be further improved by including the endotracheal tube in the model. This further simplifies clinical use since measuring tracheal pressure is not common. Also, we can use our method and try to find elements that are not identifiable in single fits such as tissue resistance (R_t). In addition, simulation studies could be conducted to study the sensitivity of such elements on the overall results. For instance, we can use a 4-element topology in forward modeling and a 3-element RCC topology in inverse modeling to study the sensitivity of R_t on lung mechanics.

BIBLIOGRAPHY

- [1] Courtney, Sherry E., David J. Durand, Jeanette M. Asselin, Mark L. Hudak, Judy L. Aschner, and Craig T. Shoemaker. "High-Frequency Oscillatory Ventilation versus Conventional Mechanical Ventilation for Very-Low-Birth-Weight Infants." *The New England Journal of Medicine* 347, no. 9 (August 29, 2002): 643–52.
- [2] Weber, Kaye, Sherry E. Courtney, Kee H. Pyon, Gordon Y. Chang, Paresh B. Pandit, and Robert H. Habib. "Detecting Lung Overdistention in Newborns Treated with High-Frequency Oscillatory Ventilation." *Journal of Applied Physiology* 89, no. 1 (July 1, 2000): 364–72.
- [3] Rachana Singh, Sherry E. Courtney, Michael D. Weisner, and Robert H. Habib. "Respiratory Mechanics during High-Frequency Oscillatory Ventilation: A Physical Model and Preterm Infant Study." *Journal of Applied Physiology* 112, no. 7 (April 1, 2012): 1105–13.
- [4] Habib, Robert H., Kee H. Pyon, and Sherry E. Courtney. "Optimal High-Frequency Oscillatory Ventilation Settings by Nonlinear Lung Mechanics Analysis." *American Journal of Respiratory and Critical Care Medicine* 166, no. 7 (October 1, 2002): 950–53.
- [5] Courtney, Sherry E., and Jeanette M. Asselin. "High-Frequency Jet and Oscillatory Ventilation for Neonates: Which Strategy and When?" *Respiratory Care Clinics of North America* 12, no. 3 (September 2006): 453–67.
- [6] Van Genderingen, H.R., A. Versprille, T. Leenhoven, D.G. Markhorst, A.J. van Vught, and R.M. Heethaar. "Reduction of Oscillatory Pressure along the Endotracheal Tube Is Indicative for Maximal Respiratory Compliance during High-Frequency Oscillatory Ventilation: A Mathematical Model Study." *Pediatric Pulmonology* 31, no. 6 (June 1, 2001): 458–63.

- [7] Casserly, Brian, F. Dennis Mccool, Jigme M. Sethi, Eyad Kavar, Richard Read, and Mitchell M. Levy. “A Method for Determining Optimal Mean Airway Pressure in High-Frequency Oscillatory Ventilation.” *Lung* 191, no. 1 (February 2013): 69–76.
- [8] Yamada, Y., J. G. Venegas, D. J. Strieder, and C. A. Hales. “Effects of Mean Airway Pressure on Gas Transport during High-Frequency Ventilation in Dogs.” *Journal of Applied Physiology* 61, no. 5 (November 1, 1986): 1896–1902.
- [9] Van Kaam, Anton H. “Bedside Parameters to Optimize Lung Volume during High-Frequency Oscillatory Ventilation*.” *Critical Care Medicine* 41, no. 1 (January 2013): 365–66.
- [10] Torres, Adalberto, and John K. Rendle. “Measuring Lung Volume During High-Frequency Oscillatory Ventilation in Neonates—Ready for Prime Time?.” *Critical Care Medicine* 41, no. 11 (November 2013): 2649–50.
- [11] Dellacà, Raffaele L., Emanuela Zannin, Maria L. Ventura, Giulio Sancini, Antonio Pedotti, Paolo Tagliabue, and Giuseppe Miserochi. “Assessment of Dynamic Mechanical Properties of the Respiratory System During High-Frequency Oscillatory Ventilation*.” *Critical Care Medicine* 41, no. 11 (November 2013): 2502–11.
- [12] Vilstrup, C. T., L. J. Bjorklund, A. Larsson, B. Lachmann, and O. Werner. “Functional Residual Capacity and Ventilation Homogeneity in Mechanically Ventilated Small Neonates.” *Journal of Applied Physiology* 73, no. 1 (July 1, 1992): 276–83.
- [13] Kavvadia, V., A. Greenough, G. Dimitriou, and Y. Itakura. “Lung Volume Measurements in Infants with and without Chronic Lung Disease.” *European Journal of Pediatrics* 157, no. 4 (March 1998): 336–39.

- [14] Wood, Brian, Padmani Karna, and Alicia Adams. "Specific Compliance and Gas Exchange during High-Frequency Oscillatory Ventilation." *Critical Care Medicine July 2002* 30, no. 7 (2002): 1523–27.
- [15] Klaus, M., W. H. Tooley, K. H. Weaver, and J. A. Clements. "Lung Volume in the Newborn Infant." *Pediatrics* 30, no. 1 (July 1, 1962): 111–16.
- [16] Dimitriou, G., A. Greenough, and B. Laubscher. "Appropriate Positive End Expiratory Pressure Level in Surfactant-Treated Preterm Infants." *European Journal of Pediatrics* 158, no. 11 (October 1, 1999): 888–91.
- [17] Giovanni Vento, Milena Tana, Chiara Tirone, Claudia Aurilia, Alessandra Lio, Sarah Perelli, Cinzia Ricci, and Costantino Romagnoli. "Unexpected Effect of Recruitment Procedure on Lung Volume Measured by Respiratory Inductive Plethysmography (RIP) during High Frequency Oscillatory Ventilation (HFOV) in Preterm Neonates with Respiratory Distress Syndrome (RDS)." *Journal of Maternal-Fetal and Neonatal Medicine* 24, no. S1 (October 2011): 159–62.
- [18] Thome Ulrich, Andreas Topfer, Peter Shaller, and Frank Pohland. "Effect of Mean Airway Pressure on Lung Volume during High-Frequency Oscillatory Ventilation of Preterm Infants." *American Journal of Respiratory and Critical Care Medicine* 157, no. 4 (April 1, 1998): 1213–18.
- [19] Yuksel, B., and A. Greenough. "Airways Resistance and Lung Volume before and after Bronchodilator Therapy in Symptomatic Preterm Infants." *Respiratory Medicine* 88, no. 4 (April 1994): 281–86.
- [20] Radford, M. "Measurement of Airway Resistance and Thoracic Gas Volume in Infancy." *Archives of Disease in Childhood* 49, no. 8 (August 1974): 611–15.
- [21] Cindy McEvoy, Diane Schilling, Dawn Peters, Carrie Tillotson, Patricia Spitale, Linda Wallen, Sally Segel, Susan Bowling, Michael Gravett, and Manuel Durand.

“Respiratory Compliance in Preterm Infants after a Single Rescue Course of Antenatal Steroids: A Randomized Controlled Trial.” *American Journal of Obstetrics and Gynecology* 202, no. 6 (June 2010): 544.e1–544.

[22] Eugenio Baraldi, Andrea Pettenazzo, Marco Filippone, G. Piero Magagnin, O. Sergio Saia, and Franco Zacchello. “Rapid Improvement of Static Compliance after Surfactant Treatment in Preterm Infants with Respiratory Distress Syndrome.” *Pediatric Pulmonology* 15, no. 3 (March 1, 1993): 157–62.

[23] Choukroun, M. L., B. Llanas, H. Apere, M. Fayon, R. I. Galperine, H. Guenard, and J. L. Demarquez. “Pulmonary Mechanics in Ventilated Preterm Infants with Respiratory Distress Syndrome after Exogenous Surfactant Administration: A Comparison between Two Surfactant Preparations.” *Pediatric Pulmonology* 18, no. 5 (November 1, 1994): 273–78.

[24] Masendu Kalenga, Oreste Battisti, Anne François, Jean-Paul Langhendries, Dale R. Gerstmann, and Jean-Marie Bertrand. “High-Frequency Oscillatory Ventilation in Neonatal RDS: Initial Volume Optimization and Respiratory Mechanics.” *Journal of Applied Physiology* 84, no. 4 (April 1, 1998): 1174–77.

[25] Dorkin, H L, A R Stark, J W Werthammer, D J Strieder, J J Fredberg, and I D Frantz. “Respiratory System Impedance from 4 to 40 Hz in Paralyzed Intubated Infants with Respiratory Disease.” *Journal of Clinical Investigation* 72, no. 3 (September 1983): 903–10.

[26] Baswa, S., H. Nazeran, P. Nava, B. Diong, and M. Goldman. “Evaluation of Respiratory System Models Based on Parameter Estimates from Impulse Oscillometry Data,” 2958–61. IEEE, 2005.

[27] Lutchen, K.R., and K.D. Costa. “Physiological Interpretations Based on Lumped Element Models Fit to Respiratory Impedance Data: Use of Forward-Inverse

Modeling.” *IEEE Transactions on Biomedical Engineering* 37, no. 11 (November 1990): 1076–86.

[28] David W. Kaczka, Edward P. Ingenito, Bela Suki, and Kenneth R. Lutchen. “Partitioning Airway and Lung Tissue Resistances in Humans: Effects of Bronchoconstriction.” *Journal of Applied Physiology* 82, no. 5 (May 1, 1997): 1531–41.

[29] Lutchen, K. R., J. R. Everett, and A. C. Jackson. “Impact of Frequency Range and Input Impedance on Airway-Tissue Separation Implied from Transfer Impedance.” *Journal of Applied Physiology* 74, no. 3 (March 1, 1993): 1089–99.

[30] Langston, C., K. Kida, M. Reed, and W. M. Thurlbeck. “Human Lung Growth in Late Gestation and in the Neonate.” *The American Review of Respiratory Disease* 129, no. 4 (April 1984): 607–13.

APPENDIX

A. Other Research Results

Table A.1: Lung volume literature summary.

Name Of Study/Paper	Number of Patients	Patient Information	Weight (kg)	Method To Determine FRC	Pressure and Frequency	Further Information	FRC (ml)	FRC/weight (ml/kg)	Journal/Year Published
Functional Residual Capacity and Ventilation Homogeneity in Mechanically Ventilated Small Neonates (T. Vilstrup L. Bjorklund A. Larsson B. Lachmann O. Werner)	15	Neonates with mild to moderate RDS	0.7-1.95	SF6 washout method	2-4 cmH ₂ O PEEP	Most infants were given a muscle relaxant	13-43	22	American Physiological Society 1992
Lung Volume Measurements in Infants with and without Chronic Lung Disease (Kavvadia A. Greenough G. Dinitrou Y. Iakura)	24	Divided into three groups -Group 1: CLD <27 weeks GA -Group 2: CLD >27 weeks GA -Group 3: Control (without CLD)	0.584-1.558	Helium Gas Dilution	<=3 cmH ₂ O PEEP	Few infants were given surfactant	8-56	14-36	Eur J Pediatr 1998
Lung Volume in the Newborn Infant (M. Klaus H. Tooley H. Weaver A. Clements)	37	Infants aged 7 minutes to 17 days.	2.3-4.12	Based on Boyle's Law. (V=(Pb-PH2O)/ΔV/AP - Vn) Measurements needed are barometric pressure, changes in lung volume, alveolar pressure, and volume of mask dead space.	NA	No infant showed RDS after birth. All infants healthy. Some babies were born vaginally others cesarean.	38-145	26.5 (vaginal) 24.7 (cesarian)	Pediatrics 1962
Measurement of Thoracic Gas Volume in the Newborn Infant (M. Auld M. Nelson B. Cherry J. Rudolph A. Smith)	27	10 infants normal 7 infants mild RDS 10 infants RDS. Study lasted from birth (hours) till days.	2.03-3.77	Plethysmograph (Boyle's Law)	NA	Measurements were taken also during RDS recovery	normal: 46-137 mild RDS: 56-142 RDS: 37-136	normal: 36 mild RDS: 38 RDS: 27	Journal of Clinical Investigation 1963
Appropriate Positive End Expiratory Pressure Level in Surfactant-treated Preterm Infants (G. Dinitrou A. Greenough B. Laubsther)	8	Eight premature infants with RDS and with a median gestational age of 28 weeks.	0.576 -2.142	Helium Gas Dilution	0, 3 and 6 cmH ₂ O PEEP	Study was done after surfactant was applied to preterm infants	5-69 ml	0 PEEP: 16 3 PEEP: 18.3 6 PEEP: 22.3	Eur J Pediatr 1999
Unexpected Effect of Recruitment Procedure on Lung Volume Measured by Plethysmography During High Frequency Oscillatory Ventilation in Preterm Neonates with Respiratory Distress Syndrome (G. Venio M. Tana C. Tirone C. Aurilia A. Lio S. Ferilli C. Ricci C. Romagnoli)	4		0.978±0.188	Plethysmography (Respiratory Inductive Plethysmography)	12-18cm H ₂ O CDP	Study was able to identify changes in lung volume but not the actual value. Study showed FRC drop at high CDP (around 15cm H2O)	NA	NA	Journal of Maternal-Fetal and Neonatal Medicine 2011
Effect of Mean Airway Pressure on Lung Volume During High-Frequency Oscillatory Ventilation of Preterm Infants (U. Thome A. Topper P. Schaller F. Pohlandt)	13	13 preterm infants with RDS	0.63-1.14	Sulfur Hexafluoride washout method SF6	3-14 cmH ₂ O at 10Hz		14-46 ml	14.7-45.4 depending on MAP	Journal of Respiratory Critical Care Medicine 1998

Table A.2: Airway resistance literature summary.

Name Of Study/Paper	Number of Patients	Patient Information	Weight (Kg)	Method To Determine Raw	Pressure and Frequency	Further Information	Raw (cmH ₂ O.s/L)	Year Published
Airways resistance and lung volume before and after bronchodilator therapy in symptomatic preterm infants. (B.Yuksel A.Greenough)	34	study conducted at age of 6-10 months.	0.656-1.93 at birth	Plethysmography	NA	Infants were born preterm and followed up. Bronchodilator treatment was applied	pre-treatment: 22-100 (mean:43.8) post-treatment: 19-63 (mean 33.6)	Respiratory Medicine 1994
Measurement of airway resistance and thoracic gas volume in infancy (M.Radford)	21	normal infants aged 1 to 10 months	approximately 3 to 7	Plethysmography	NA	Study did not consider the flow dependence of resistance. I.e: they compared resistance values from different flows.	22.6±8.9	Archives of Disease in Childhood 1974

Table A.3: Compliance literature summary. Values of respiratory resistance are also included when available.

Name Of Study/Paper	Number of Patients	Patient Information	Weight (Kg)	Method To Determine Crs	Pressure and Frequency	Further Information	Crs (mL/cmH ₂ O/Kg)	FRC/Weight (ml/Kg)	Year Published
Respiratory compliance in preterm infants after a single rescue course of antenatal steroids: a randomized controlled trial (C.McEvoy, D.Schilling D.Peters et al.)	AS: 49 Placebo: 49	Preterm Infants. GA at birth AS: 31.9±3.3 Placebo: 32.3±2.9	AS: 1.806±0.778 Placebo: 1.83±0.657	Crs: Single Breath Occlusion Technique FRC: Nitrogen Washout Method	NA	Randomized trial. Some mothers were given steroids (AS) others a placebo. Measurements were taken no more than 72 hours after birth	AS: 1.21±0.53 Placebo: 1.01±0.51	AS: 24.8±8.8 Placebo: 22.0±7.9	American Journal of Obstetrics and Gynecology 2010
Rapid Improvement of Static Compliance After Surfactant Treatment in Preterm Infants With Respiratory Distress Syndrome (E.Baraldi, A. Pettenzzo M. Filippone G. Piero, O.Sergio F.Zacchello)	24	Two Groups Early and Late GA early: 29.3±2.2 late: 31.7±1.8	1.37±0.45	Single Breath Occlusion Technique	PEEP: 3.2±0.4 cmH ₂ O PIP: 23±3.8cmH ₂ O	Rrs was also measured: 0.13±0.07 cmH ₂ O/ml/s	0.40 ± 0.14		Pediatric Pulmonology 2005
Pulmonary Mechanics in Ventilated Preterm Infants With Respiratory Distress Syndrome After Exogenous Surfactant Administration: A Comparison Between Two Surfactant Preparations (M.Choukron B.Lianas, H.Agape M.Fayon R.Galperine H.Guenard J.Demarquez)	24	All preterm infants have RDS GA at birth: 27-33.4 weeks	0.9-2	Passive expiratory flow-volume method.	7-15.5 cmH ₂ O PEEP	Objective was to compare two surfactants. Rrs was also measured: 0.07-0.19 cmH ₂ O/ml/s	0.23-0.51		Pediatric Pulmonology 1994
High-frequency oscillatory ventilation in neonatal RDS: initial volume optimization and respiratory mechanics. (M.Kalenga, O Battisti A. Francois, J.Langhendries D.Gerstmann, J.Bertrand)	17	Premature infants with RDS GA at birth: 31.5±1.6 weeks	1.744±0.411	Single Occlusion Technique	7.5-12.5 cmH ₂ O at 10 Hz	Crs was inversely related to mean airway pressure and increased pressure amplitude Study was conducted hours after birth Rrs was also measured: 0.13±0.04 cmH ₂ O/ml/s	0.45 ± 0.14		Journal of Applied Physiology 1998
Respiratory System Impedance from 4 to 40 Hz in Paralyzed Intubated Infants with Respiratory Disease (H.Darkin A.Stark J.Werthammer D.Streder J.Fredberg I.Frantz)	6	All infants had RDS. GA at birth: 31-36 weeks	1.91±0.26	Pressure Flow Measurements (Impedance Analysis)	NA	Rrs was also measured: 22-34 cmH ₂ O/ml/s Irs was measured: 0.0056-0.047cmH ₂ O/l/s ² Resonant frequency: 13-23 Hz	0.22-0.68 ml cmH ₂ O		Journal of Clinical Investigation 1983

B. Data Selection and Preparation for Fitting

Figure B.1 shows baby data taken at one Paw three ΔP settings for two different babies. In the first case, we observe high reproducibility of data, whereas in the other (baby 7) pressure data probably includes interferences. Those could be due to heartbeat, breathing cycle, noise or other sources. Even after filtering, the effect of these interferences was not completely removed. In that case, we went over the data and eliminated these interferences manually. Figures B.2, B.3, and B.4 show how data is collected across settings. It shows the different data used in the 2 Element fit, Model 1, Model 2, and Model 3.

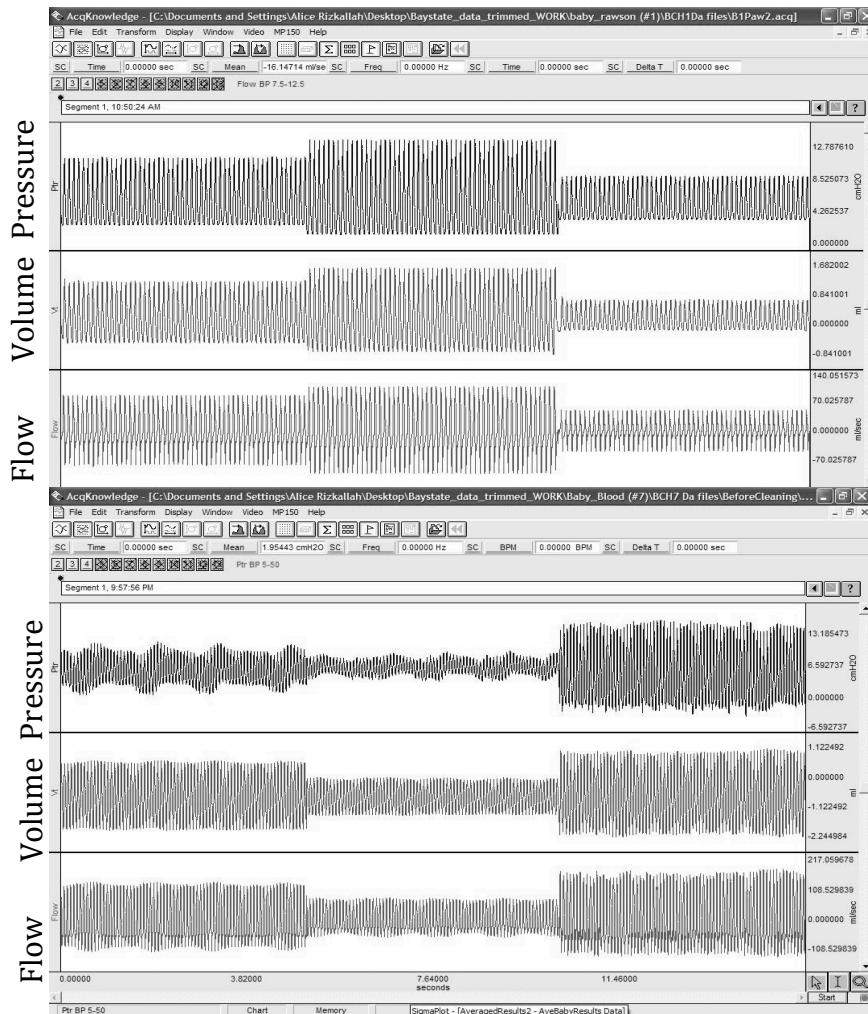


Figure B.1: Measurements at one Paw 3 ΔP settings taken for two babies. Notice how the signal could be distorted.

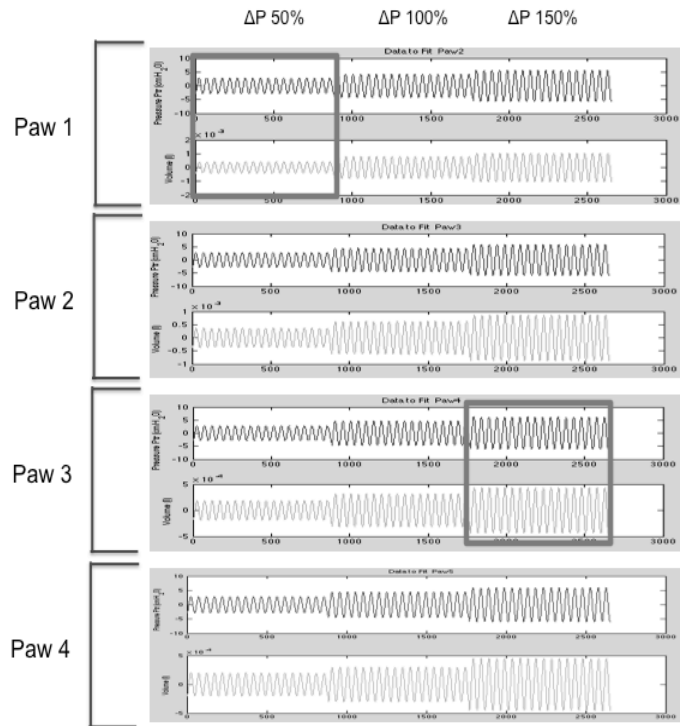


Figure B.2: Pressure (1st signal) and Volume (2nd signal) measurements taken at 4 Paws and 3 ΔP settings. In a 2 Element fit every setting is studied separately. In total we have 24 fits.

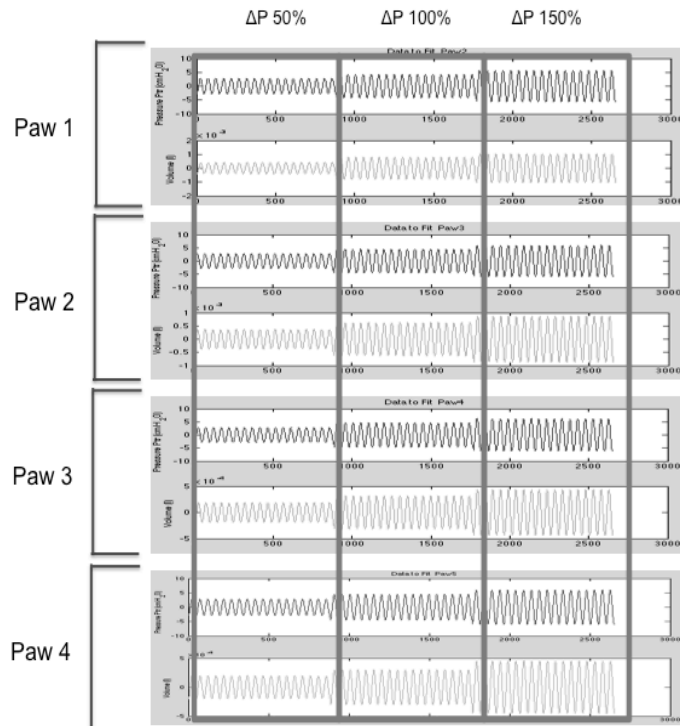


Figure B.3: Pressure (1st signal) and Volume (2nd signal) measurements taken at 4 Paws and 3 ΔP settings. When fitting across Paw (Model 2), we combine data at every ΔP setting. In total, we fit 3 times.

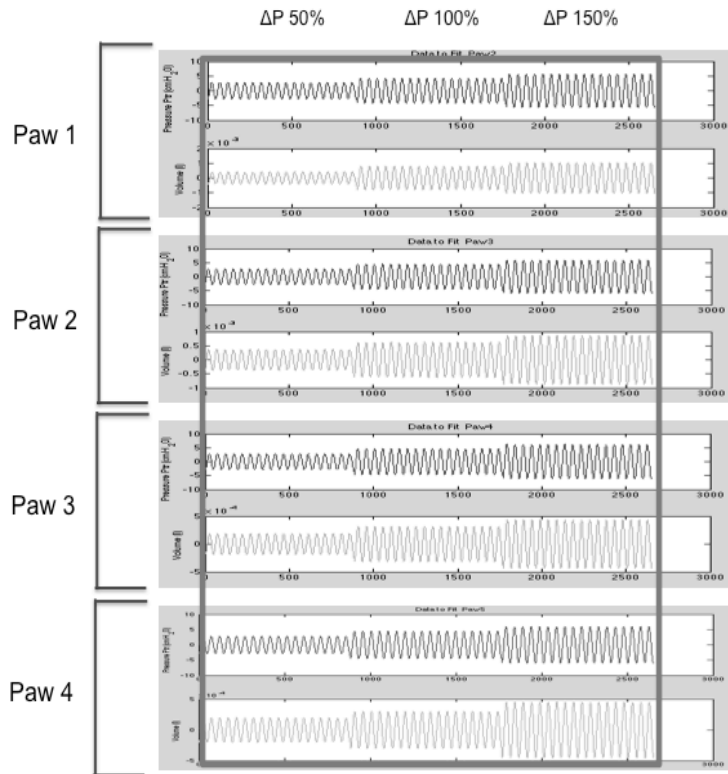


Figure B.4: Pressure (1st signal) and Volume (2nd signal) measurements taken at 4 Paws and 3 ΔP settings. When fitting across all settings (Model 2 and 3) all the data is taken. Thus only one fit is needed.

C. Baby and Model Guide

Summarized is data related to baby demographics, model information, and HFOV settings.

Table C.1: Baby demographics

Demographics						
Baby*	Gender	Birth Weight (Kg)	Study Weight (Kg)	GA (weeks)	Age (days)	Diagnosis**
1	Male	0.84	0.872	25	1	RDS, IVH
2	Female	0.542	0.542	24	1	RDS,sepsis
4	Female	0.41	0.41	26	1	RDS, IUGR
5	Male	0.819	0.819	25	1	RDS
6	Female	0.57	0.57	24	1	RDS,PDA
7	Female	0.788	0.71	26	4	RDS
9	Female	0.73	0.69	25	2	RDS,PDA,PE
10	Male	0.77	0.73	25	1	RDS, PDA
$\mu \pm \sigma$		0.6836±0.0553	0.6679±0.0539	25.0±0.2673	1.5±0.378	

*Baby 3 not analyzed due to leakage

*Baby 8 not analyzed due to flow sensor failure

**RDS= Respiratory Distress Syndrome

**IVH= Intra-Ventricular Hemorrhage

**IUGR= Intra-uterine Growth Retardation

**PDA = Patent Ductus Arteriosus

**PE= Pericardial Effusion

Table C.2: Model information.

Model Information	
2 Element RC Fit	Fitted each setting alone (single Paw, single ΔP setting)
Model 1	Fitted multiple Paws with a single ΔP setting.
Model 2	Fitted multiple Paws with the three different ΔP settings. Assumed lung volume independent of ΔP .
Model 3	Fitted multiple Paws with the three different ΔP settings. Allowed lung volume to vary with ΔP .

Table C.3: Data Fitted

Fitting Information			
Baby	Data quality	Cycles fitted per setting	Band pass filter applied (Hz)
1	Good	20	5-15
2	Poor	9	7.5-12.5
4	Poor	10	7.5-12.5
5	Fair	10	11.25-18.75
6	Good	20	11.25-18.75
7	Good	20	11.25-18.75
9	Good	20	11.25-18.75
10	Good	20	11.25-18.75
1 PS	Good	20	5-15

Table C.4: HFOV settings.

HFOV Settings (Paw, ΔP) and Measured Tidal Volume Amplitude ΔV										
Baby	F. (Hz)	ΔP 50%			ΔP 100%			ΔP 150%		
		Paw (cmH ₂ O)	ΔP (cmH ₂ O)	ΔV (mLiter)	Paw (cmH ₂ O)	ΔP (cmH ₂ O)	ΔV (mLiter)	Paw (cmH ₂ O)	ΔP (cmH ₂ O)	ΔV (mLiter)
1	10	5.22	5.73	0.84	5.54	8.41	1.58	5.47	11.46	2.11
		7.78	5.69	0.75	7.91	9.18	1.26	7.85	12.04	1.75
		9.16	5.80	0.39	9.23	9.35	0.64	9.21	12.50	0.88
		11.24	5.83	0.41	11.24	9.04	0.61	11.11	12.03	0.91
2	10				3.98	5.99	0.37	4.19	7.87	0.49
		6.47	4.22	0.28	6.54	5.08	0.43	6.44	7.27	0.51
		8.74	4.49	0.32	8.79	5.34	0.38	8.48	6.59	0.53
		10.13	3.74	0.31	10.32	4.90	0.41	10.05	6.54	0.55
4	10	11.51	5.78	0.54	11.48	7.06	0.62	11.40	8.73	0.84
		13.26	5.87	0.55	13.32	7.20	0.71	13.50	8.29	1.08
		15.59	4.59	0.57	15.59	6.82	0.87	15.47	8.63	0.98
		17.85	4.53	0.47	17.77	5.60	0.66	17.68	8.28	0.84
5	15	4.19	2.04	0.86	4.65	4.26	1.30	4.28	5.31	1.75
		6.35	2.15	0.78	6.32	3.63	1.25	6.23	5.04	1.73
		8.35	2.01	0.74	7.95	3.05	1.25	8.00	4.75	1.72
		10.40	2.27	0.73	10.24	3.40	1.19	9.79	5.56	1.68
6	15	4.77	2.22	0.38	4.78	3.75	0.53	4.66	5.81	0.64
		6.58	2.22	0.39	6.53	3.31	0.52	6.11	5.33	0.68
		8.71	2.05	0.38	8.50	3.30	0.52	8.35	4.72	0.73
		10.60	2.16	0.39	10.71	3.11	0.52	10.20	4.73	0.67
7	15	6.34	3.72	0.99	5.62	7.06	1.80	4.73	17.31	2.25
		8.35	3.63	1.03	7.51	6.59	1.97	6.29	10.70	2.53
		10.54	4.48	0.95	9.18	6.55	1.80	8.63	12.66	2.29
		12.38	4.14	0.96	11.17	6.93	1.79	10.54	10.07	2.48
9	15	5.06	2.64	1.83	4.72	5.46	2.76	4.26	10.69	2.82
		7.10	3.65	1.50	6.71	5.99	2.56	5.92	8.02	3.92
		9.16	3.38	2.27	8.51	5.91	3.17	8.18	8.97	4.75
					10.49	5.26	4.16	10.26	7.14	7.15
10	15	5.67	3.79	1.54	5.33	6.44	2.43	3.94	9.49	3.49
		8.23	3.16	1.35	7.55	6.76	2.23	6.51	8.84	3.20
		9.60	3.09	1.37	9.39	6.30	2.28	8.66	8.68	3.08
		12.00	3.50	1.32	11.41	6.00	2.18	10.59	8.81	2.87
1 PS*	10	6.31	6.30	0.66	6.66	11.58	1.29	6.86	16.25	1.78
		8.84	6.78	0.64	8.93	11.99	1.36	8.81	16.76	1.98
		10.88	6.90	0.62	10.87	12.50	1.21	10.46	17.84	2.03
		12.74	6.48	0.65	12.49	11.88	1.28	11.88	15.85	2.25

*PS: Post-Surfactant. Baby 1 was analyzed prior to surfactant treatment and after treatment.

When we fit across P_{aw} , we combine and fit each ΔP alone. Figure 29 shows the data fitted at ΔP 150%. As suggested earlier, in this type of fitting we should have one ΔP . However, we notice for some babies this is not the case. The baby shown for example starts at a much higher ΔP than the other three settings. It could be that the physician observed difficulty in breathing and so the setting was altered. In any case, the drawback becomes that the model (Model 1) does not account for this variation.

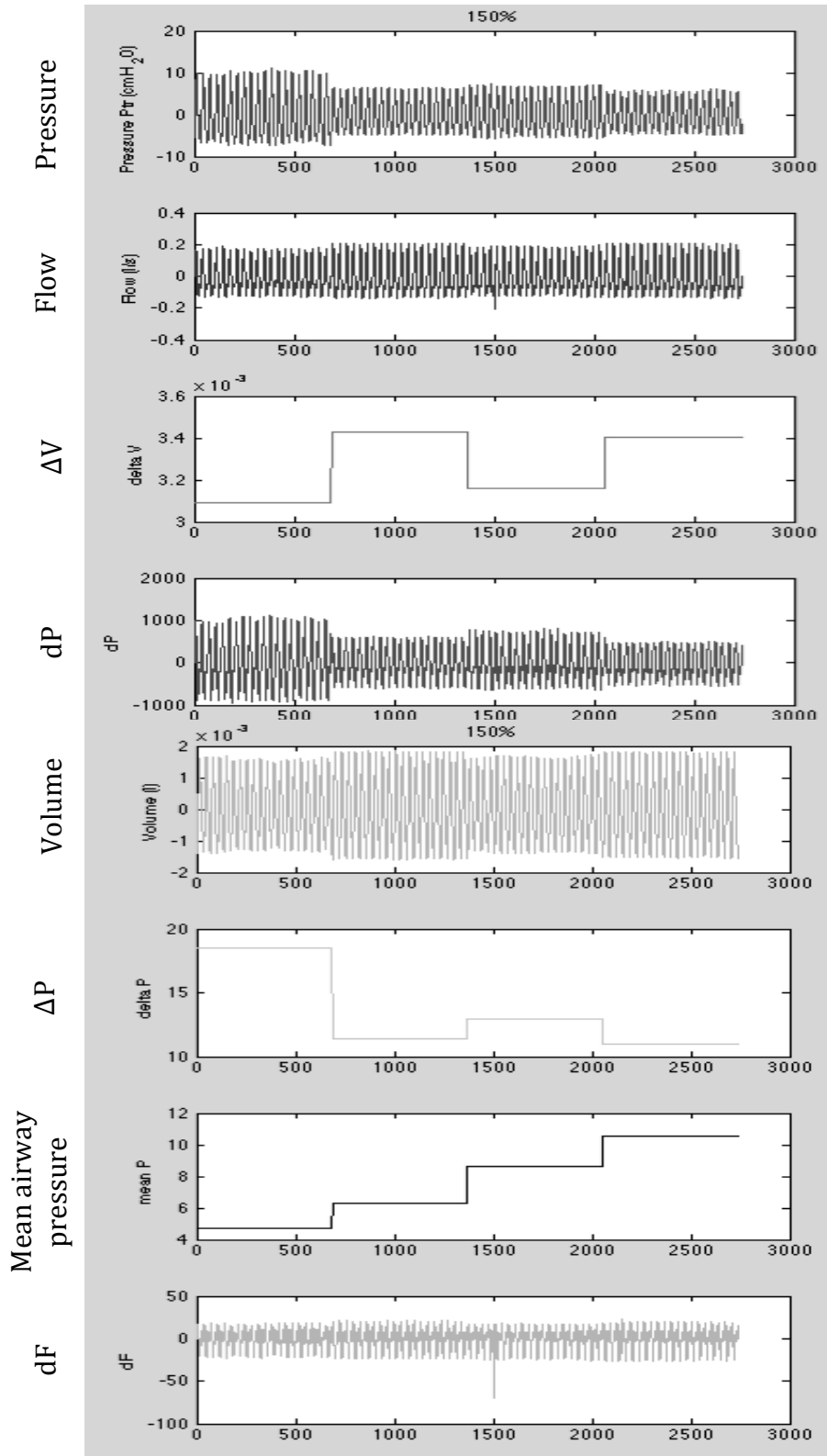


Figure C.1: Example of data while fitting across ΔP . dP is pressure derivative. dF is flow derivative.

When we fit across ΔP and P_{aw} together this is no longer the problem since the model (Model 2 and 3) accepts variation in ΔP (Figure 30). Finally, also notice that the mean, for example in this baby, is not uniform even across ΔP (i.e.: the protocol keeps a constant P_{aw} across three different ΔP s before increasing P_{aw})

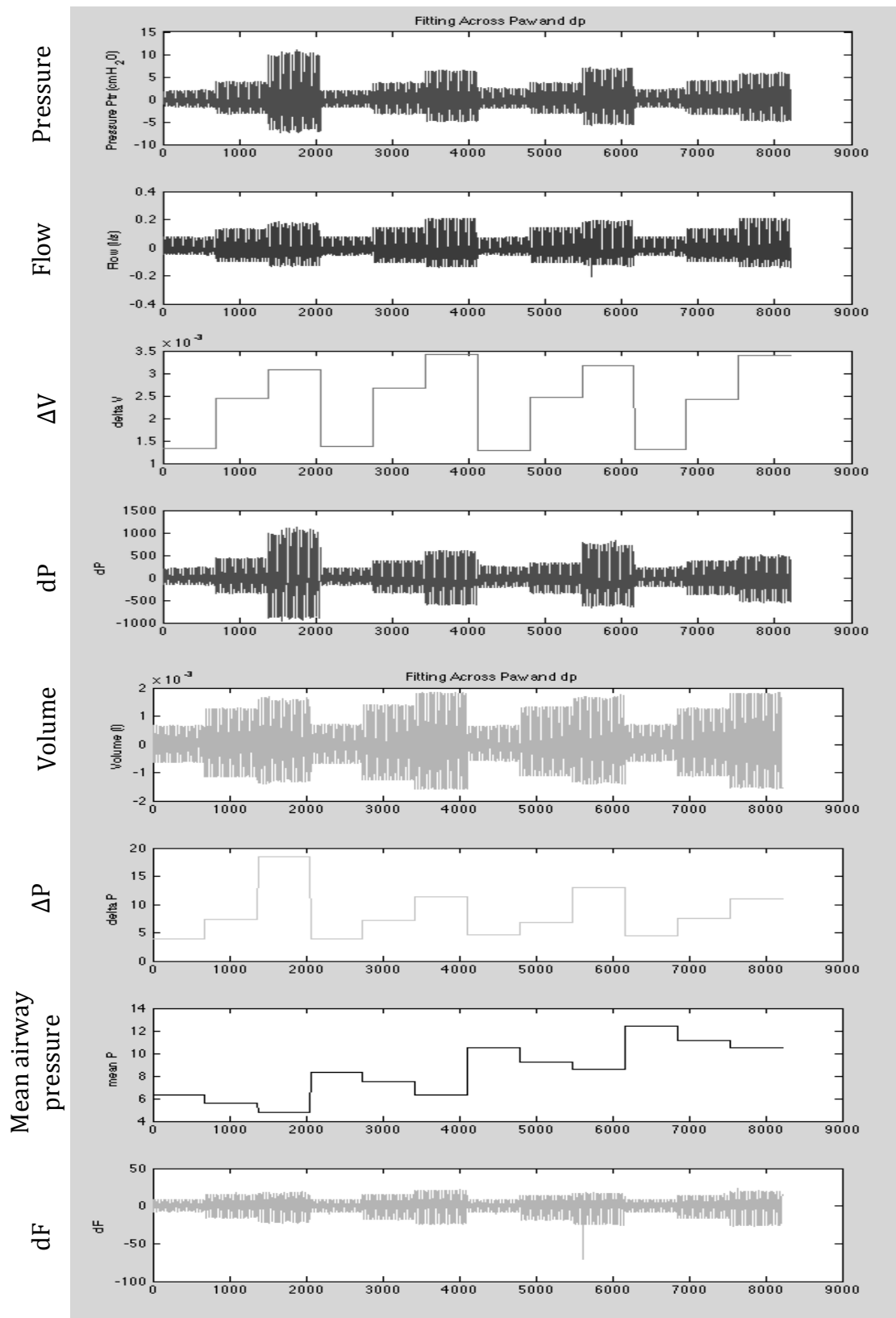


Figure C.2: Example of data while fitting across both settings.

D. Averaged Baby Results

Figures D.1 and D.2 show averaged results with standard error bars for Raw, Crs, Ct, Vo per weight, Crs/Vo, and Ct/Vo. Averaging was done between Paw of 6.5 and 10 cmH₂O since that range included most of the infant data. In order to average, we interpolated the results of the infants from Paw 6.5 to 10 cmH₂O with an interval of 0.5 cmH₂O.

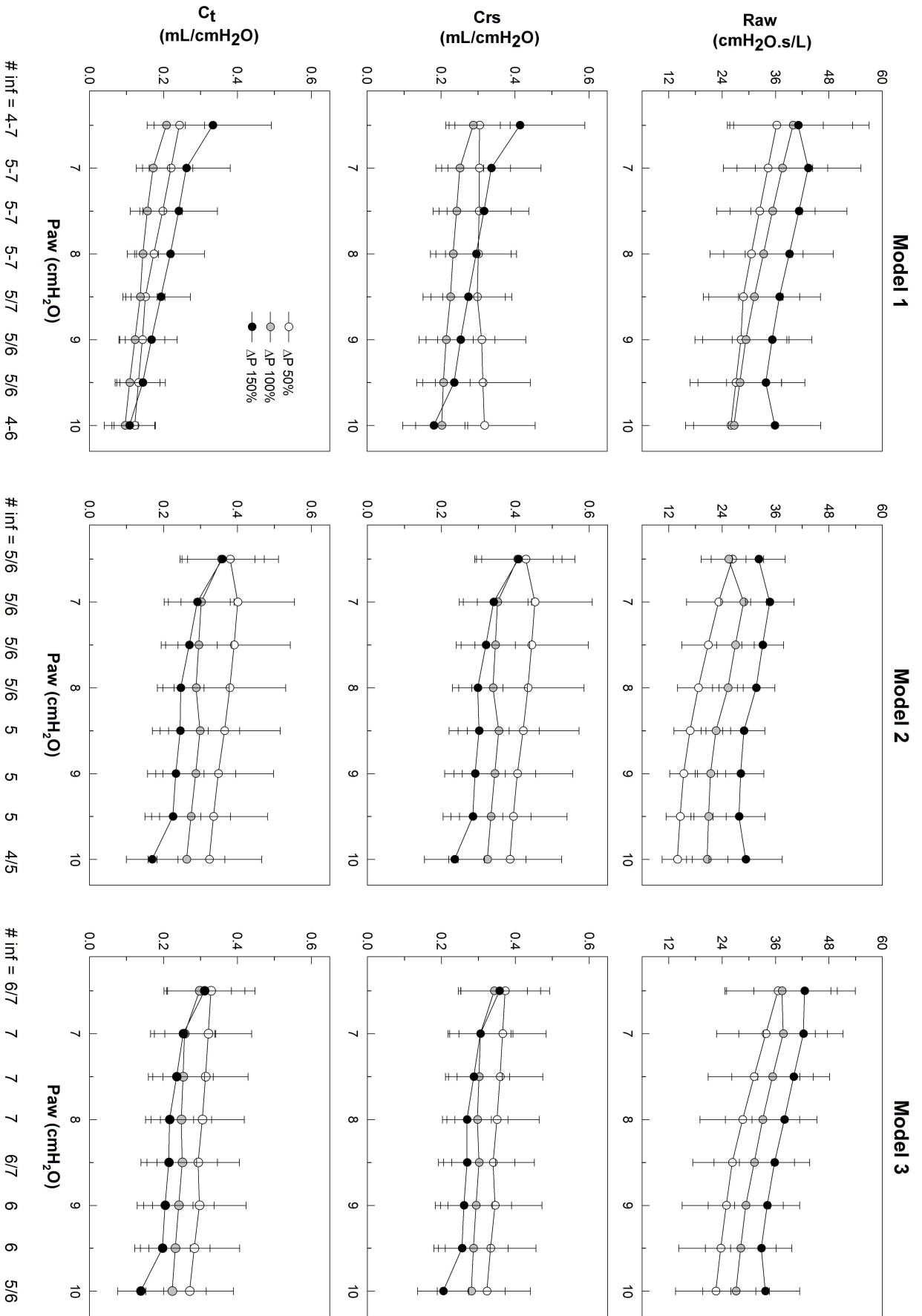


Figure D.1: Averaged baby results. (Raw, Crs, Ct)

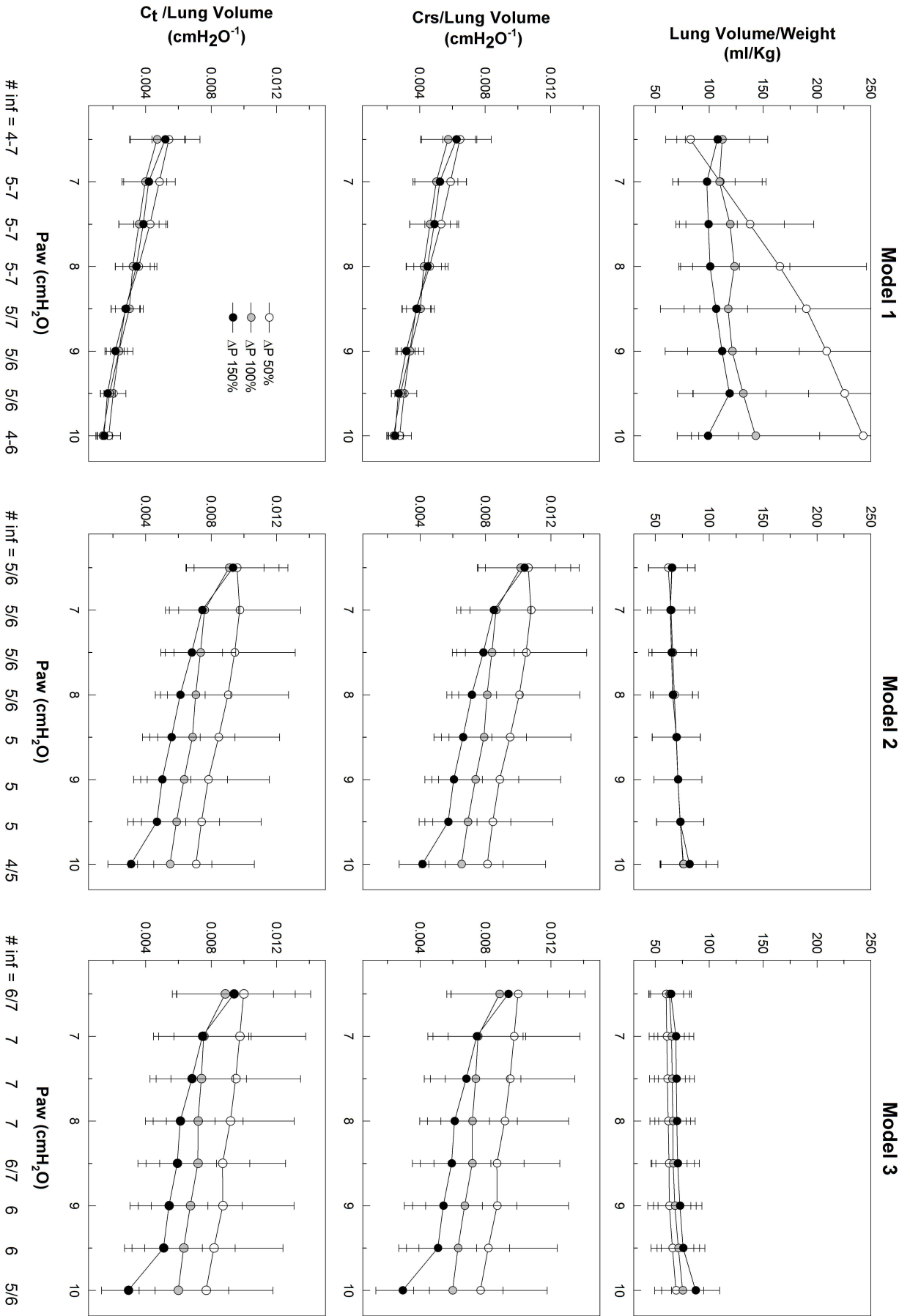


Figure D.2: Averaged baby results. Vo per weight, Crs/Vo, and Ct/Vo

E. Inertance Effect

In our model, we neglected inertance stating that even at high HFOV frequencies inertance does not contribute to lung mechanics. We decided to try to relax this assumption for baby 1 and see how values would differ. First, we attempted to fit the same data (filtered from 5-15Hz) with an Inertance. We modeled the inertance as a power-law; however, we did not restrain it to increasing values as we did for the lung. For the 5-15 filtered data, we failed to detect any inertance. Second, we filtered the data with a band pass filter between 5 and 50 Hz. Then we fitted this data with and without an inertance.

The element I_{aw} was allowed to vary as such across P_{aw}

$$\rightarrow I_{aw} = i_o + i_1 \left(\frac{P_{aw} - \min(P_{aw})}{\max(P_{aw} - \min(P_{aw}))} \right)^{i_2} \quad i_o > 0$$

in case fitting across both P_{aw} and ΔP

$$\rightarrow I_{aw} = \left(i_o + i_1 \left(\frac{P_{aw} - \min(P_{aw})}{\max(P_{aw} - \min(P_{aw}))} \right)^{i_2} \right) \times \left(\frac{\Delta P}{\max(\Delta P)} \right)^{\alpha_{Iaw}} \quad i_o > 0$$

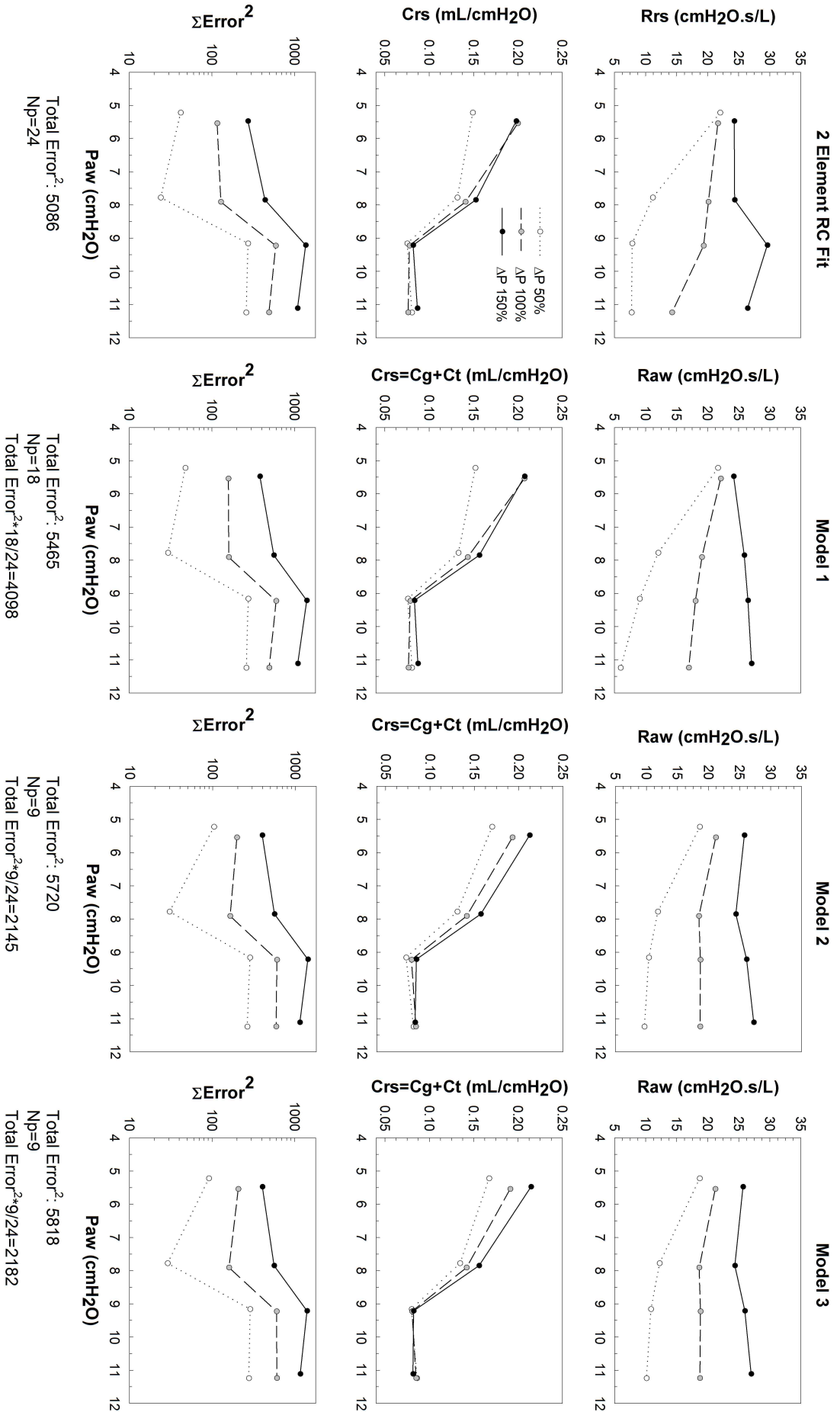
however, both i_o and α_{Iaw} were not needed in the fit.

thus the final behaviour applied for I_{aw} was reduced to:

$$\rightarrow I_{aw} = i_1 \left(\frac{P_{aw} - \min(P_{aw})}{\max(P_{aw} - \min(P_{aw}))} \right)^{i_2} \quad i_1 > 0$$

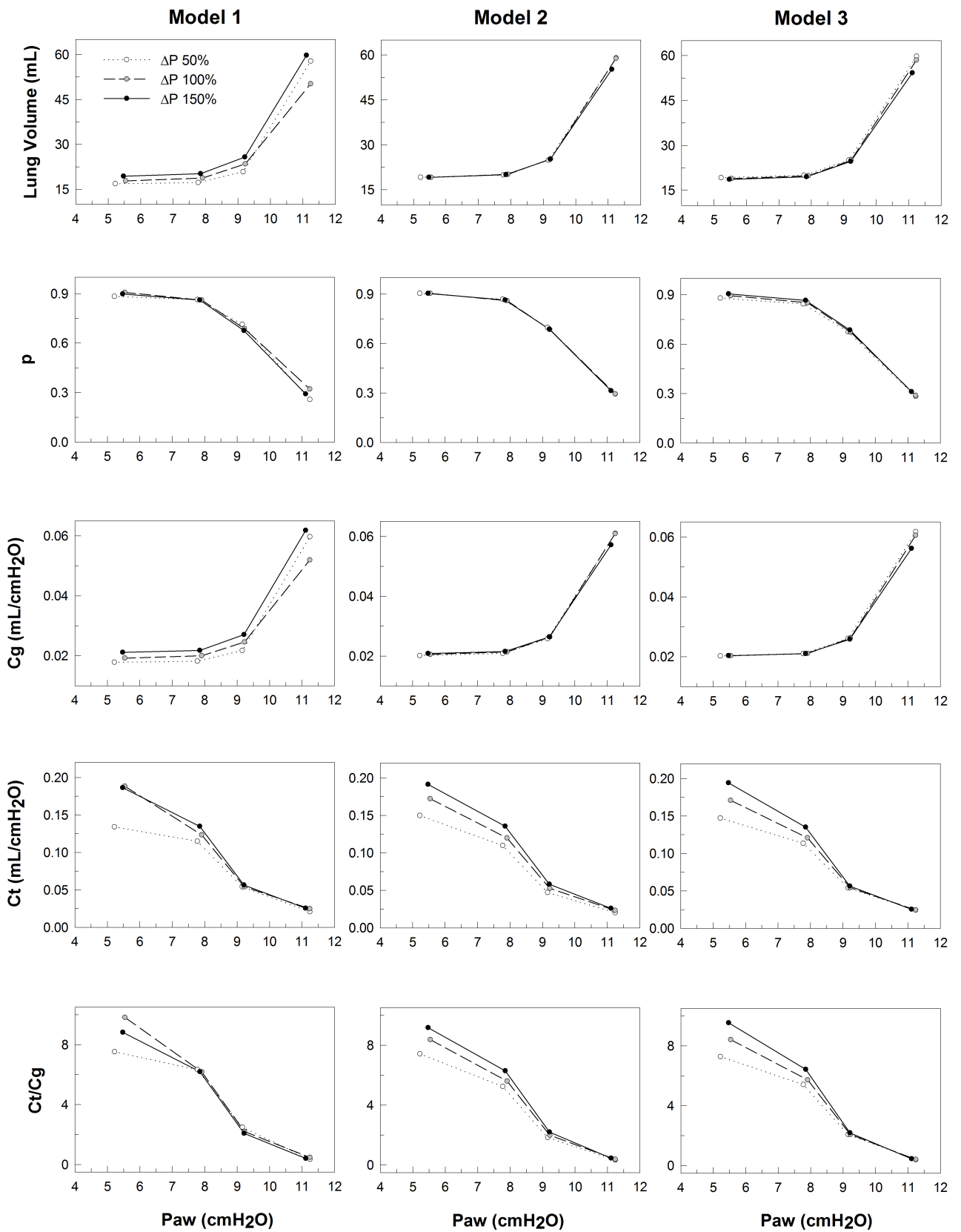
the fact that α_{Iaw} was not needed shows that airway inertance is independent of ΔP .

Figures E.1 and E.2 show results for the 5-50 Hz filtered data without modeling for inertance. Then inertance is included (Figures E.3 and E.4). The effects of including inertance in the model on the respiratory elements (R_{aw} , C_{rs} , and lung volume) are shown in figures E.5, E.6, and E.7.



Baby 1, Male, 0.872 Kg, 50 Hz Natural Frequency, **Filter BP 5-50 Hz**, 20 cycles per setting

Figure E.1: Results for 5-50Hz band pass filter without modeling for inertance.



Baby 1 , Male, 0.872 Kg, 10 Hz Natural Frequency, **Filter BP 5-50 Hz**, 20 cycles per setting

Figure E.2: Results for 5-50Hz band pass filter without modeling for inertance.

Baby 1, Male, 0.872 Kg, 10 Hz Natural Frequency, Filter BP 5-50 Hz, 20 cycles per setting

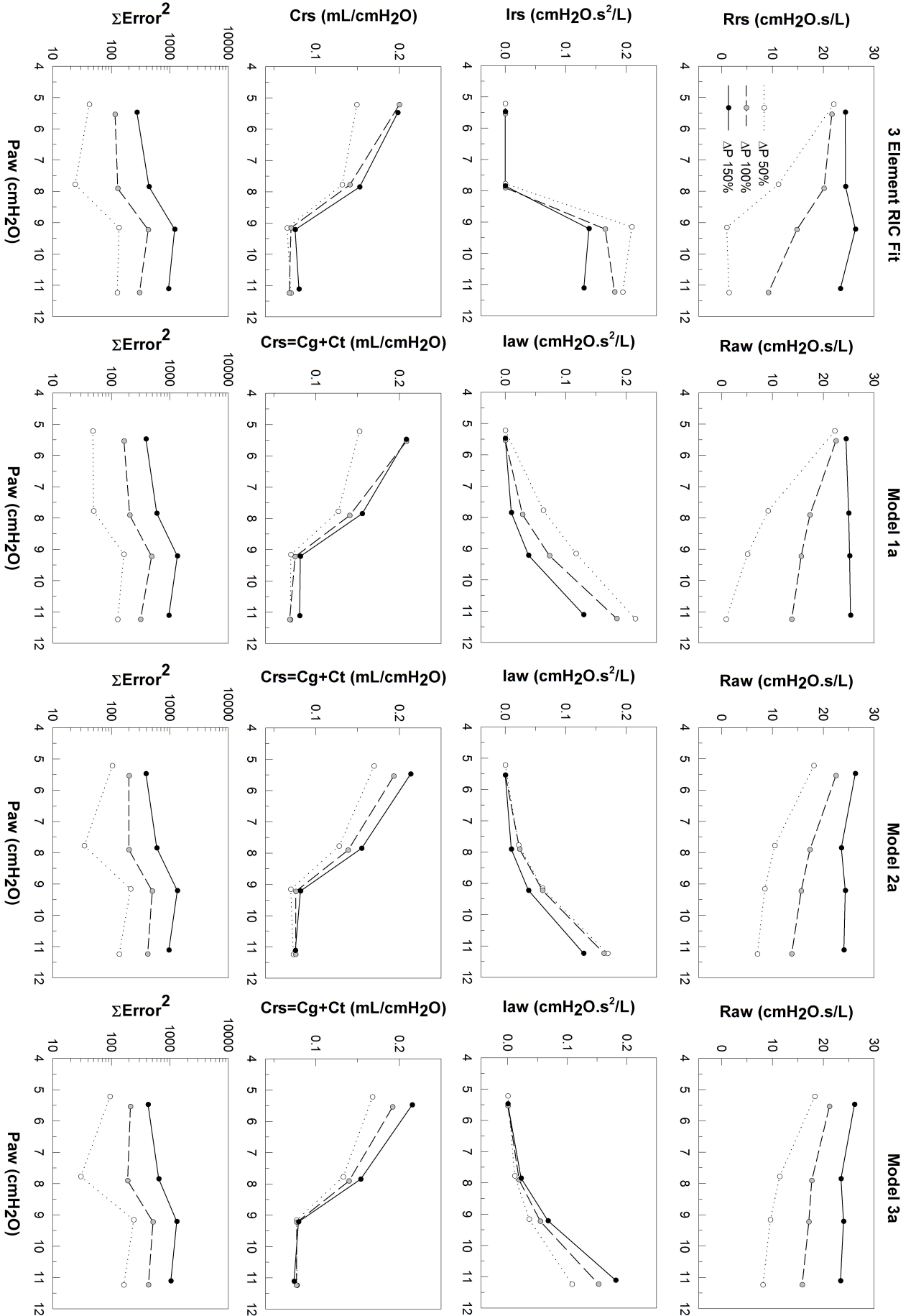
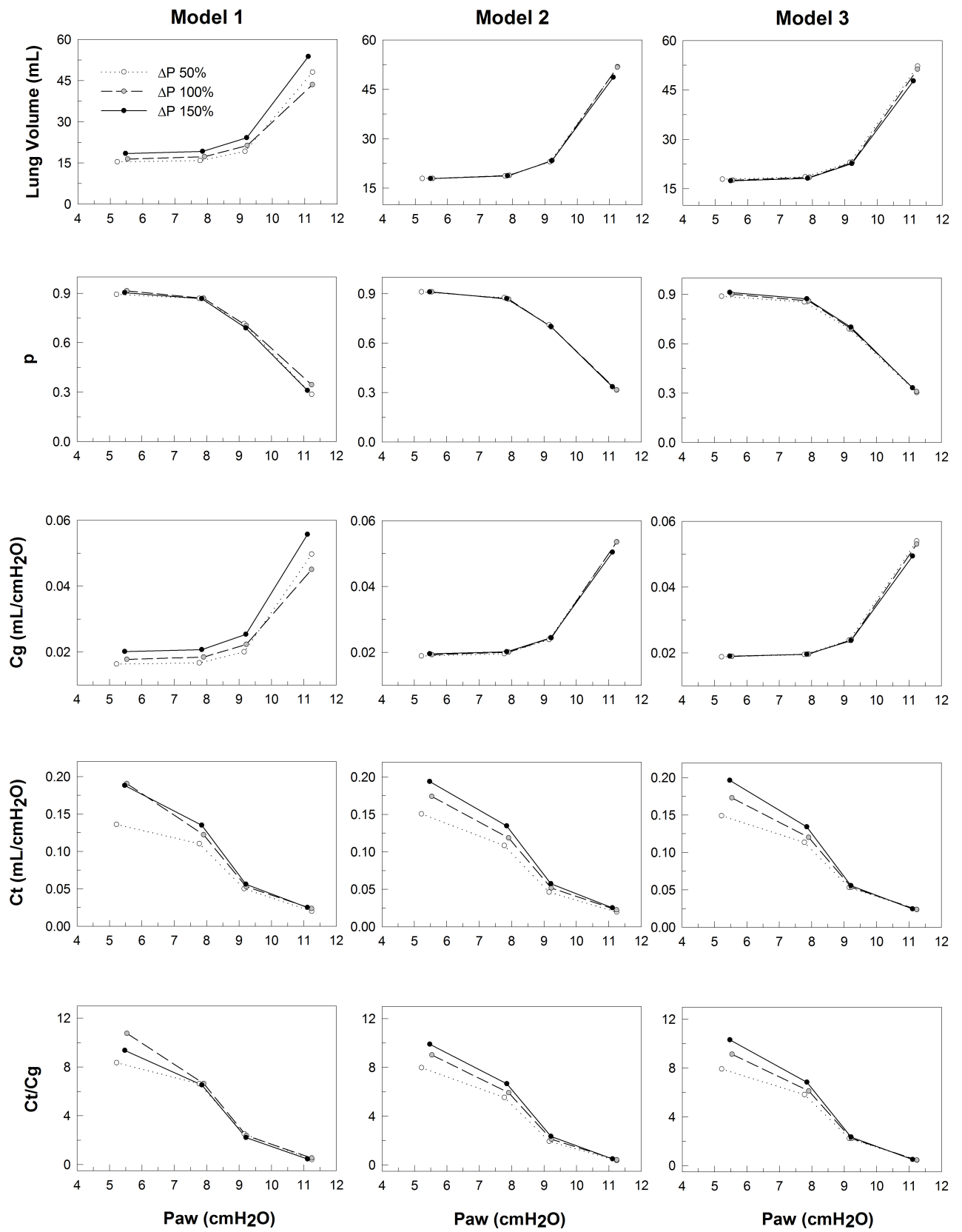
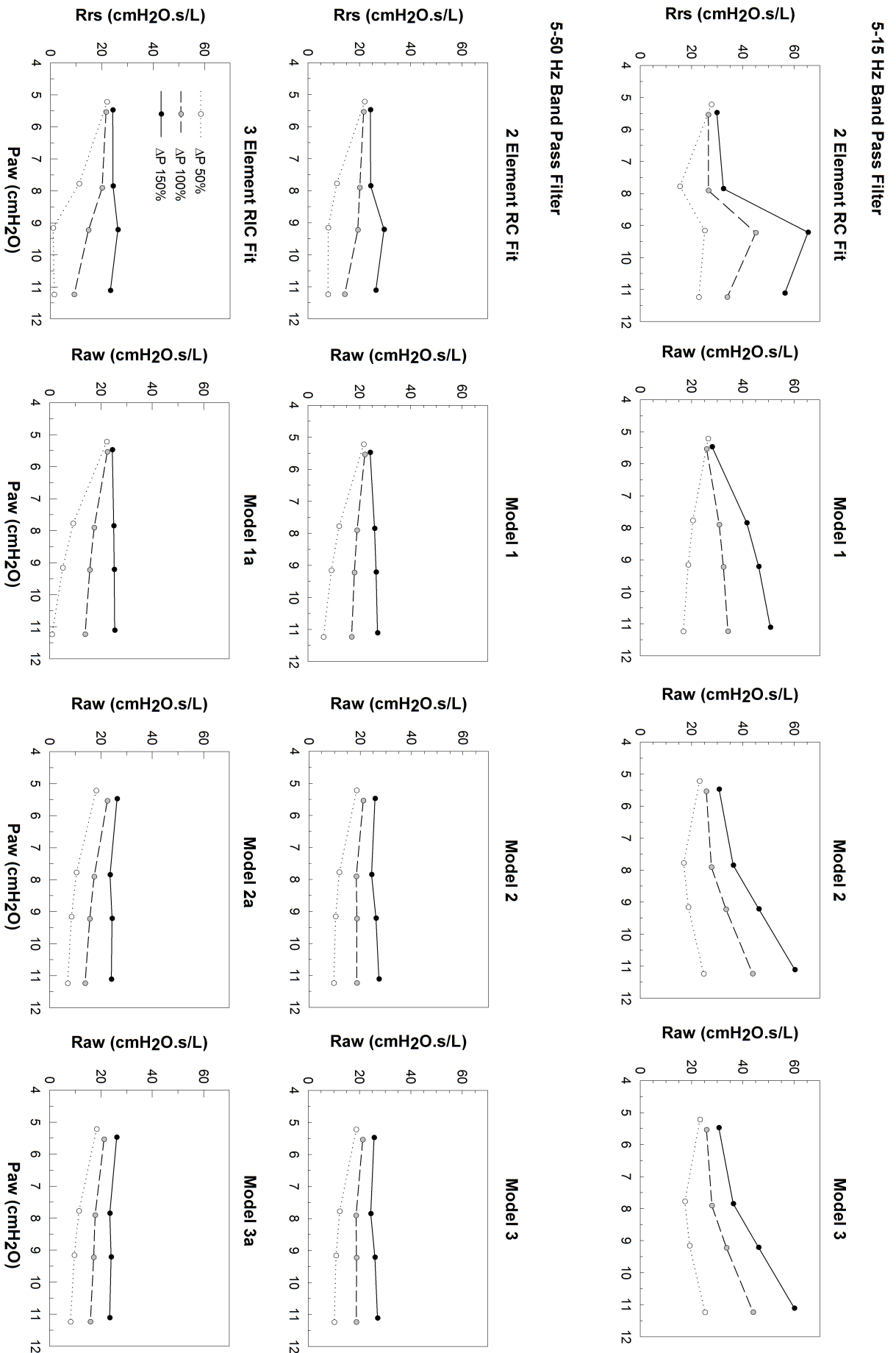


Figure E.3: Results for 5-50Hz band pass filter including inertia/L model.



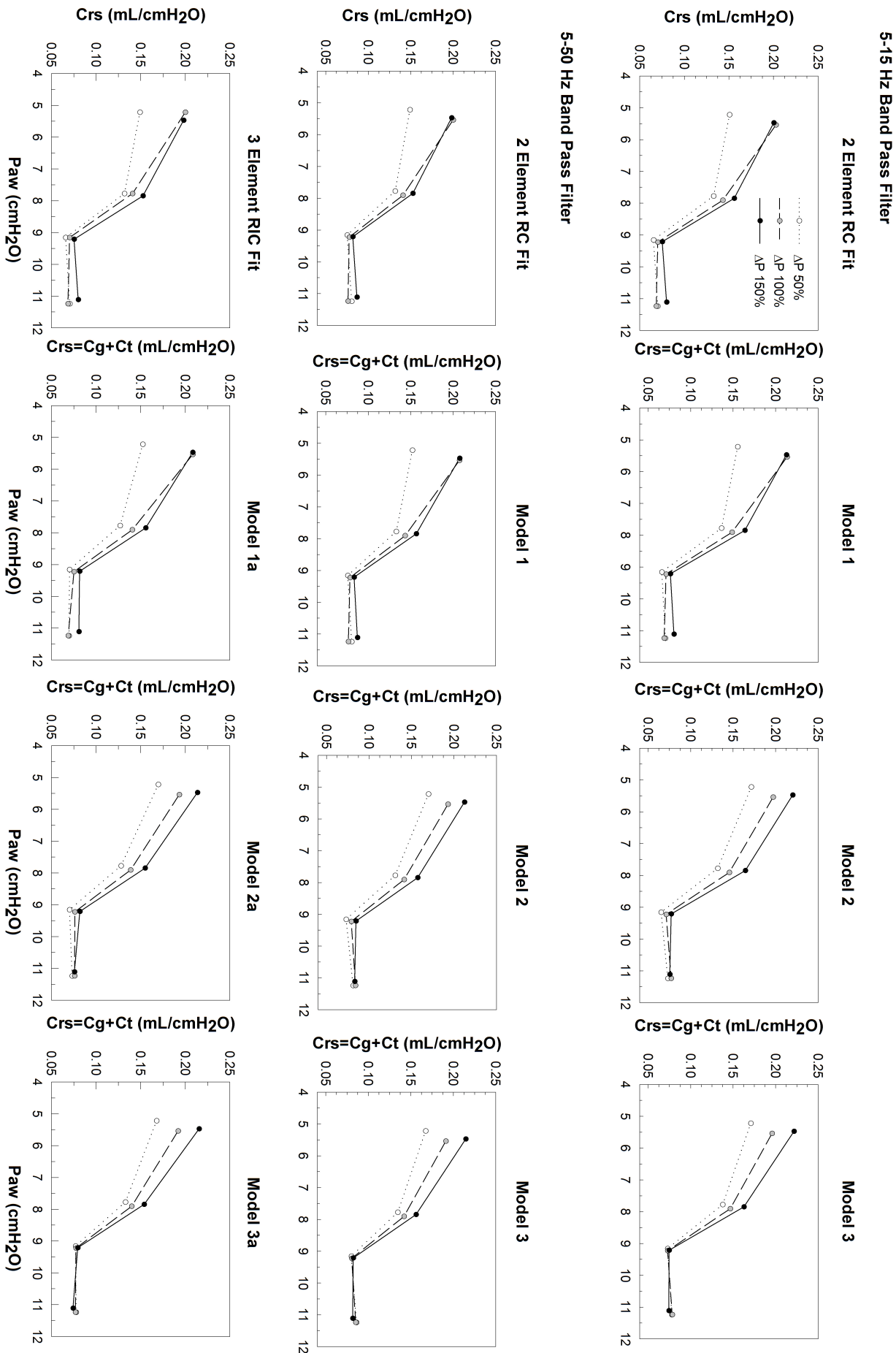
Baby 1 , Male, 0.872 Kg, 10 Hz Natural Frequency, Filter BP 5-50 Hz, 20 cycles per setting

Figure E.4: Results for 5-50Hz band pass filter including inertance model.



Baby 1, Male, 0.872 Kg, 10 Hz Natural Frequency, 20 cycles per setting

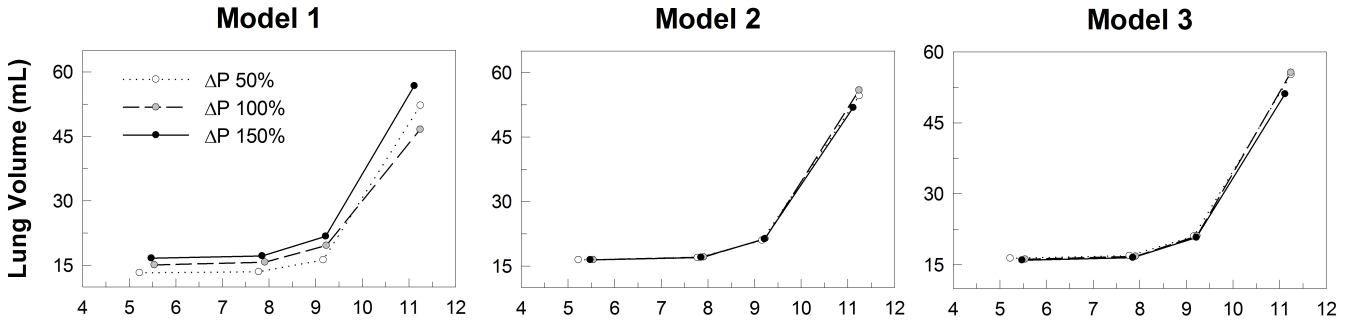
Figure E.5: Filtering effects on resistance values.



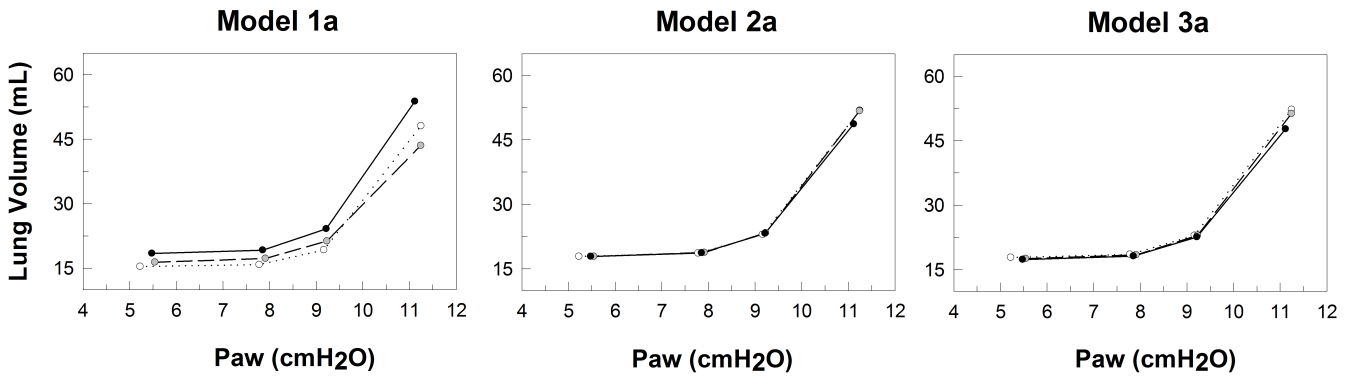
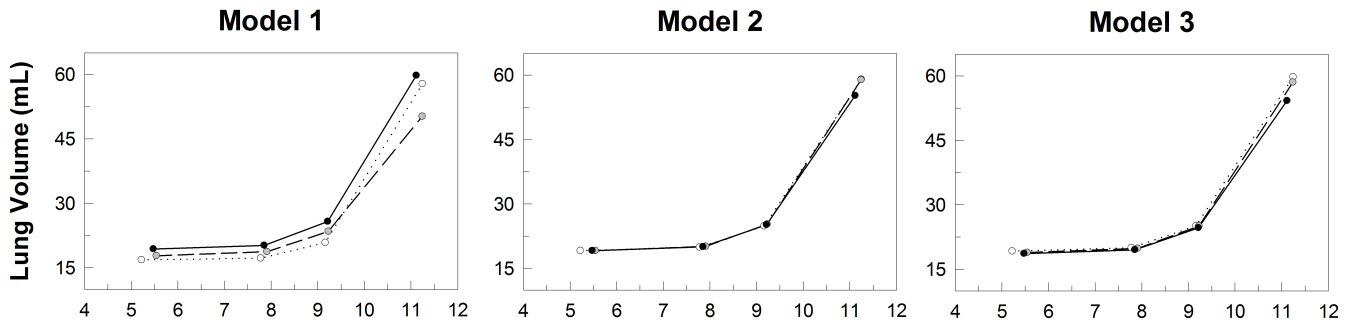
Baby 1, Male, 0.872 Kg, 10 Hz Natural Frequency, 20 cycles per setting

Figure E.6: Filtering effects on compliance values.

5-15 Hz Band Pass Filter



5-50 Hz Band Pass Filter



Baby 1 , Male, 0.872 Kg, 10 Hz Natural Frequency, 20 cycles per setting

Figure E.7: Filtering effects on lung values.

Resistance

Resistance values drop significantly when we use a wider frequency range. This is true whether the model includes an airway inertance or doesn't. The main point here is that we observe frequency dependent behavior for airway resistance. Since the data filtered between 5 and 50 Hz has more frequency content observing lower resistance values is expected since, as mentioned earlier, resistance drops with frequency.

Compliance

On the other hand, system compliance barely changes and can be said to be frequency independent.

Lung Volume

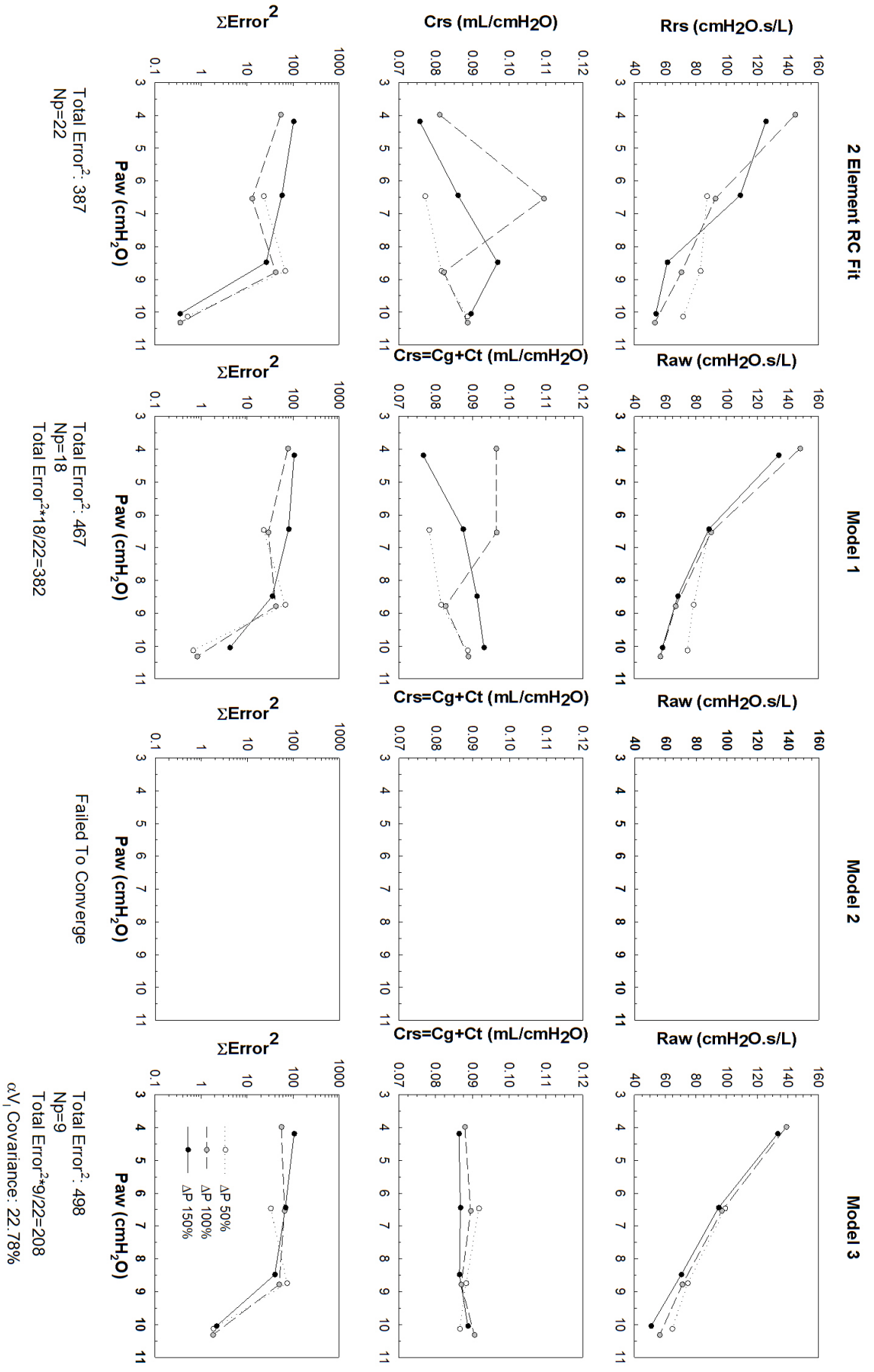
With a wider range of frequency and neglecting inertance, lung volume was just slightly overestimated (a maximum of 5ml). More precisely, the higher the P_{aw} is, the higher the difference. At small P_{aw} where inertance was not identified the difference was not considerable. Adding an inertance to the model decreased that difference. Having said that, we believe that also the lung dependence on frequency is arguably negligible.

Inertance

Inertance was observed to be negligible at small P_{aws} . Only at higher P_{aws} it was considerable. Inertance represents the mass of air in the airway. Since airways are compliant, then with increasing P_{aw} , more mass can accumulate in the airway leading to higher values of inertance. This could be a possible explanation to our finding.

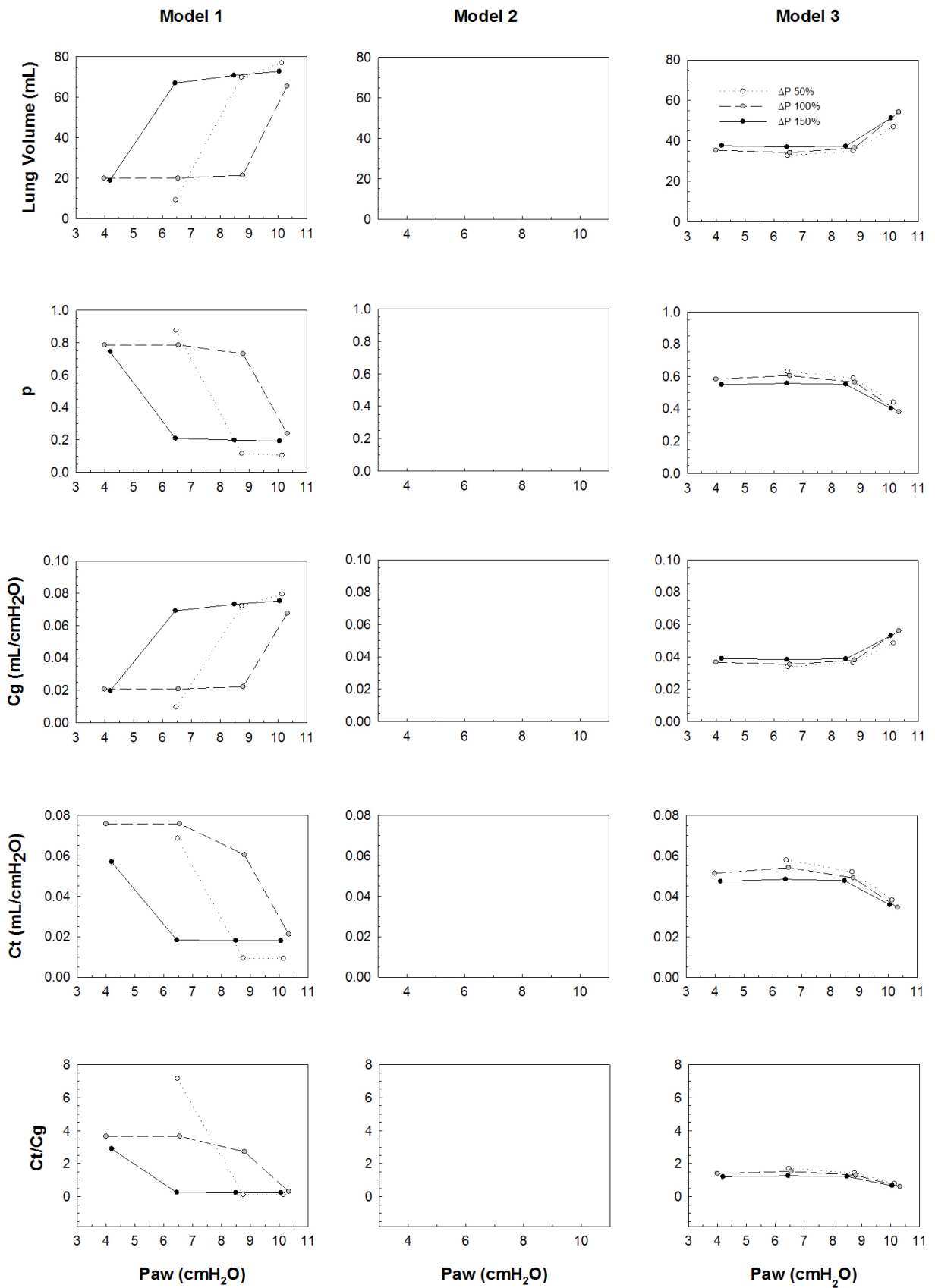
F. Individual Baby Results

Figures F.1 till F.14 show individual baby results.



Baby 2, Female, 0.542 Kg, 10 Hz Natural Frequency, Filter BP 7.5-12.5 Hz, 9 cycles per setting

Figure F.1: Baby 2 results. Rrs, Crs, and Error.



Baby 2 , Female, 0.542 Kg, 10 Hz Natural Frequency, Filter BP 7.5-12.5 Hz, 9 cycles per setting

Figure F.2: Baby 2 results. Vo, p, Cg, Ct, and Ct/Cg.

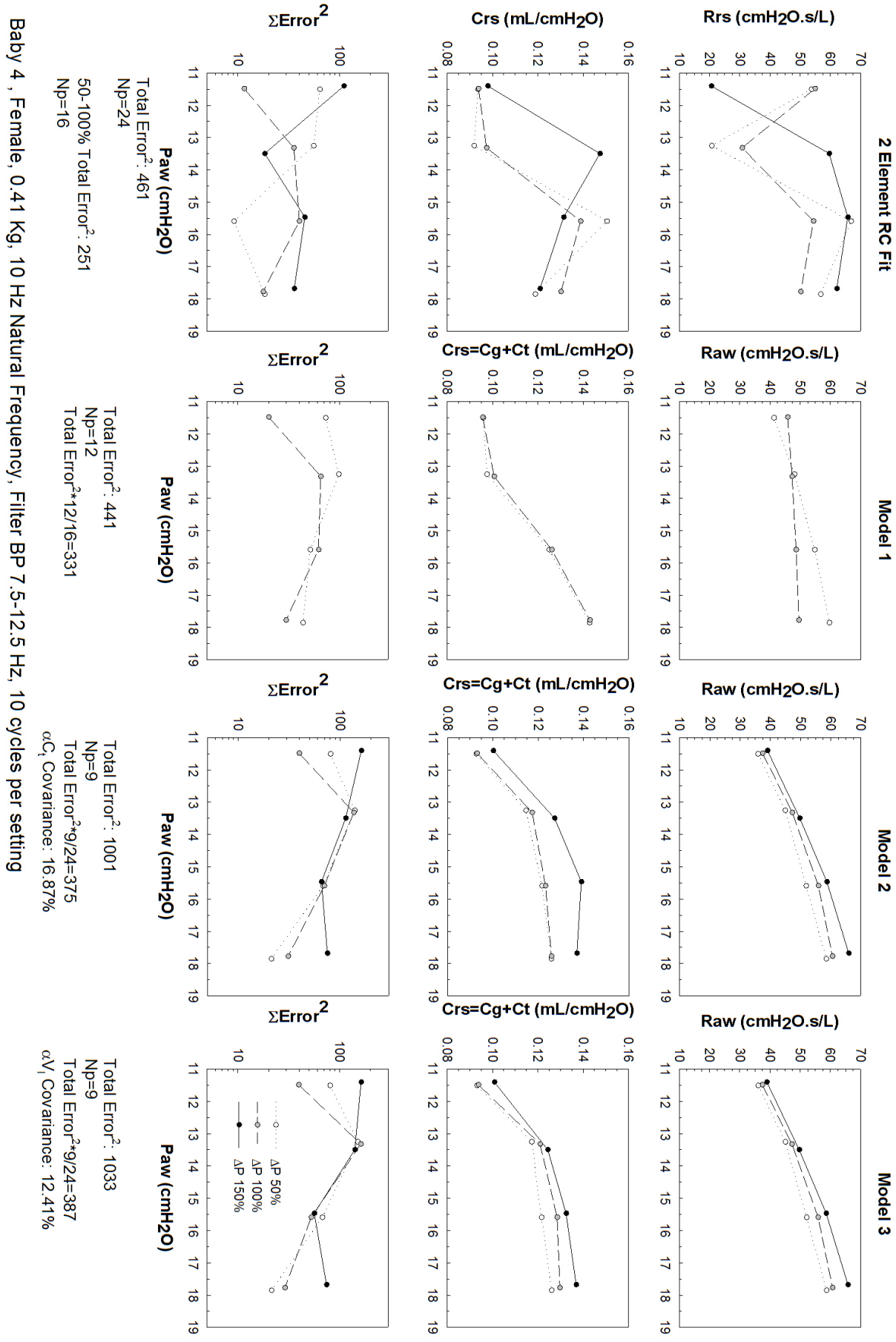
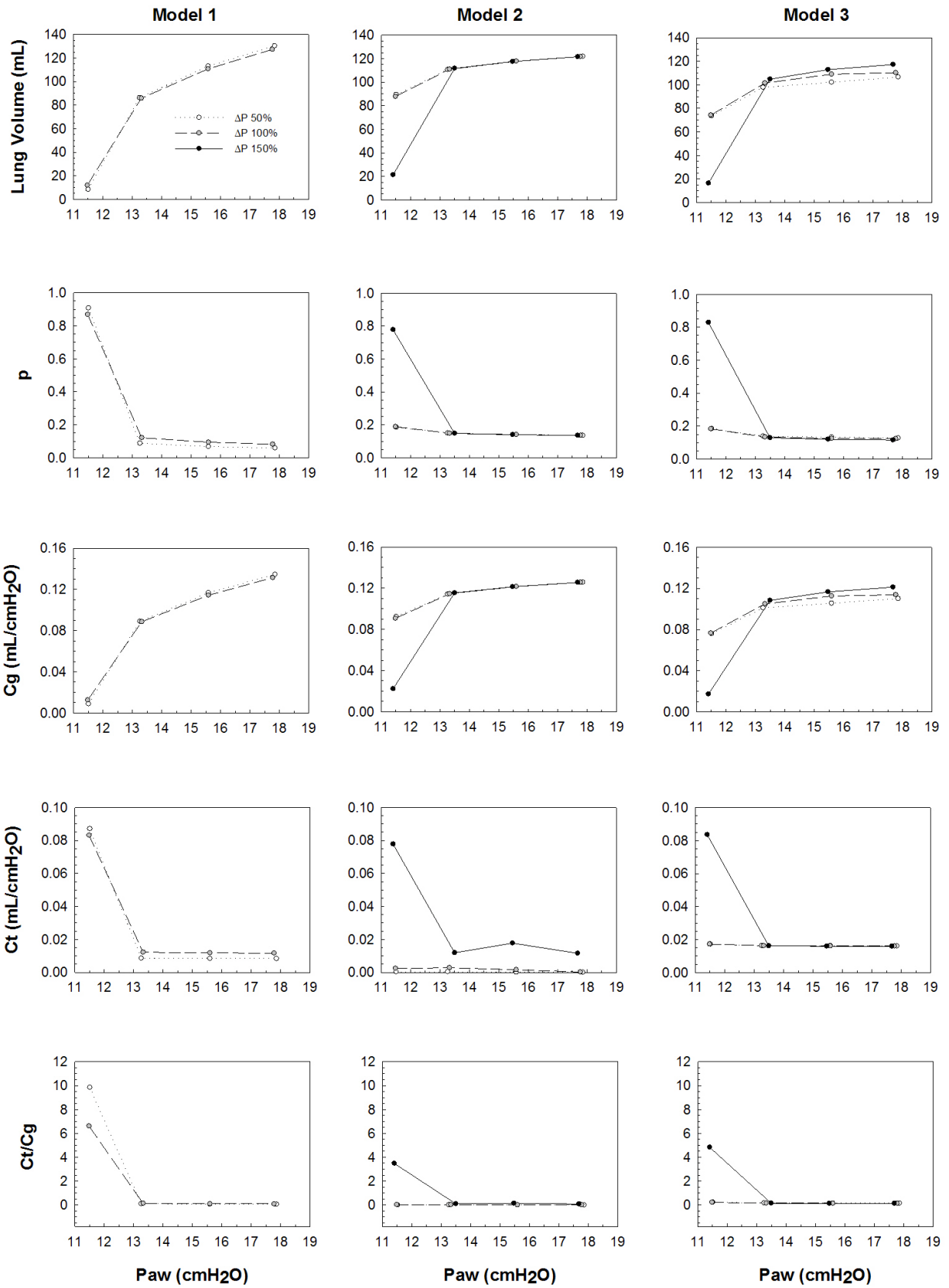


Figure F.3: Baby 4 results. Rrs. Crs. and Error.



Baby 4 , Female, 0.41 Kg, 10 Hz Natural Frequency, Filter BP 7.5-12.5 Hz, 10 cycles per setting

Figure F.4: Baby 4 results. Vo, p, Cg, Ct, and Ct/Cg.

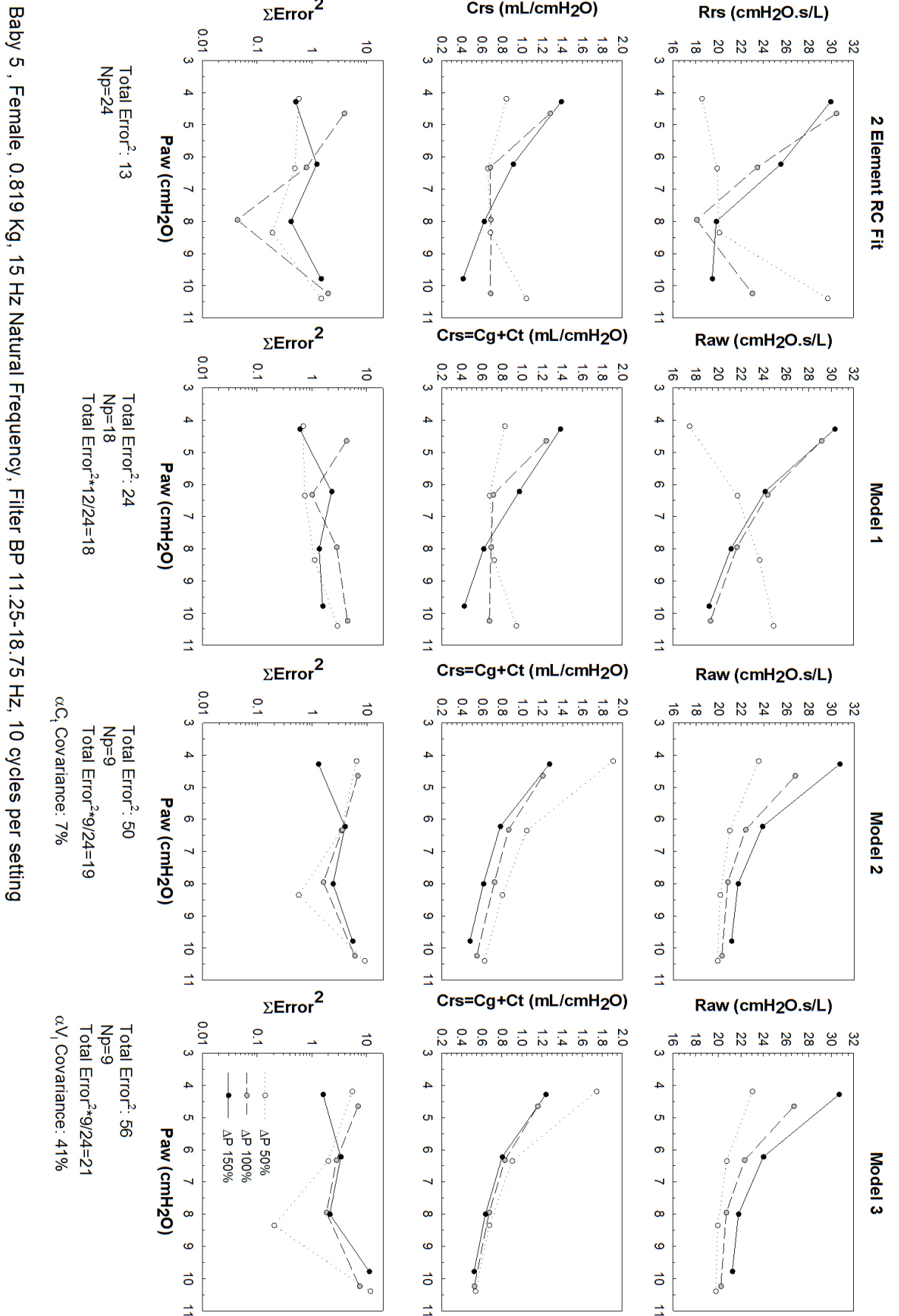
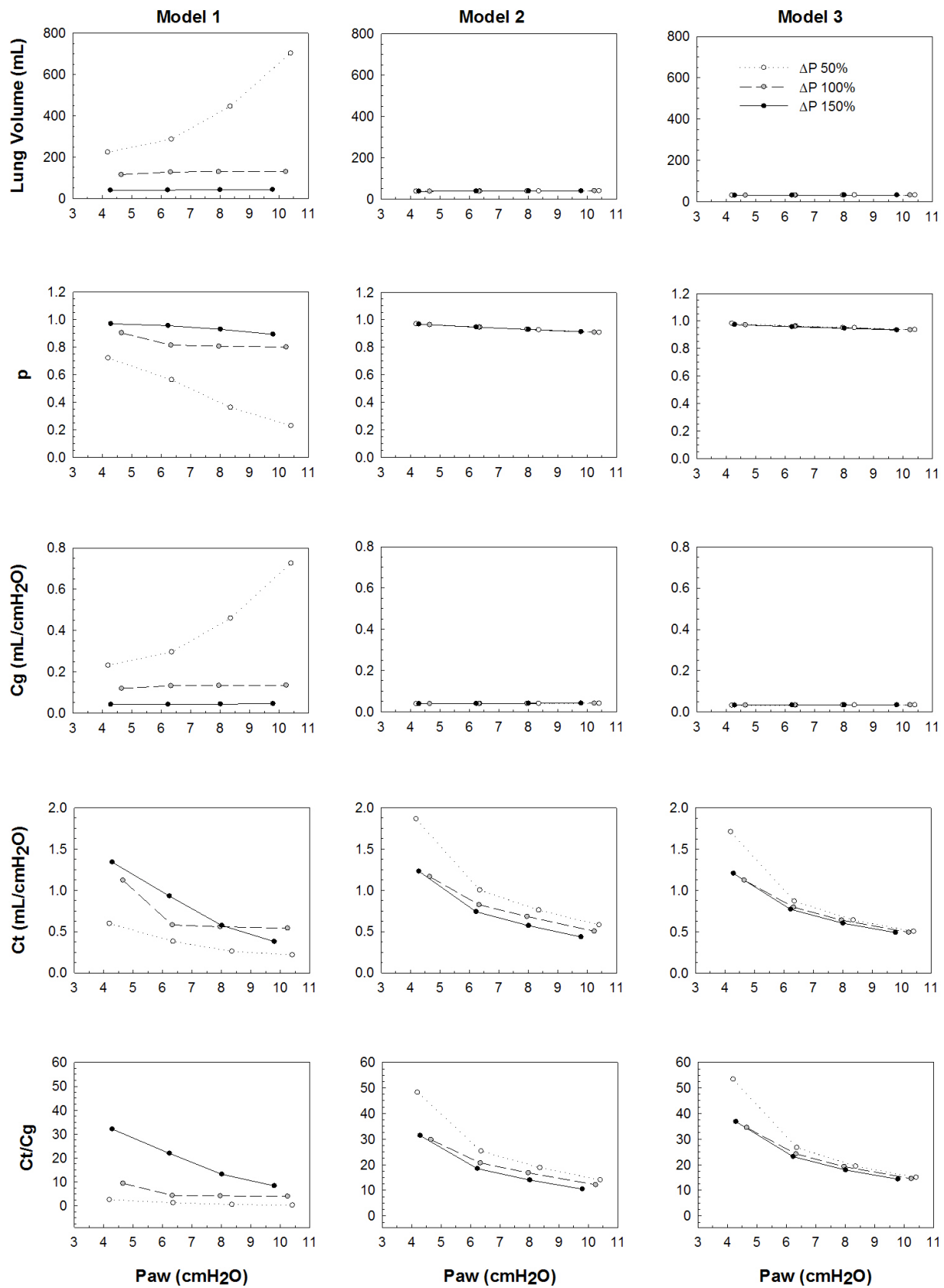


Figure F.5: Baby 5 results. Rrs, Crs, and Error.



Baby 5, Female, 0.819 Kg, 15 Hz Natural Frequency, Filter BP 11.25-18.75 Hz, 10 cycles per setting

Figure F.6: Baby 5 results. Vo, p, Cg, Ct, and Ct/Cg.

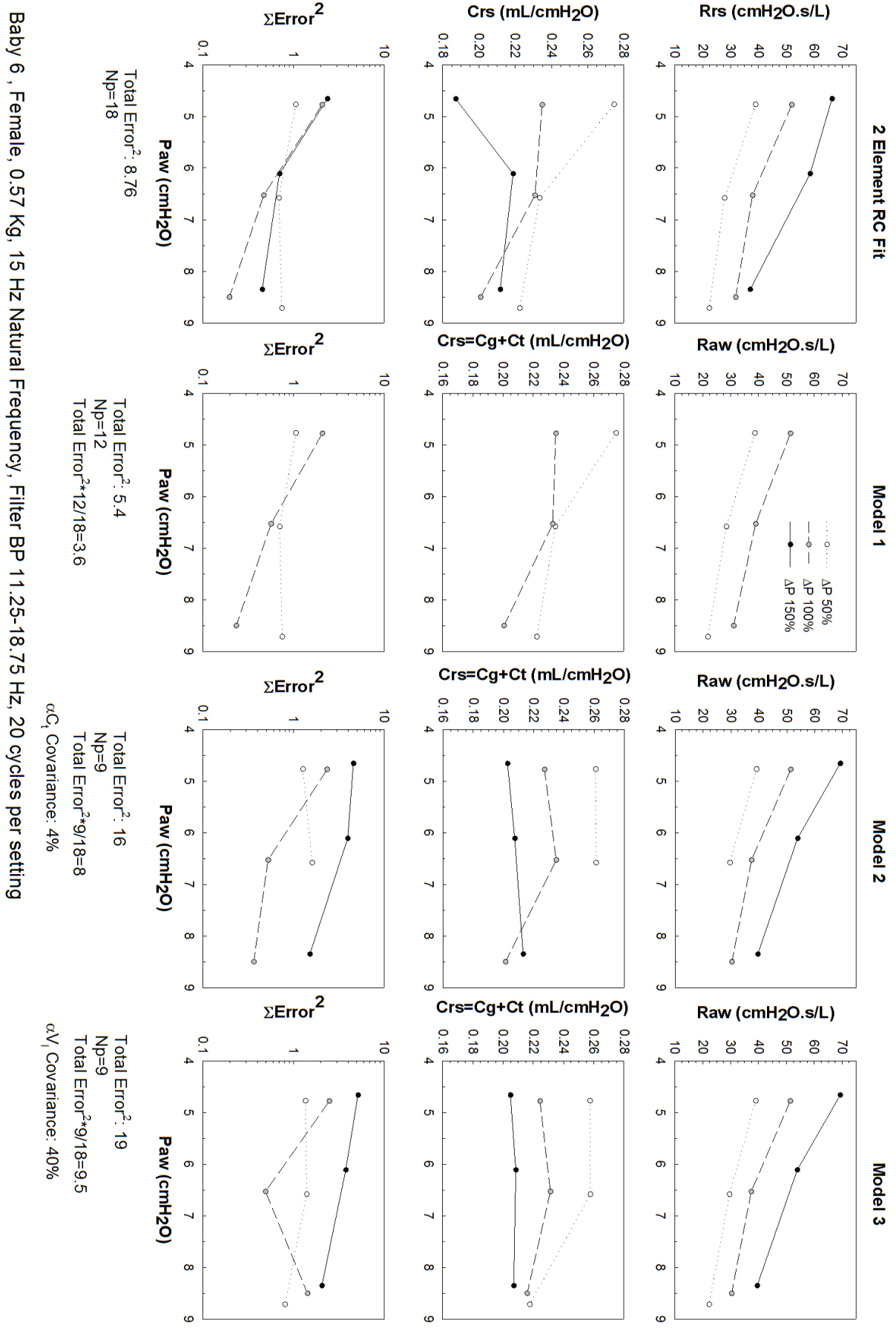
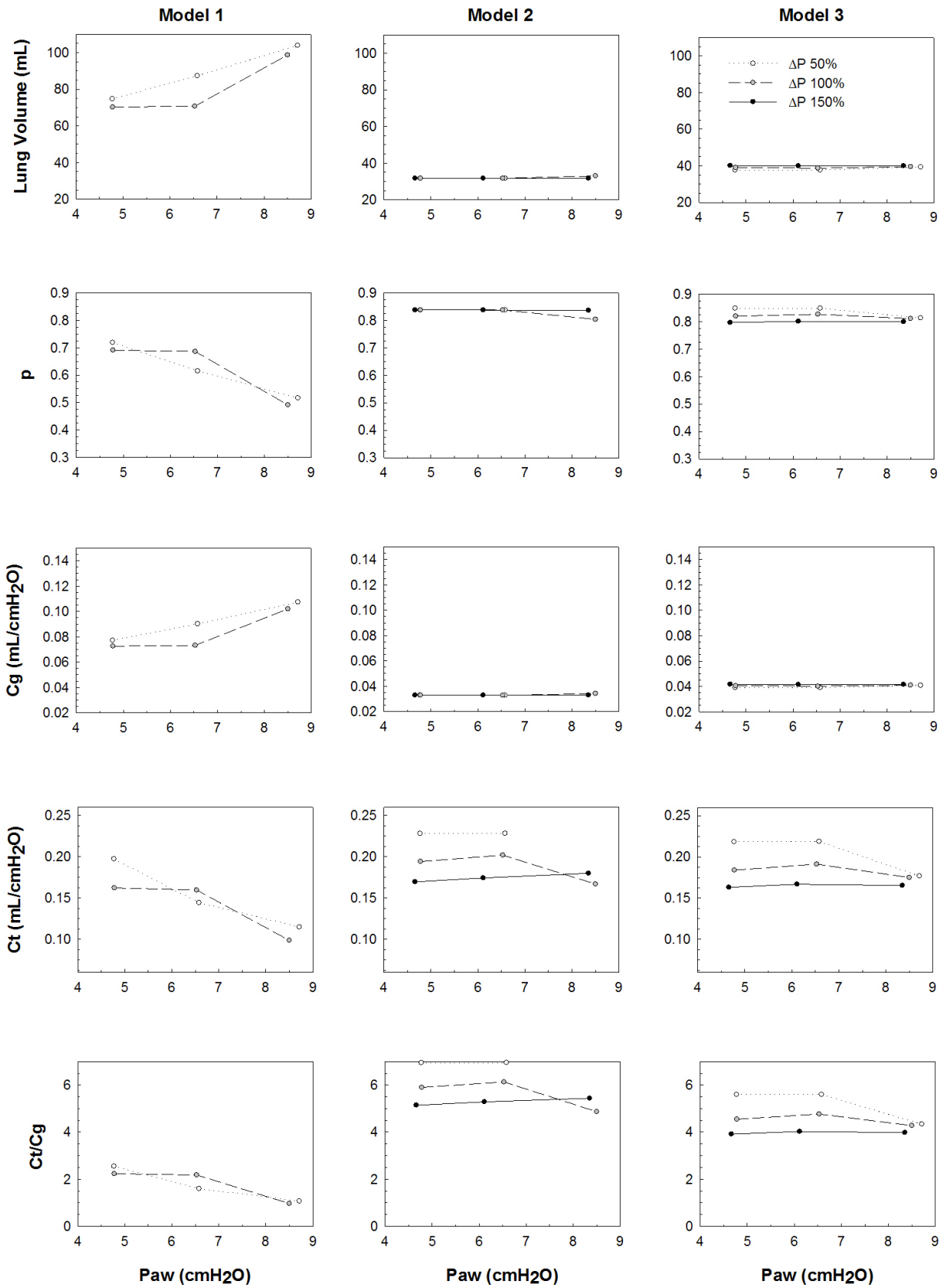


Figure F.7: Baby 6 results. Rrs, Crs, and Error.



Baby 6 , Female, 0.57 Kg, 15 Hz Natural Frequency, Filter BP 11.25-18.75 Hz, 20 cycles per setting

Figure F.8: Baby 6 results. Vo, p, Cg, Ct, and Ct/Cg.

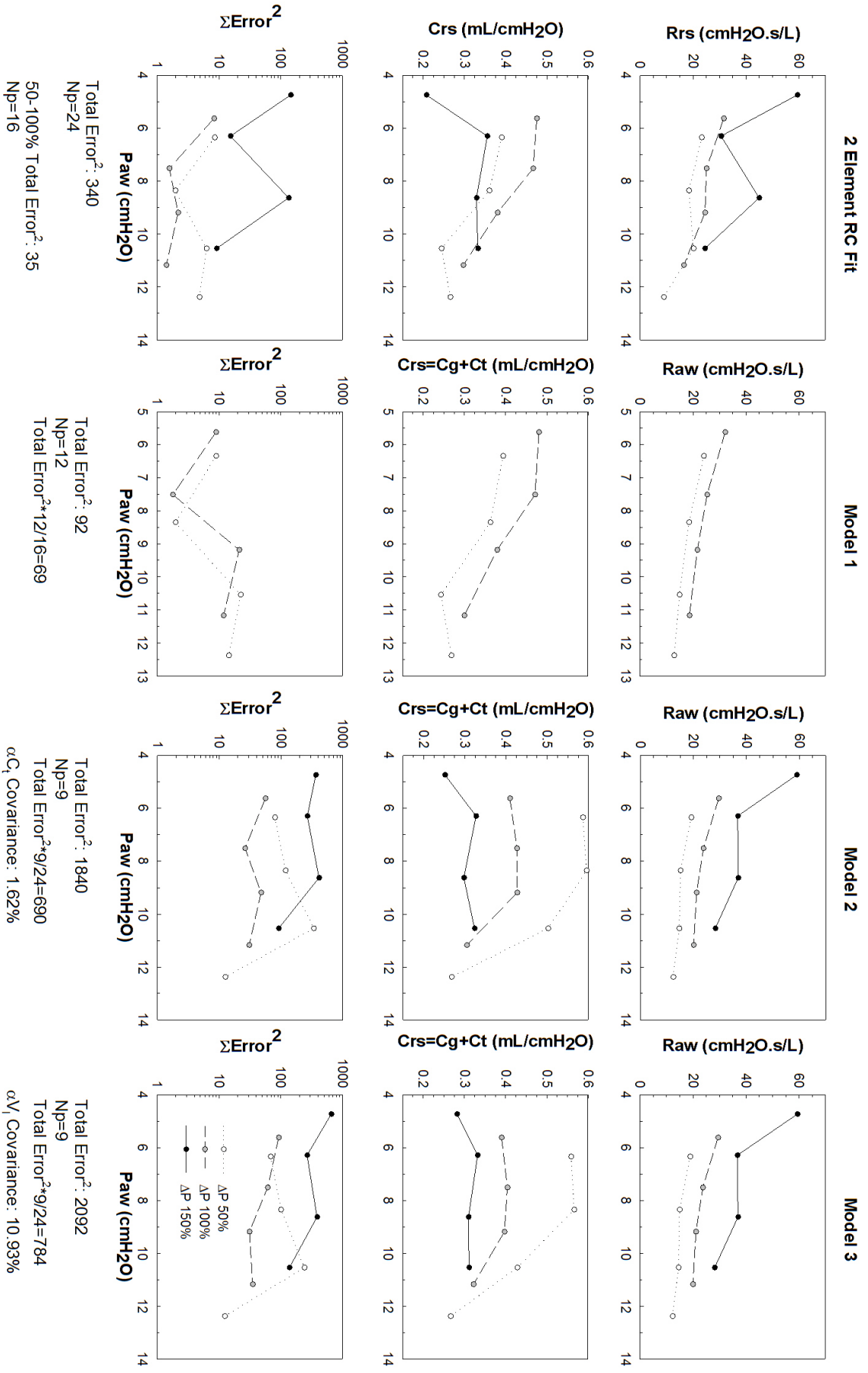
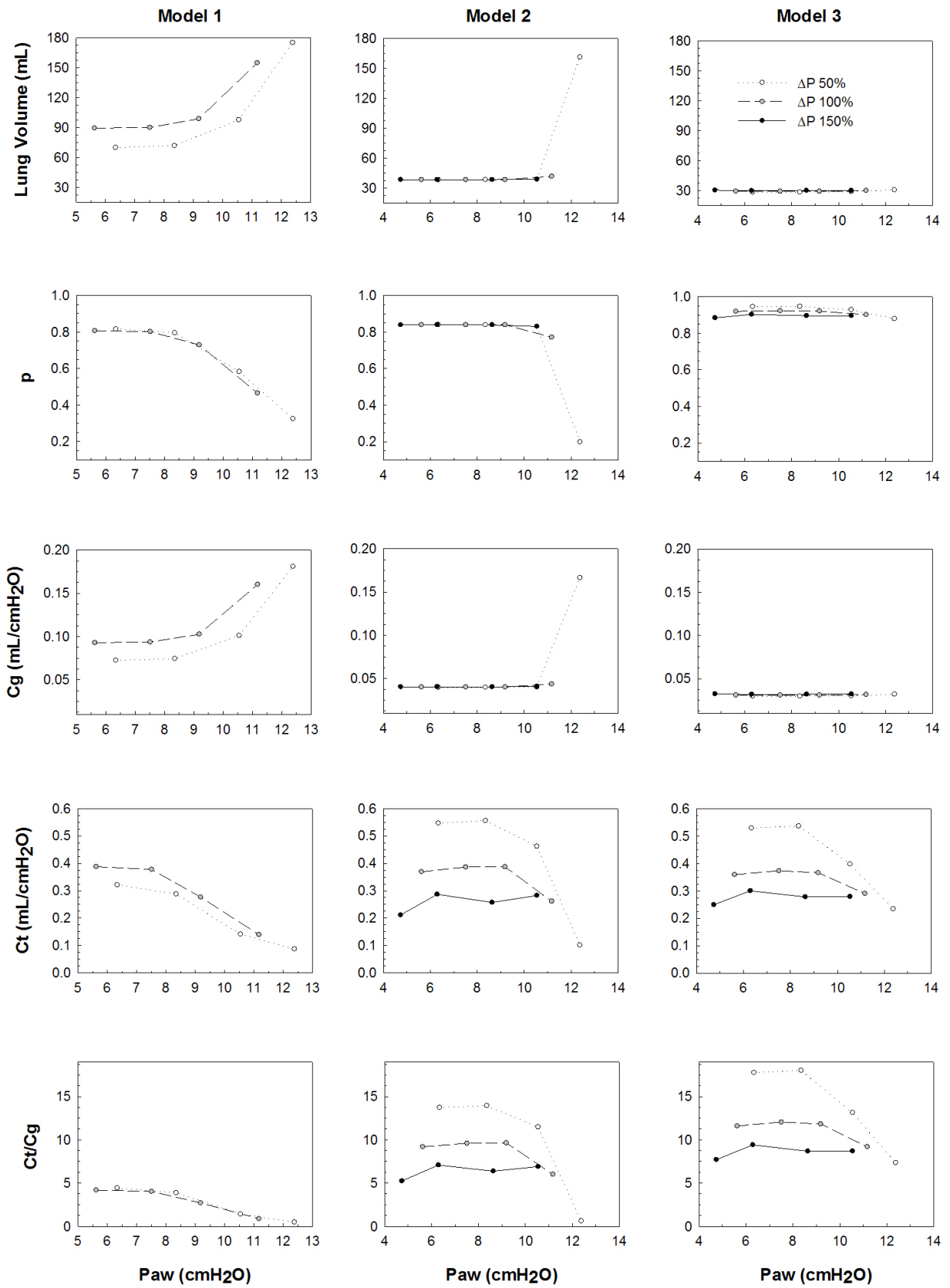


Figure F.9: Baby 7 results. Rrs, Crs, and Error.



Baby 7 , Female, 0.788 Kg, 15 Hz Natural Frequency, Filter BP 11.25-18.75 Hz, 20 cycles per setting

Figure F.10: Baby 7 results. Vo, p, Cg, Ct, and Ct/Cg.

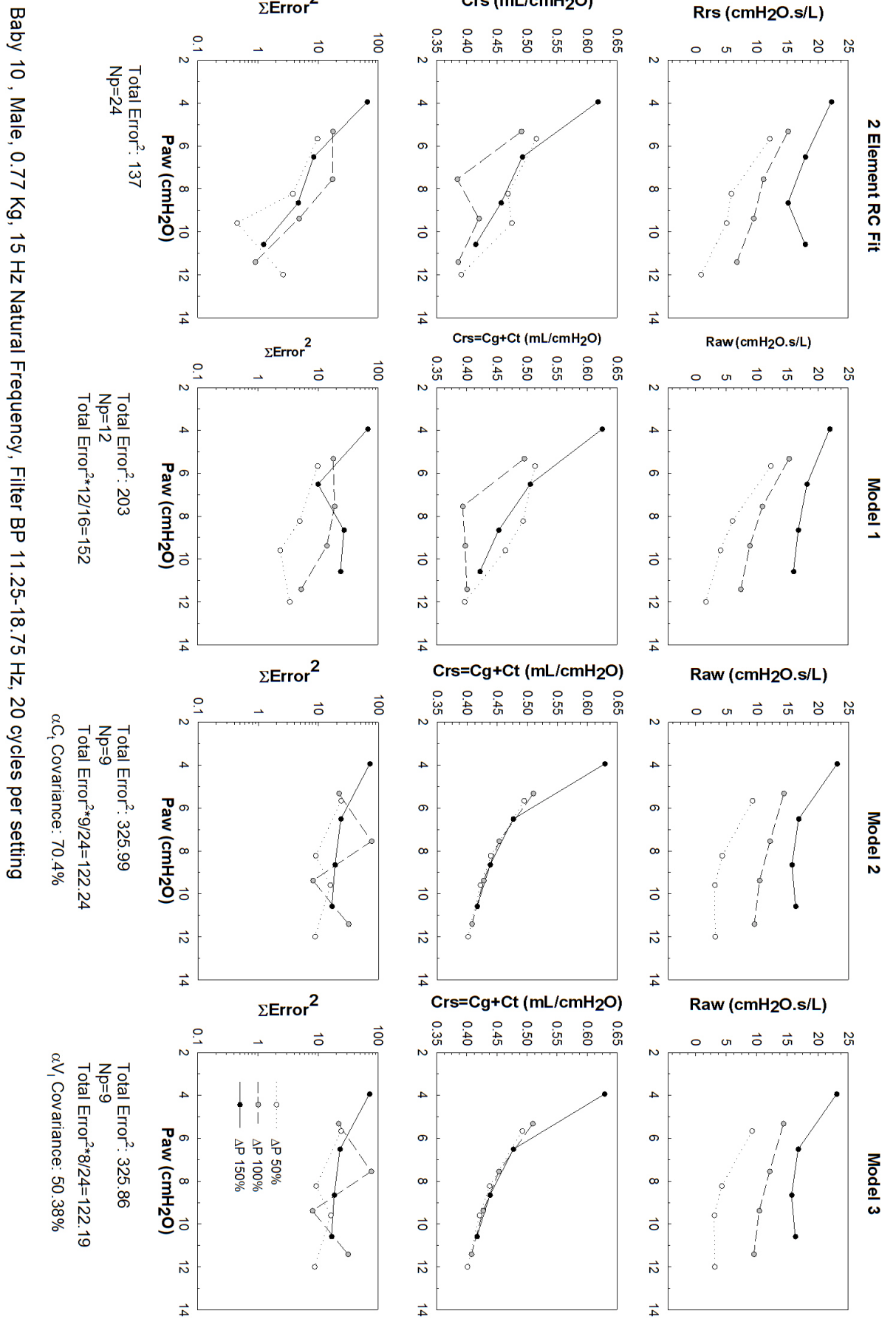
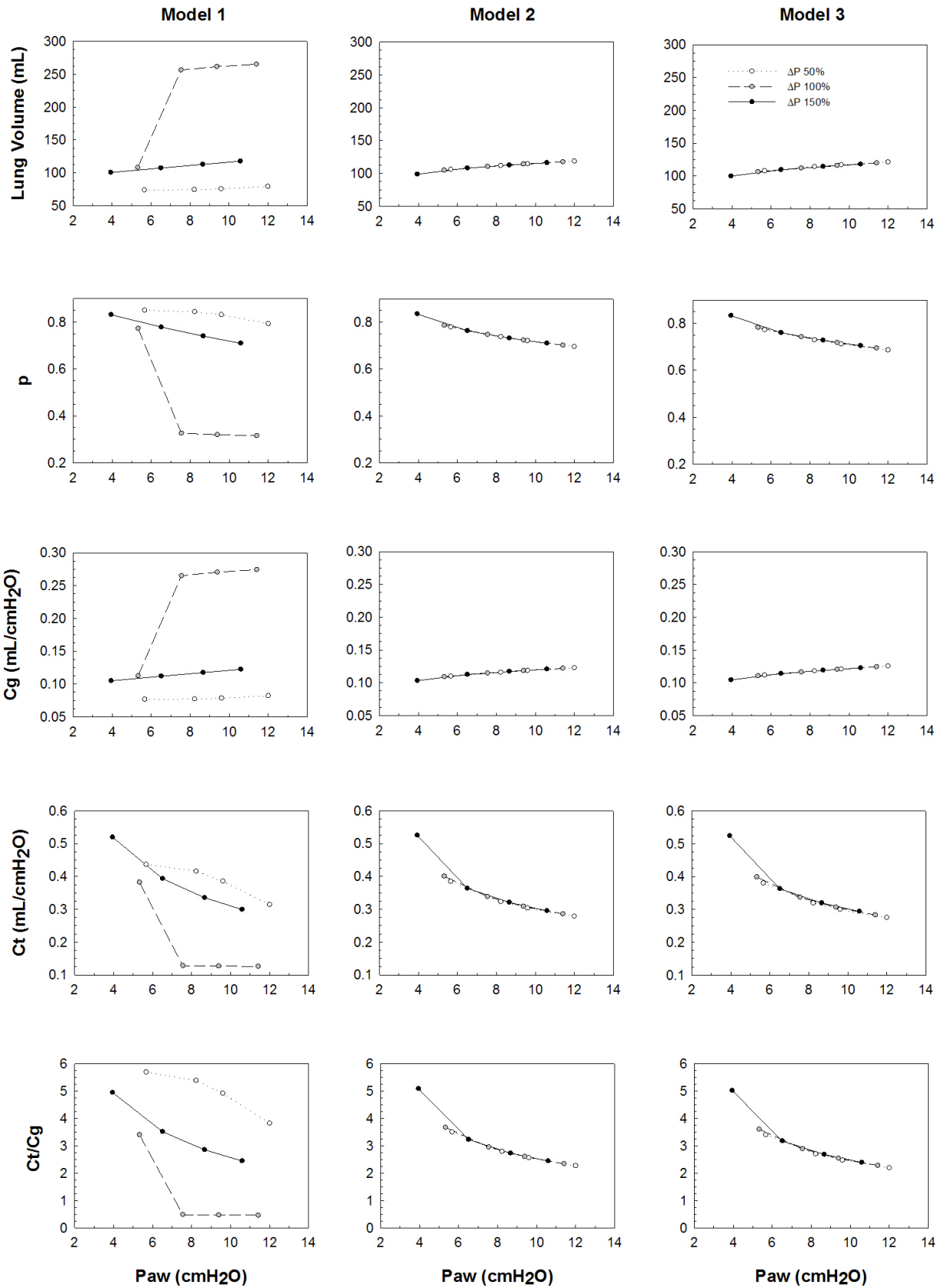
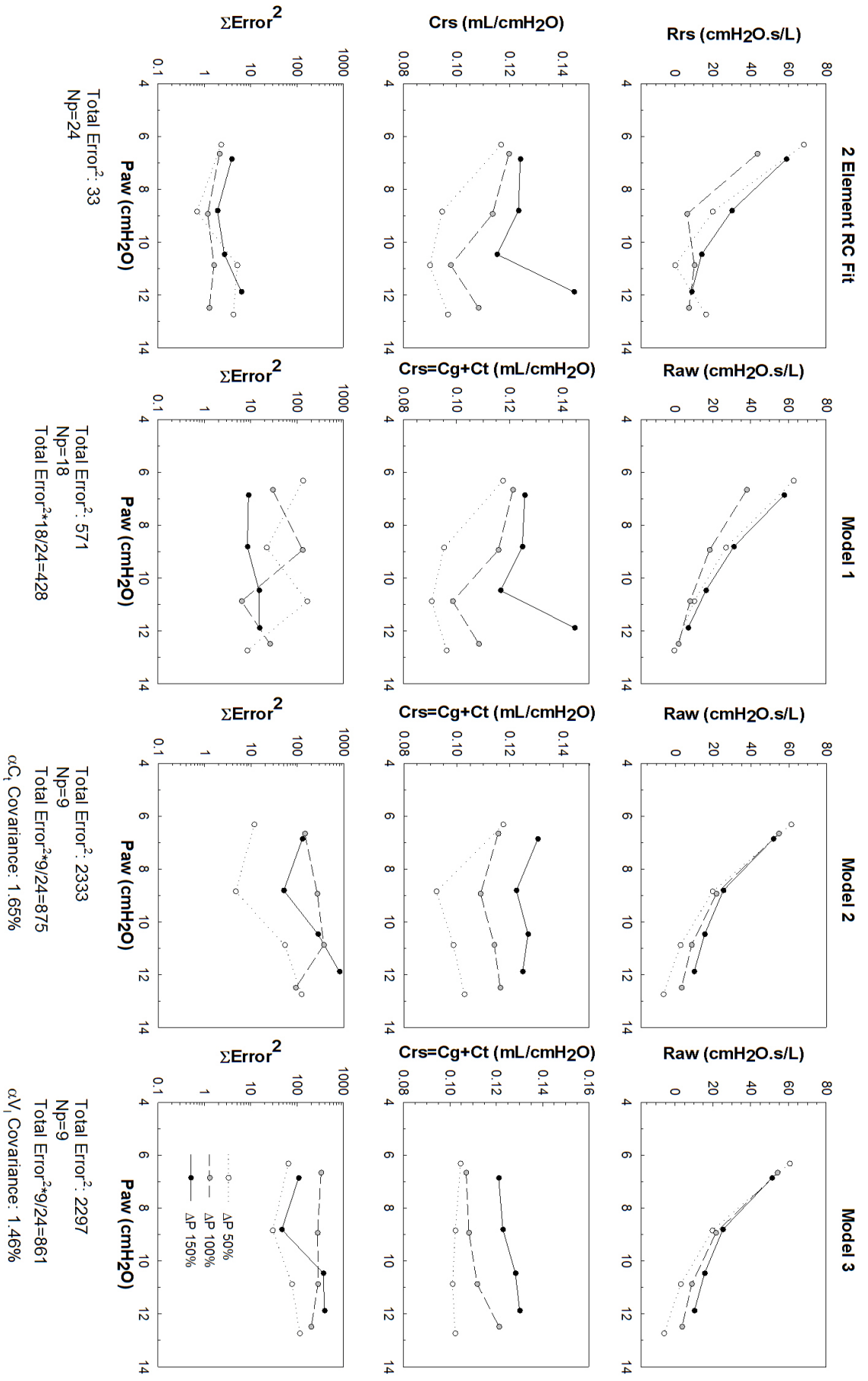


Figure F.11: Baby 10 results. Rrs, Crs, and Error.



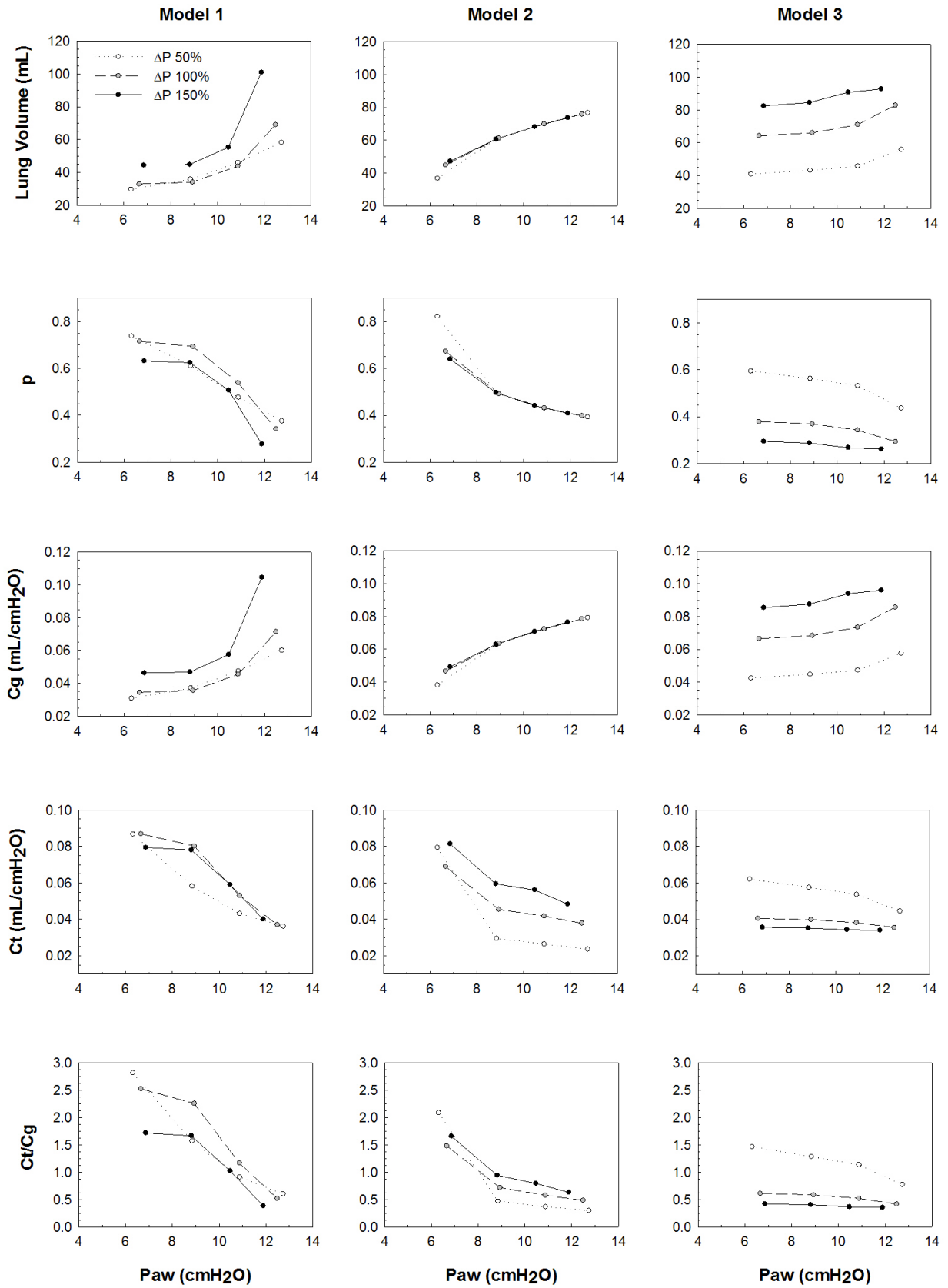
Baby 10 , Male, 0.77 Kg, 15 Hz Natural Frequency, Filter BP 11.25-18.75 Hz, 20 cycles per setting

Figure F.12: Baby 10 results. Vo, p, Cg, Ct, and Ct/Cg.



Baby 1 post-surfactant, Male, 0.872 Kg, 10 Hz Natural Frequency, Filter BP 5-15 Hz, 20 cycles per setting

Figure F.13: Baby 1 post-surfactant results. Rrs, Crs, and Error.



Baby 1 post-surfactant , Male, 0.872 Kg, 10 Hz Natural Frequency, Filter BP 5-15 Hz, 20 cycles per setting

Figure F.14: Baby 1 post-surfactant results. Vo, p, Cg, Ct, and Ct/Cg.